DEVELOPMENT OF STARCH-BASED MATERIALS

Thesis committee

Thesis supervisor
Prof. dr. ir. R. M. Boom
Professor of Food Process Engineering
Wageningen University

Thesis co-supervisor
Dr. ir. A. J. van der Goot
Associate Professor
Wageningen University

Other members
Prof. dr. E. van der Linden
Professor of Food Physics
Wageningen University

Prof. dr. G. Eggink
Wageningen University

Prof. dr. A.A. Broekhuis
University of Groningen

Dr. Job Ubbink
Nestlé Research Center, Lausanne, Switzerland

This research was conducted under the auspices of the VLAG Graduate School.

DEVELOPMENT OF STARCH-BASED MATERIALS

Edwin A. Habeych N.

Thesis

Submitted in partial fulfillment of the requirements for the degree of doctor
at Wageningen University
by the authority of the Rector Magnificus
Prof. dr. M.J. Kropff,
in the presence of the
Thesis Committee appointed by the Doctorate Board
to be defended in public
on Monday 26th of October 2009
at 1:30 PM in the Aula.

Edwin A. Habeych N.
Development of starch-based materials

Thesis, Wageningen University, The Netherlands, 2009
With summaries in English, Spanish, and Dutch

ISBN: 978-90-8585-433-3

Dedicado a mi padre, mi madre, a Nacho y a Rochy

Contents

CHAPTER 1	GENERAL INTRODUCTION	**1**
CHAPTER 2	PREDICTION OF PERMEATION FLUXES OF SMALL VOLATILE COMPONENTS THROUGH STARCH-BASED FILMS	**13**
CHAPTER 3	ON THE APPLICABILITY OF FLORY-HUGGINS THEORY TO TERNARY STARCH-WATER-SOLUTE SYSTEMS	**31**
CHAPTER 4	STARCH-ZEIN BLENDS FORMED BY SHEAR FLOW	**57**
CHAPTER 5	*IN SITU* COMPATIBILIZATION OF STARCH-ZEIN BLENDS UNDER SHEAR FLOW	**81**
CHAPTER 6	COMPATIBILIZATION OF STARCH-ZEIN BLENDS UNDER SHEAR FLOW	**103**
CHAPTER 7	GENERAL DISCUSSION	**113**
SUMMARY		**123**
RESUMEN		**127**
SAMENVATTING		**131**
ACKNOWLEDGEMENTS		**135**
PUBLICATION LIST		**139**
OVERVIEW OF COMPLETED TRAINING ACTIVITIES		**141**
CURRICULUM VITAE		**143**

General introduction

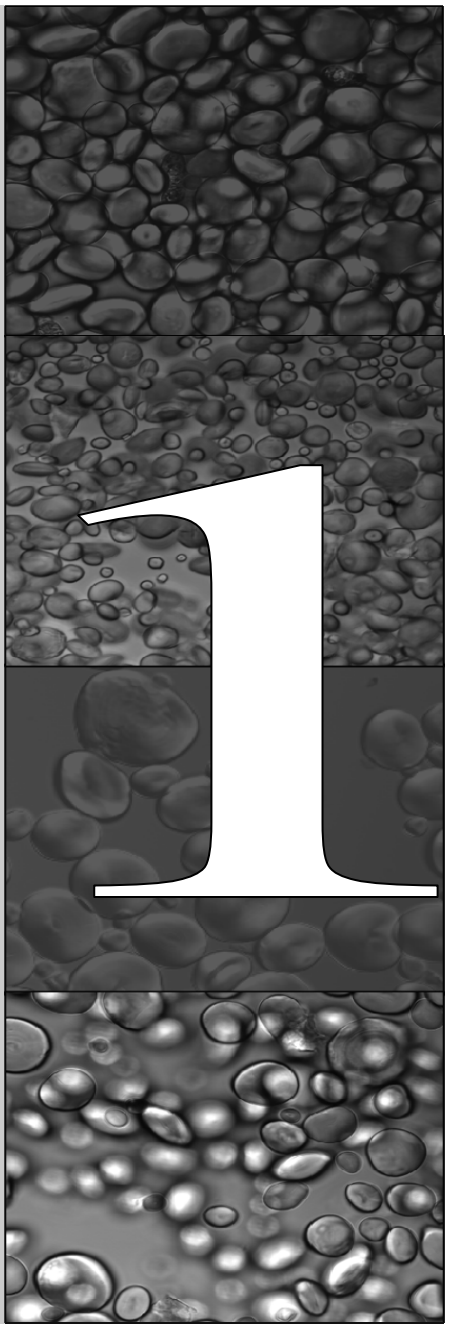

1. Starch and starch-based materials

Starch is the principal component for energy storage in plants and is one of the most abundant and available biopolymers. The most important sources for starch are corn, potato, wheat, and tapioca while barley, sorghum, rice, sago, arrowroot, and some others serve as smaller sources (Ratnayake & Jackson, 2008). Starch has become a multifunctional and significant contributor to the commercial food industry, because of its unique thermal properties and functionality (Rouilly & Rigal, 2002). It is used as thickener, stabilizer, bulking agent, gel former, and viscosity builder (Eliasson, 2004). Starch can be hydrolyzed chemically and/or enzymatically to obtain products such as glucose, maltose, maltodextrins, and cyclodextrins (Ratnayake & Jackson, 2008). Furthermore, being a biodegradable polymer, it has great potential as a versatile, renewable resource for various material applications. For example, biodegradable materials based on starch have been proposed as part of the new generation of materials yielding to contribute to the reduction of environmental problems such as green-house effect (Bastioli, 2001) compared to non-biodegradable materials. Biodegradable starch-based materials may perform as traditional plastics, but be completely biodegradable within a composting cycle through the action of living organisms. Furthermore, physical, chemical or biochemical modification of starch can result in starches with even greater functionality. This will stimulate the development of new products, processes and market trends (Eliasson, 2004), such as for packaging (trash bags, wrappings, loose-fill foam, food containers, film wrapping, laminated paper), ingredient delivery (drugs encapsulation), hygiene (diaper back sheets, cotton swabs), consumer goods (fast-food tableware, containers, toys), and agriculture (mulch films) (Gross & Kalra, 2002).

Unfortunately, so far the use of starch-based materials has been limited because of their poor tolerance for water and weak mechanical properties under moist conditions. For this reason, starch is frequently blended with other polymers with the aim to extend its applicability (Avérous, 2004). By varying the components in the blend and controlling their interaction with starch, the morphology and hence the properties can be controlled. Therefore, a clear understanding over the mechanism that control process-structure-function relationship in the blend is key in the development of a new generation of biodegradable starch-based blends.

2. Preparation of starch-based materials

Starch-based plastics are obtained from native starch by disruption of its native, granular structure and plasticization using plasticizing agents (e.g., water, glycerol and other

polyols) under the action of heat and mechanical work. The material obtained is referred as thermoplastic starch (TPS) (Van Soest et al., 1996a). The role of a plasticizer added to the starch is first to decrease the melting point below the decomposition temperature of starch and second to improve the mechanical properties of the material by, for example, increasing its ductility (Lourdin et al., 1997). Furthermore, thermo-mechanical treatment of starch is required to transform the partially crystalline polymer into a homogeneous, essentially amorphous polymeric matrix (Van Soest & Knooren, 1997).

The TPS prepared in this way still swells or even dissolves in water, ages, while its mechanical properties under moist conditions are poor (Follain, 2005). To overcome these limitations while maintaining its biodegradability, blending of plasticized starch with another polymer is a mode to obtain a low-cost material with physical properties that differ from those of the pure components (Gáspár et al., 2005). Blends containing TPS have been obtained by blending with synthetic polymers such as aliphatic polyesters, e.g., polycaprolactone, polyesteramide, polylactic acid and poly-(hydroxybutyrate-co-valerate) (Avérous, 2004). From the viewpoint of biodegradability, other biopolymers, such a proteins are considered as more suitable materials for blending with TPS than regular synthetic polymers (Corradini et al., 2006; Habeych et al., 2008; Lawton, 2002; Shukla & Cheryan, 2001). For example, the combination of the good gas barrier properties of starch with the hydrophobic corn zein may lead to a material for barrier films with the right combination of mechanical and permeability properties. However, for the development of robust materials with good applicability, it is important to understand how the morphology of the blend influences the properties of the final blend, and how this morphology is created during processing (Petersson et al., 2005). We will therefore discuss here three of the most important related aspects: gelatinization of starch, plasicization and blending with other (bio)polymers.

2.1 Starch gelatinization

Granular starch is a partially crystalline, granular solid (i.e., 15-39% crystallinity) (Jenkins & Donald, 1998; Slade & Levine, 1987). It consists of approximately 25% w/w of the linear polysaccharide amylose and 75% w/w of the branched polysaccharide amylopectin (Imberty et al., 1991). The starch chain can form a number of crystal polymorphs. Type A is found in cereals such as wheat; type B is found in tubers and high-amylose cereals, while type C is typically found in legumes. The A and B forms can be distinguished based on the packing of double helices: type A shows a monoclinic unit cell (Imberty et al., 1991) while

type B is hexagonally packed (Perry & Donald, 2000) arrays, respectively. Type C is known to be a mixture of types A and B (Eliasson, 2004).

When starch is heated above a certain temperature in the presence of excess water (>66% w/w), it undergoes a series of structural changes, which are collectively termed gelatinization (Ratnayake & Jackson, 2007). These changes are defined as melting in case of low water conditions. During gelatinization or melting, the principal changes that occur in the starch granules are: granule disruption, loss of order, swelling, exudation of amylose, and increase of viscosity (Ratnayake & Jackson, 2007; Sopade et al., 2004).

To study gelatinization, various technologies have been developed, such as DSC, X-Ray scattering, (visible) light scattering, optical microscopy, NMR, and thermomechanical analysis (TMA). However, different experimental methods lead to different values for the gelatinization temperature, since they all measure different aspects of the transitions during melting and gelatinization. This makes it difficult to unambiguously determine the gelatinization temperature (Baks et al., 2007).

Gelatinization and subsequent plasticization of the amorphous regions of native granular starch by the plasticizers are processes that occur after the initial swelling of the granule (Slade & Levine, 1994). Before plasticization may begin, water or another low molecular weight solvent should diffuse to the amorphous regions of starch. This explains why the plasticization process is very slow at temperatures below the initial glass transition temperature (T_g) of starch, but it occurs more rapidly at higher temperatures (Van Soest et al., 1996b). During the production of TPS-based products, heating and mechanical forces (shear) are often applied simultaneously to achieve full gelatinization (Van den Einde et al., 2004). A classical example is the extrusion cooking of starch (Barron et al., 2001). In the extruder, the thermo-mechanical treatment of starch induces various changes, such as melting of crystallites, disruption of granules and molecular breakdown of amylopectin, which have a direct relation with the properties of the material.

Various authors have tried to explain the changes that occur during gelatinization of starch, but often, their explanations remain ambiguous and even inconsistent (Ratnayake & Jackson, 2008). This situation stresses the need for new approaches to explain starch gelatinization. But, a universal explanation is not trivial due to the different factors that influence the gelatinization of starch: botanic origin, amylose to amylopectin ratio, and other polymer characteristics that can be attributed to the botanical source of a given starch

and its growth environment. In view of this need, it is useful to study the mechanism involve during gelatinization of starch. This knowledge will of course have high impact on the development of new starch-based materials because functional properties of starch are directly influenced by thermo-mechanical treatment or processing conditions (Ratnayake & Jackson, 2008).

2.2 Plasticization of starch

Fully gelatinized or melted starch can undergo a range of transitions. Plasticization is the softening of an amorphous polymer, or its amorphous fraction, from a glassy state to a more mobile rubbery state (i.e., glass transition - T_g). This glass transition relates to the phenomena observed when a brittle glass is changed upon heating into a super-cooled liquid or a rubbery material, or conversely when a super-cooled, malleable liquid or rubbery material is changed into a solid glass upon cooling (Figure 1). Water, polyols, small sugars, and other low molecular weight molecules may act as a plasticizer (Habeych et al., 2009). Those components have a strong influence on depressing the glass transition temperature, plasticizing the material, and modifying its mechanical properties (Myllarinen et al., 2002; Nashed et al., 2003; Rodriguez-Gonzalez et al., 2004; Sopade et al., 2004).

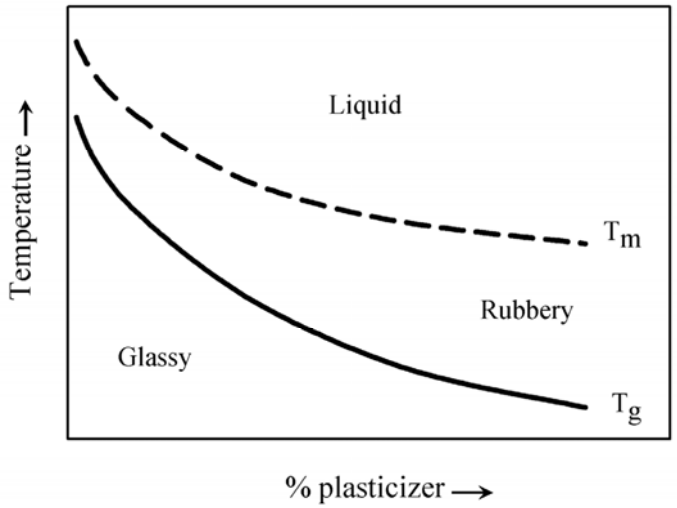

Figure 1. *Schematic state diagram for amorphous starch. T_g: glass transition temperature and T_m: melting temperature.*

The glass to rubber or liquid transition is accompanied by changes in physical properties of the material with temperature and a decrease in both rigidity and viscosity. These changes can be used to determine T_g of the material but because the glass transition is a kinetic process rather than a thermodynamic process, the temperature at which the system vitrifies depends on the cooling/heating rate (Roudaut, 2004). The most widely used techniques to determine the glass transition temperature in starch are differential scanning calorimetry (DSC) and dynamic mechanical thermal analysis (DMTA).

The plasticization of starch is an important mean to physically modify this biopolymer having high impact on its structure-function relationships. Therefore, a better knowledge about the plasticization of starch is important for the rational design of new starch-based materials with improved properties (i.e., thermal, mechanical, and structural properties).

2.3 Blending of starch-based materials

Blending is one of the most common techniques of polymer technology to produce materials with physical properties that are different from those of the pure components (Wang, 2006). Blending may yield to:

(i) materials with a favorable set of desired properties without having to synthesize completely new materials; or

(ii) materials with improved specific properties (e.g., impact strength or moisture resistance).

Starch has already been blended with synthetic polymers such as aliphatic polyesters (Avérous, 2004) and also with other agro-materials, e.g., proteins (Corradini et al., 2006; Lawton, 2002; Shukla & Cheryan, 2001). Proper processing of the blends is essential to obtain a specific morphology that leads to enhanced properties, e.g., for barrier applications. These can be achieved through the presence of an oriented hydrophobic phase within the starch matrix. Figure 2 shows a schematic distribution of a dispersed hydrophobic phase in the starch matrix. This anisotropic distribution of the disperse phase retards the diffusion of water by increasing the tortuous path through the matrix.

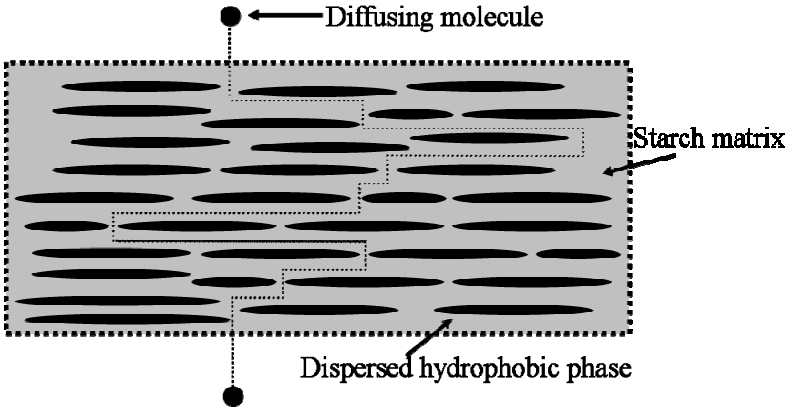

Figure 2. *Explanatory model for improved barrier properties in starch-based materials.*

Those and other novel structures with starch as base polymer may result in novel food and other starch-based products. Unfortunately, controlling the structure is difficult with traditional processes such as extrusion and mixing. The principal reason for this is in the flow and deformation patterns applied to the material during processing, which are complex and not well understood (Van der Goot et al., 2008). A first step is a better understanding of the role of flow and deformation. This may lead to an improvement of traditional equipment, but a more radical approach is the development of new process equipment based on well-defined conditions which allows better control over the final structure of the material. Thus, we consider new process concepts dedicated to structuring to be key in the development of new materials (Van der Goot et al., 2008).

Due to their low entropy of mixing, most polymer pairs are immiscible and need to be compatibilized. Compatibilization is required (Utracki, 2002):

(i) to enhance adhesion between the phases,
(ii) to stabilize the morphology against high stresses during forming, and
(iii) to reduce the interfacial tension.

Good compatibilization has significant effects on the flow behaviour and the final performance of the material. It can be accomplished either by the addition of a compatibilizer or by reactive processing (Utracki, 2002). Extensive work can be found in compatibilization strategies in synthetic polymers, however, little work has been done on compatibilization of starch-based materials, which makes this an issue of attention for the development of rationally designed starch-based biomaterials.

3. Motivation, Objectives and Outline

The overall goal of this thesis is to develop scientific insight on how the properties of starch-based materials emerge from the combination of processing and ingredients, and to devise and explore new processing routes based on this insight. Properties of choice are the moisture permeability and the mechanical properties of the materials. We therefore study the relation between the permeability of a number of permeants as function of the composition of a starch-based film, the gelatinization process in highly concentrated systems containing several solutes, and the properties of a starch-based blend, as function of its structure and composition. Figure 3 shows a scheme of the different aspects studied in this thesis.

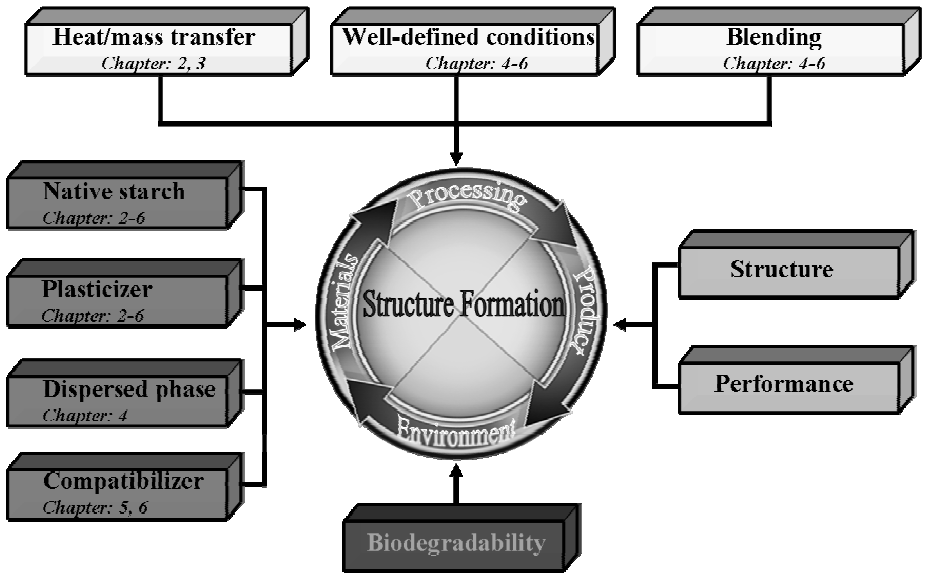

Figure 3. *Schematic representation of structure formation of starch-based materials.*

Chapter 2 describes the permeation fluxes of volatile diffusive species through starch films and relates this to the structure and composition of the starch films. Estimations of the Maxwell-Stefan diffusion rates of trace volatile compounds through polymeric films in multicomponent mixtures were developed based on the free-volume theory and the Flory-Huggins-Maxwell-Stefan (FHMS) equation. The model correctly predicts the trends and the order of magnitude of the permeation fluxes of diacetyl and carvone through starch films.

Chapter 3 studies the effect of a solute (i.e., glucose and glycerol) on the gelatinization of highly concentrated starch mixtures. An extended form of the well-known Flory–Huggins equation was used to interpret and predict the gelatinization and melting behavior of ternary starch-based systems. The chapter summarizes some of the results with ternary phase diagrams for the systems starch-water-glycerol and starch-water-glucose.

Chapter 4 introduces the use of simple shear flow as a process parameter for structure formation in starch-protein blends. A shearing device was developed to explore the formation of new types of microstructure in concentrated starch-zein blends. The use of this device allowed the formation of different morphologies ranging from isotropic to anisotropic. Their mechanical properties of the obtained materials were tested and their behavior was explained by using models for blends with poor adhesion. The chapter concludes with identifying a generic process parameter for the structure formation of starch-zein blends with a proposed mechanism for structuring.

Chapter 5 reports on the improvement of the adhesion properties of starch-zein blends by the addition of a component that contains a reactive functional group (aldehyde), which reacts during blending with the components present on the interface between the phases, creating a compatibilizer *in situ*. The properties of the created materials were evaluated and related to the processing conditions and the composition.

Chapter 6 explores the addition of an extract from rice bran as a non-reactive, food-grade compatibilizing component for the compatibilization of starch-zein blends. This rice bran extract shows radical scavenging functionality, is antioxidative, and shows emulsifying properties. The chapter compares the influence of rice bran extract with that of aldehyde starch (cf. **Chapter 5**) as compatibilizers for starch-zein blends under shear conditions.

Chapter 7 combines the conclusions of the preceding chapters into a general conclusion, and from this perspective then discusses the applicability of the concepts presented in this thesis, in different practical contexts.

References

1. Avérous, L. (2004). Biodegradable multiphase systems based on plasticized starch: A review. *Journal of Macromolecular Science - Polymer Reviews*, 44(3), 231-234.
2. Baks, T., Ngene, I.S., Van Soest, J.J.G., Janssen, A.E.M., & Boom, R.M. (2007). Comparison of methods to determine the degree of gelatinisation for both high and low starch concentrations. *Carbohydrate Polymers*, 67(4), 481-490.
3. Barron, C., Bouchet, B., Della Valle, G., Gallant, D.J., & Planchot, V. (2001). Microscopical study of the destructuring of waxy maize and smooth pea starches by shear and heat at low hydration. *Journal of Cereal Science*, 33(3), 289-300.
4. Bastioli, C. (2001). Global status of the production of biobased packaging materials. *Starch/Staerke*, 53(8), 351-355.
5. Corradini, E., De Medeiros, E.S., Carvalho, A.J.F., Curvelo, A.A.S., & Mattoso, L.H.C. (2006). Mechanical and morphological characterization of starch/zein blends plasticized with glycerol. *Journal of Applied Polymer Science*, 101(6), 4133-4139.
6. Eliasson, A.C. (2004). *Starch in food: Structure, function and applications*. Cambridge, England: Woodhead Publishing Ltd.
7. Follain, N., Joly, C., Dole, P., & Bliard, C. (2005). Mechanical properties of starch-based materials. I. Short review and complementary experimental analysis. *Journal of Applied Polymer Science*, 97(5), 1783-1794.
8. Gáspár, M., Benko, Z., Dogossy, G., Réczey, K., & Czigány, T. (2005). Reducing water absorption in compostable starch-based plastics. *Polymer Degradation and Stability*, 90(3), 563-569.
9. Gross, R.A. & Kalra, B. (2002). Biodegradable polymers for the environment. *Science*, 297(5582), 803-807.
10. Habeych, E., Dekkers, B., Van der Goot, A.J., & Boom, R. (2008). Starch-zein blends formed by shear flow. *Chemical Engineering Science*, 63(21), 5229-5238.
11. Habeych, E., Guo, X., Van Soest, J.J.G., Van der Goot, A.J., & Boom, R. (2009). On the applicability of Flory-Huggins theory to ternary starch-water-solute systems. *Carbohydrate Polymers*, 77(4), 703-712.
12. Imberty, A., Buleon, A., Tran, V., & Perez, S. (1991). Recent advances in knowledge of starch structure. *Starch-Starke*, 43(10), 375-384.
13. Jenkins, P.J. & Donald, A.M. (1998). Gelatinisation of starch: a combined SAXS/WAXS/DSC and SANS study. *Carbohydrate Research*, 308(1-2), 133-147.

14. Lawton, J.W. (2002). Zein: A history of processing and use. *Cereal Chemistry*, 79(1), 1-18.
15. Lourdin, D., Bizot, H., & Colonna, P. (1997). "Antiplasticization" in starch-glycerol films? *Journal of Applied Polymer Science*, 63(8), 1047-1053.
16. Myllarinen, P., Partanen, R., Seppälä, J., & Forssell, P. (2002). Effect of glycerol on behaviour of amylose and amylopectin films. *Carbohydrate Polymers*, 50(4), 355-361.
17. Nashed, G., Rutgers, R.P.G., & Sopade, P.A. (2003). The plasticisation effect of glycerol and water on the gelatinisation of wheat starch. *Starch/Staerke*, 55(3-4), 131-137.
18. Perry, P.A. & Donald, A.M. (2000). The effects of low temperatures on starch granule structure. *Polymer*, 41(16), 6361-6373.
19. Petersson, M., Lorén, N., & Stading, M. (2005). Characterization of phase separation in film forming biopolymer mixtures. *Biomacromolecules*, 6(2), 932-941.
20. Ratnayake, W.S. & Jackson, D.S. (2007). A new insight into the gelatinization process of native starches. *Carbohydrate Polymers*, 67(4), 511-529.
21. Ratnayake, W.S. & Jackson, D.S. (2008). Chapter 5: Starch gelatinization, *Advances in Food and Nutrition Research*, Vol. 55: 221-268.
22. Rodriguez-Gonzalez, F.J., Ramsay, B.A., & Favis, B.D. (2004). Rheological and thermal properties of thermoplastic starch with high glycerol content. *Carbohydrate Polymers*, 58(2), 139-147.
23. Roudaut, G., Simatos, D., Champion, D., Contreras-Lopez, E., & Le Meste, M. (2004). Molecular mobility around the glass transition temperature: A mini review. *Innovative Food Science and Emerging Technologies*, 5(2), 127-134.
24. Rouilly, A. & Rigal, L. (2002). Agro-materials: A bibliographic review. *Journal of Macromolecular Science - Polymer Reviews*, 42(4), 441-479.
25. Shukla, R. & Cheryan, M. (2001). Zein: the industrial protein from corn. *Industrial Crops and Products*, 13(3), 171-192.
26. Slade, L. & Levine, H. (1987). Recent advances in starch retrogradation. *Industrial Polysaccharides*, 387-430.
27. Slade, L. & Levine, H. (1994). Water and the glass transition - dependence of the glass transition on composition and chemical structure: Special implications for flour functionality in cookie baking. *Journal of Food Engineering*, 22(1-4), 143-188.

28. Sopade, P.A., Halley, P.J., & Junming, L.L. (2004). Gelatinisation of starch in mixtures of sugars. II. Application of differential scanning calorimetry. *Carbohydrate Polymers*, 58(3), 311-321.
29. Utracki, L.A. (2002). Compatibilization of polymer blends. *Canadian Journal of Chemical Engineering*, 80(6), 1008-1016.
30. Van den Einde, R.M., Bolsius, A., Van Soest, J.J.G., Janssen, L.P.B.M., Van der Goot, A.J., & Boom, R.M. (2004). The effect of thermomechanical treatment on starch breakdown and the consequences for process design. *Carbohydrate Polymers*, 55(1), 57-63.
31. Van der Goot, A.J., Peighambardoust, S.H., Akkermans, C., & Van Oosten-Manski, J.M. (2008). Creating novel structures in food materials: the role of well-defined shear flow. *Food Biophysics*, 3(2), 120-125.
32. Van Soest, J.J.G., De Wit, D., & Vliegenthart, J.F.G. (1996a). Mechanical properties of thermoplastic waxy maize starch. *Journal of Applied Polymer Science*, 61(11), 1927-1937.
33. Van Soest, J.J.G., Hulleman, S.H.D., De Wit, D., & Vliegenthart, J.F.G. (1996b). Crystallinity in starch bioplastics. *Industrial Crops and Products*, 5(1), 11-22.
34. Van Soest, J.J.G. & Knooren, N. (1997). Influence of glycerol and water content on the structure and properties of extruded starch plastic sheets during aging. *Journal of Applied Polymer Science*, 64(7), 1411-1422.
35. Wang, Z.G. (2006). Challenges and opportunities in polymer theory. *Journal of Polymer Science, Part B: Polymer Physics*, 44(24), 3445-3447.

Prediction of permeation fluxes of small volatile components through starch-based films

This chapter has been published as: Habeych, E., Van der Goot, A.J., & Boom, R. (**2007**). Prediction of permeation fluxes of small volatile components through starch-based films. *Carbohydrate Polymers*, 68(3), 528-536.

Abstract

Simple formulas for estimating the Maxwell-Stefan diffusion of trace volatile compounds through polymeric films in multicomponent mixtures are developed based on free-volume theory and Flory-Huggins-Maxwell-Stefan (FHMS) equation. The model includes the solution-diffusion theory, and predicts the order of magnitude of the permeation fluxes of diacetyl and carvone through starch films. The permeability of volatile components within starch films was dominated by the swelling of the matrix. The methodology required only some physical properties of the components sorption equilibrium.

1. Introduction

Quantitative prediction of permeation of volatile components through polymeric films is relevant for a great number of applications. Predictions of permeation of aroma compounds through food matrices can be important to develop suitable matrices for flavor encapsulation. Another important application is the permeation of drug molecules through matrixes for drug delivery (Kumar & Kumar, 2001). The transfer of compounds within the product and their release from it depends on the nature of the compounds, the composition and the structure of the matrix (Seuvre et al., 2006). Model predictions can be used to show the rate of release, or how the performance of the system will be affected by any change made to it. Furthermore, the use of predictive models of permeation allows the quantification of a rate of release of particular compound within a specific matrix.

The rate of permeation of small components through a polymeric matrix is affected by the size and geometry of the molecules as well as by their physical-chemical affinity to the polymer. A common approach used to describe the diffusion through matrices is the solution-diffusion model (Fornasiero et al., 2005a), where the polymeric-matrix/solute system is considered to be a molecular solution in which solute transport is through diffusion only. Usually, the description of diffusion in these systems has been treated through three different approaches: by using the generalized Fick's law, the Maxwell-Stefan expression (MS), or via the thermodynamics of irreversible processes (Wesselingh & Krishna, 2000). Even though these formulations are formally equivalent, the MS-description of diffusion is usually preferred (Taylor & Krishna, 1993) and is adopted in this work. The MS approach requires information about thermodynamic and kinetic components of the system. The thermodynamic part can be described using the Flory-Huggins theory (FH), which can be readily incorporated in the MS due to their similar treatment of the microscopic molecular structure (Schaetzel et al., 2001).

The kinetic parameters can be obtained using the so-called Free-volume theory (FV). This theory has been used to describe the mobility of small penetrant though rubbery polymer systems with good accuracy (Wang et al., 2001; Wesselingh & Bollen, 1997). In this approach the prediction of permeability values through polymeric films makes use of only physical data together with the sorption equilibrium for each component in the mixture. The model proposed in this study is based on the assumption that the diffusivity of each permeant depends uniquely on the total volume fraction occupied by the permeant molecules, whatever their nature. Combined with the Maxwell-Stefan/Flory-Huggins (MSFH) theory the model allows predictions of permeation values.

The aim of this chapter is to describe the permeation rates of the volatile diffusive species through starch films and to relate these estimates to the structure and composition of the starch films. The model is first checked with permeation data reported in the literature for starch-volatile (Yilmaz et al., 2004) and then analyzed to explore its sensitivity to different parameters and produce guidelines for design of (edible) barriers.

2. Model

The simulations are based on Maxwell-Stefan, Flory-Huggins, and Free-volume theories. The theoretical background and the assumptions considered in the present model are explained in the following section.

2.1 Basic considerations

The mathematical treatment of diffusion transport is based on the following assumptions:

- The system consists of: a model volatile compound being either Diacetyl (2,3-butanedione) or Carvone (p-menthe-6, 8-dien-2-one)- (component 1), Water (component 2), Glycerol (component 3), and Starch (component M);
- The matrix is considered as a homogeneous material;
- The diffusion process is considered to be isothermal and isobaric;
- The fluids on either side of the film are at equilibrium with the starch film at the interface. This assumption implies that there is a continuous gradient in chemical potential from one side of the film to the other. Thus, the rates of absorption and desorption at the matrix interface are much higher than the rate of diffusion through the film, i.e. diffusion through the film is the rate-determining step;
- The chemical potential gradient across the starch film is only a function of the composition;
- The FH interaction parameter χ was calculated using the solubility of the minor component, as outlined by Mulder (1996) and Schaetzel et al. (2001) using the following expression.

$$\chi_{iM} = -\frac{\ln \phi_i + (1-\phi_i)}{(1-\phi_i)^2}, \qquad (1)$$

Solubility data were obtained from equilibrium experiments reported by (Yilmaz et al., 2004). Using the formula for diacetyl-starch the χ values is 4.7 and 5.9 for carvone-starch. For water-starch, a constant value of 0.6 was taken from (Van den Berg, 1981).

The fact that starch molecules are enormously larger than the other compounds induces large uncertainties in the model. However, in a mixture of polymers and low-molecular weight substances, the diffusion interaction will not be with the complete polymer chain, but only with portion of it. It is therefore usual to adapt the theory to avoid this. Different authors have proposed multiples strategies (Heintz & Stephan, 1994; Paul, 2004; Fornasiero et al., 2005b; Wesselingh & Bollen, 1997). We adopted the strategy suggested by Wesselingh and Bollen, in which it is assumed that diffusion is caused by motion of the separate chain elements of the polymer. Thus, it is assumed that glucose constitutes the chain repeat element of starch. In addition, water is assumed to be associated (dimer).

3. The Maxwell-Stefan Equation

The Maxwell-Stefan approach poses a force balance in which the driving forces acting on system balance a (linear) combination of the friction forces between the species in the system.

$$-\frac{x_i}{RT}\nabla_{T,P}\mu_i = \sum_{\substack{j=1 \\ j\neq 1}}^{n} \frac{x_j N_i - x_i N_j}{c_T \text{Đ}_{ij}}, \qquad i = 1,2,...,n, \tag{2}$$

where i is one of the diffusing species; c_T is the total molar concentration; Đ_{ij} is the binary Maxwell-Stefan diffusivity; μ_i is the chemical potential; x_i is the molar fraction; N_i is the species molar flux. The MS diffusivity can be interpreted as the inverse of the intermolecular friction coefficient (Wesselingh & Krishna, 2000). The use of the MS equation requires the estimation of the binary MS diffusivities as well as the chemical potential for all the species. For the case of polymer-solvent mixtures, the chemical potential can be estimated using the Flory-Huggins theory, and the binary MS diffusivities can be predicted through the Free-volume theory.

4. Free volume theory

Here, we will use the theory proposed by (Wesselingh & Bollen, 1997) to estimate the diffusion coefficients of the mixture. The free volume theory follows three basic assumptions. The first assumption is that the total free volume in a mixture is given by the contribution of the pure components;

$$V_F = \sum_{i=1}^{n} x_i V_{Fi}, \tag{3}$$

The free volume of each component (V_{Fi}) can be calculated using two simple equations based on viscosity and molar volume data as was described by (Wesselingh & Bollen, 1997):

$$\eta_i = \sqrt{\frac{3MW_i A^{1/3} kT}{\pi^2 (V_i^{\bullet})^{4/3}}} \exp\left(0.7 \frac{V_i^{\bullet}}{V_{Fi}}\right), \tag{4}$$

and

$$V_{Fi} = V_i^{\bullet} - V_i \ , \tag{5}$$

The minimum (compressed) volume ($V^{\bullet}_i$) of each component can also be estimated using the critical volume (V_{ci}) of component *i* according to Guggenheim equation (Wesselingh & Bollen, 1997). The minimum compress volume was then used as a starting value to solve eq. 4 and 5.

$$V_i^{\bullet} = 0.289 V_{ci} \, , \tag{6}$$

The second assumption is that for molecules of different sizes, a better estimation of the free volume can be obtained if it is assumed that the free volume seen by each component is proportional to its surface fraction. When considering molecules to be spherical, the surface of a molecule scales to $V^{2/3}$. Therefore, the surface fractions of the component species are represented by:

$$\sigma_i = \frac{x_i (V_i)^{2/3}}{\sum_{k=1}^{n} x_k (V_k)^{2/3}} \, , \tag{7}$$

The free volume for each species becomes now:

$$V_{Fi} = \frac{\sigma_i V_F}{x_i} \, , \tag{8}$$

The third assumption relates to the density that we approximated as the average mass density:

$$\rho^{\bullet} = \sum_{k=1}^{n} \rho_k^{\bullet} x_k^m \, , \tag{9}$$

Finally, the expression for the MS binary diffusivity is given by:

$$Đ_{ik} = \frac{RT}{\xi_{ik}} \, , \tag{10}$$

where

$$\xi_{ik} = \frac{\xi_{i,eff}\,\xi_{k,eff}}{\sum_{m=1}^{n} x_m \xi_{m,eff}} \qquad i \neq k\ , \tag{11}$$

and

$$\xi_{i,eff} = 2A\sqrt{3kT\rho^{\bullet} d_i}\,\exp\left(0.7\frac{V_i^{\bullet}}{V_{Fi}}\right), \tag{12}$$

where $\xi_{i,eff}$, and d_i can be calculated assuming that the compressed fluid has a cubic structure:

$$d_i = \left(\frac{V_i^{\bullet}}{A}\right)^{1/3}, \tag{13}$$

5. The Maxwell-Stefan/Flory-Huggins equations (MSFH)

Following the Flory-Huggins theory for a quaternary system; the Gibbs energy of mixing (ΔG_M) is as follows:

$$\frac{\Delta G_M}{RT} = n_1 \ln\phi_1 + n_2 \ln\phi_2 + n_3 \ln\phi_3 + n_3 \ln\phi_M + n_1\phi_2\chi_{12} + n_1\phi_3\chi_{13}$$
$$n_1\phi_M\chi_{1M} + n_2\phi_3\chi_{23} + n_2\phi_M\chi_{2M} + n_3\phi_M\chi_{3M}\ , \tag{14}$$

Differentiation with regard to each component gives the change in chemical potential upon mixing for that component:

$$\Delta\mu_i = RT\ln(a_i) = \left(\frac{\partial \Delta G_M}{\partial n_i}\right)_{P,T,n_j}, \tag{15}$$

In which a_i is the activity.

We assume that the binary FH interaction parameters χ_{ij} are not concentration dependent. The latest assumption is justified, because we consider that for the low concentration range of the three non-polymeric components the binary parameters behave as constants. The resultant system is:

$$\ln(a_1) = \ln\phi_1 - \frac{V_1}{V_2}\phi_2 - \frac{V_1}{V_3}\phi_3 - \frac{V_1}{V_M}\phi_M + (1-\phi_1)\left(1+\chi_{12}\phi_2+\chi_{13}\phi_3+\chi_{1M}\phi_M\right)$$
$$-\frac{V_1}{V_2}\chi_{2M}\phi_2\phi_M - \frac{V_1}{V_2}\chi_{23}\phi_2\phi_3 - \frac{V_1}{V_M}\chi_{3M}\phi_3\phi_M, \quad (16A)$$

$$\ln(a_2) = \frac{V_1}{V_2}\ln\phi_2 - \phi_1 - \frac{V_1}{V_3}\phi_3 - \frac{V_1}{V_M}\phi_M + (1-\phi_2)\left(\frac{V_1}{V_2}+\chi_{12}\phi_1+\frac{V_1}{V_2}\chi_{23}\phi_3+\frac{V_1}{V_2}\chi_{2M}\phi_M\right)$$
$$-\chi_{1M}\phi_1\phi_M - \chi_{13}\phi_1\phi_3 - \frac{V_1}{V_M}\chi_{3M}\phi_3\phi_M, \quad (16B)$$

$$\ln(a_3) = \frac{V_1}{V_3}\ln\phi_3 - \phi_1 - \frac{V_1}{V_2}\phi_2 - \frac{V_1}{V_M}\phi_M + (1-\phi_3)\left(\frac{V_1}{V_3}+\chi_{13}\phi_1+\frac{V_1}{V_2}\chi_{23}\phi_2+\frac{V_1}{V_M}\chi_{3M}\phi_M\right)$$
$$-\chi_{1M}\phi_1\phi_M - \chi_{12}\phi_1\phi_2 - \frac{V_1}{V_2}\chi_{2M}\phi_2\phi_M, \quad (16C)$$

$$\ln(a_M) = \frac{V_1}{V_M}\ln\phi_M - \phi_1 - \frac{V_1}{V_2}\phi_2 - \frac{V_1}{V_3}\phi_3 + (1-\phi_M)\left(\frac{V_1}{V_M}+\chi_{1M}\phi_1+\frac{V_1}{V_2}\chi_{2M}\phi_2+\frac{V_1}{V_M}\chi_{3M}\phi_3\right)$$

$$-\chi_{13}\phi_1\phi_3 - \chi_{12}\phi_1\phi_2 - \frac{V_1}{V_2}\chi_{23}\phi_2\phi_3, \quad (16D)$$

The MS equation for a quaternary system in terms of volume fraction (considering unidirectional diffusion in the z axis) is as follows:

$$-\left(\frac{d\ln(a_i)}{dz}\right) = \sum_{\substack{j=1\\ j\neq 1}}^{n} \frac{\phi_j}{c_T V_j Đ_{ij}}\left(\frac{V_i N_i}{\phi_i} - \frac{V_j N_j}{\phi_j}\right), \qquad i = 1,2,3,4, \quad (17)$$

This equation extended for four components considering a zero value for the polymer flux (i.e., $N_M \cong 0$) are as follow:

$$-\left(\frac{d\ln(a_1)}{dz}\right) = \frac{\phi_2}{c_T V_2 Đ_{12}}\left(\frac{V_1N_1}{\phi_1} - \frac{V_2N_2}{\phi_2}\right) + \frac{\phi_3}{c_T V_3 Đ_{13}}\left(\frac{V_1N_1}{\phi_1} - \frac{V_3N_3}{\phi_3}\right) + \frac{\phi_M}{c_T V_M Đ_{1M}}\left(\frac{V_1N_1}{\phi_1}\right), \quad (18A)$$

$$-\left(\frac{d\ln(a_2)}{dz}\right) = \frac{\phi_1}{c_T V_1 Đ_{12}}\left(\frac{V_2N_2}{\phi_2} - \frac{V_1N_1}{\phi_1}\right) + \frac{\phi_3}{c_T V_3 Đ_{23}}\left(\frac{V_2N_2}{\phi_2} - \frac{V_3N_3}{\phi_3}\right) + \frac{\phi_M}{c_T V_M Đ_{2M}}\left(\frac{V_2N_2}{\phi_2}\right), \quad (18B)$$

$$-\left(\frac{d\ln(a_3)}{dz}\right) = \frac{\phi_1}{c_T V_1 Đ_{13}}\left(\frac{V_3N_3}{\phi_3} - \frac{V_1N_1}{\phi_1}\right) + \frac{\phi_2}{c_T V_2 Đ_{23}}\left(\frac{V_3N_3}{\phi_3} - \frac{V_2N_2}{\phi_2}\right) + \frac{\phi_M}{c_T V_M Đ_{3M}}\left(\frac{V_3N_3}{\phi_3}\right), \quad (18C)$$

$$-\left(\frac{d\ln(a_M)}{dz}\right) = \frac{\phi_1}{c_T V_1 Đ_{1M}}\left(-\frac{V_1N_1}{\phi_1}\right) + \frac{\phi_2}{c_T V_2 Đ_{23}}\left(-\frac{V_2N_2}{\phi_2}\right) + \frac{\phi_3}{c_T V_3 Đ_{3M}}\left(-\frac{V_3N_3}{\phi_3}\right), \quad (18D)$$

The exact solution requires the numerical resolution of these equations, however, we have considered several further assumptions, which are physically acceptable that allow additional simplifications. They are:

- Glycerol acts as a plasticizer in the film, and it does not leave film. Therefore, we may assume its net diffusion to be negligible (i.e., $N_3 \cong 0$).
- The permeating species are present at low concentrations, thus we neglect coupling fluxes. Even though the interaction parameters between non-permeating species will have influence on the swelling value of the system, it is only the binary interaction between permeating species and the matrix (χ_{1M} and χ_{2M}) that is important for determining the flux.

The simplified equation resulting from application of these assumptions is similar to the one given by (Schaetzel et al., 2001).

$$N_i = \frac{Đ_{iM}}{V_i^2 z_e}\left[\left(V_M - 2V_i - 2\chi_{iM}V_i + \frac{V_i^2}{V_M}\right)\cdot\frac{\left(\phi_{i0}^2 - \phi_{ie}^2\right)}{2} + \frac{2}{3}\chi_{iM}\left(V_i - V_M\right)\left(\phi_{i0}^3 - \phi_{ie}^3\right) - V_i \ln\left(\frac{1-\phi_{i0}}{1-\phi_{ie}}\right)\right], \quad (19)$$

The subscripts '0' and '*e*' refer to the initial and final side of the film, respectively, and Z_e is the thickness of the film.

To elucidate the driving parameter that governs permeation of hydrophobic compound through starch films, two simulations were performed with Mathcad (Mathsoft Engineering & Education, version 11.0, Cambridge, USA) following the steps described in previous paragraphs. Table 1 shows the parameters used for the simulations.

Table 1. *Physical data used for the simulations*

Code	Component	Molecular weight	Density (kg/m^3)	Viscosity (N·s/m^2)
1	Diacetyl	86.1	981	-
	Carvone	150.22	961	-
2	Water	[b]2 x 18.0	998	8.0 x 10^{-4}
3	Glycerol	92.09	1261	1.07 x 10^{0}
M	Glucose	180.16	1544	[a]1.61 x 10^{11}

Data taken from (Weast, 1973). [a]data generated using ASPEN Plus. [b]water is taken as a dimmer.

6. Results and Discussion

6.1 Validation of the model

To verify the model, we used the experimental results reported by (Yilmaz et al., 2004) concerning the permeation data of diacetyl and carvone through starch films at 20 °C. The experimental data extracted to verify the model are summarized in Table 2.

Table 2. Characteristics of different Starch films[a] (Yilmaz et al., 2004)

Film No.	Film thickness (mm)	Solubility (mg cm^{-3})	Moisture contain after equilibration (% mol/mol)	Flux ($mol \cdot m^{-2}\ s^{-1}$)*10^8	Crystallinity (%)
1	0.351 ± 0.002	2.11 ± 0.04	32.2	42.3	19 ± 1
2a	0.164 ± 0.002	2.41 ± 0.03	47.7	153	20 ± 2
2b	0.348 ± 0.002	2.42 ± 0.02	47.1	71.9	22 ± 1
[b]3	0.353 ± 0.002	2.41 ± 0.02	56.8	117	17 ± 1
[c]4	0.356 ± 0.004	3.30 ± 0.03	66.5	169	21 ± 1
5	0.352 ± 0.005	3.14 ± 0.03	55.2	117	24 ± 1
6	0.354 ± 0.003	2.14 ± 0.02	56.8	36.1	31 ± 3
7	0.347 ± 0.007	2.18 ± 0.02	47.8	172	None
8a	0.165 ± 0.002	0.60 ± 0.03	47.7	13.7	19 ± 2
8b	0.351 ± 0.002	0.61 ± 0.03	47.1	5.18	21 ± 1
9	0.351 ± 0.003	0.43 ± 0.14	32.8	3.88	19 ± 2
[b]10	0.352 ± 0.002	0.62 ± 0.02	56.5	5.55	18 ± 1
[c]11	0.352 ± 0.005	0.63 ±0.05	66.0	7.21	22 ± 2
12	0.348 ± 0.003	0.76 ± 0.02	54.4	10.2	24 ± 1
13	0.350 ± 0.004	0.57 ±0.04	57.9	3.33	31 ± 2
14	0.351 ± 0.007	0.67 ± 0.01	47.1	12.8	None

[a]Films 1-7 were used for permeation experiments with diacetyl; films 8a-14 were used for the permeation experiments with carvone.
[b]Films where the permeation experiments were carried out at relative humidity (RH) of 60%.
[c]The permeation experiments were carried out at RH of 90%. All the rest films were equilibrated at RH of 30%.

First of all, MS binary diffusivities were calculated using the procedure previously described. The estimated MS diffusivities are shown Figure 1. Water concentration in the films turned out to be the main parameter in the diffusivities of all components. According

to the FV theory, the diffusion coefficient is a strong function of the volume fractions of the individual species. For this reason, the addition of small molecules such as water or polar solutes results in increase in free volume, strongly increasing the molecular mobility of the mixture (plasticizing effect). This plasticizing effect upon starch films caused by water and glycerol is synergistic and enhances the diffusion rate, which facilitates the penetration of the volatile components as was also observed by Yilmaz et al. (2004) for this specific system. Another aspect observed is the effect of the size of the permeants in the diffusivities values. Thus, water is the smallest molecule in this system and consequently the fastest to diffuse. In contrast, carvone is the biggest and therefore the slowest diffusive species. Diacetyl and glycerol have similar molecular weights, and therefore their diffusion coefficients are similar.

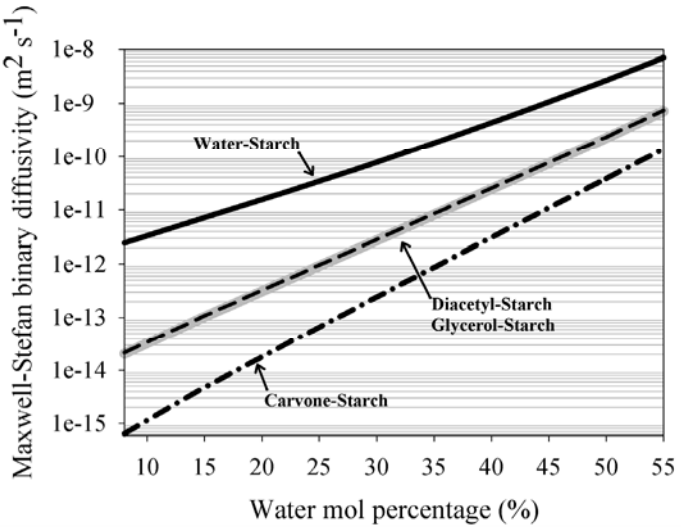

Figure 1. *Binary Maxwell-Stefan diffusivities at 20 ℃.*

Figure 2 and 3 show the fluxes estimations for diacetyl and carvone. Most of the estimations are of the same order of magnitude as the experimental results. Furthermore, the flux of water shows concordance with the result for carvone and diacetyl, it increases when the water content in the film increases (Figure 4). As a result, this model results very attractive to make predictions of diffusion of small components through starch-based films. Some of the values for diacetyl show less precise predictions. The deviations from the experiments may be related to the effect of crystallinity, cross-linking, or other inhomogeneities that are not taken into consideration in the present model. For example,

film 6 for diacetyl has the highest crystallinity and its prediction deviates strongly from the experimental results. A similar situation occurs with film 13 for carvone but, although a less pronounced effect.

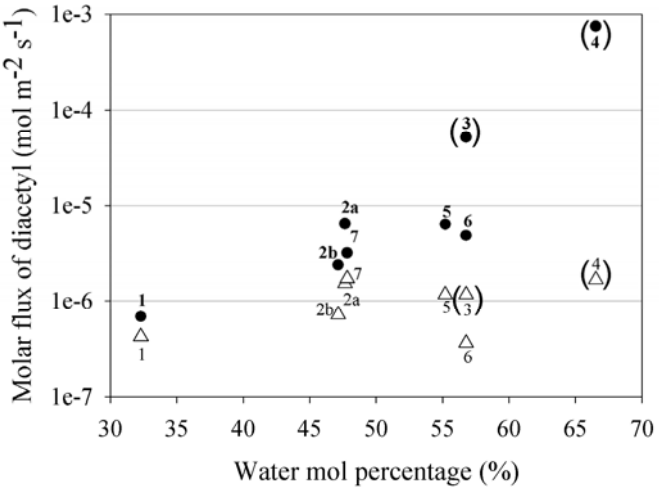

Figure 2. *Permeation flux of diacetyl through starch films (no. 1-7; Table 2) at 20 ℃ as a function of the water mol percentage. (△) experimental values, (●) simulated values.*

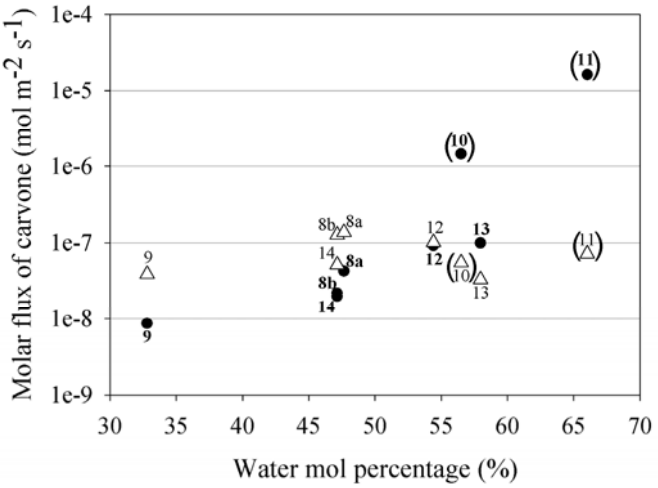

Figure 3. *Permeation flux of carvone through starch films (no. 8a-14; Table 2) at 20 ℃ as a function of the water mol percentage. (△) experimental values, (●) simulated values.*

Films 3-4 for diacetyl, and films 10-11 for carvone differ more than one order of magnitude from the experimental results. In addition, Figure 4 shows that the highest water flux values correspond to the anomalous films mentioned above. Table 2 shows that the permeability experiments with these films were carried out at high relative humidity (60 and 90% RH), while they were prepared at low humidity (30% RH). In consequence, it is possible that the films were not measured at equilibrium conditions leading to a lower permeation values, violating the fourth assumption of our model. Hence, the model suggests that the relative independence of these experimental points on the water contains might be due to data obtained in non-equilibrium (non-steady state) conditions. This suggestion is supported by the results of Standing and co-workers who found a direct effect of the surrounding humidity on the film microstructure and permeability properties. They reported that for glycerol-plasticized amylose films, the network microstructure changed from dense and homogeneous to a more open structure with fluctuations in the pore size when the surrounding RH was increased (Stading et al., 2001). This change in morphology was attributed to plasticization of the amorphous areas due to the increased water content, leading to higher mobility in the network and subsequent higher permeability values. This observation supports our interpretation of the disagreement between model and experiments for these films.

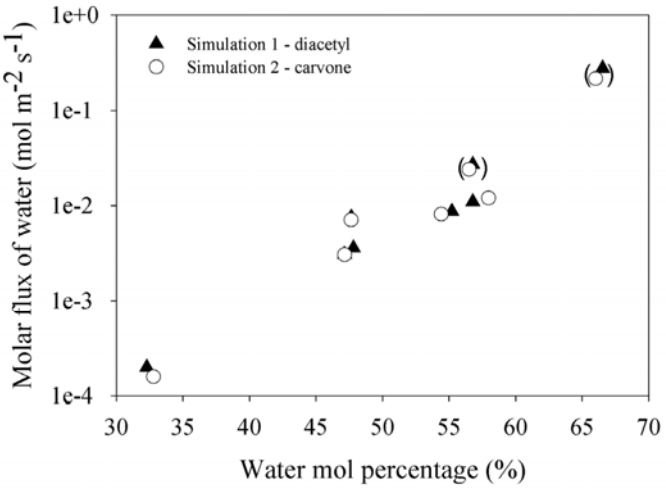

Figure 4. *Permeation flux of water through starch films at 20 ℃.*

In summary, the diacetyl/carvone permeation fluxes through starch films are satisfactorily predicted with the Free-volume/Maxwell-Stefan/Flory-Huggins (FV-MSFH)

equation without the need of any adjustable parameters. For the prediction, only a number of physical properties of the components sorption equilibrium values were required.

6.2 Consequences for film design

Now, the model can be used to explore the effect of film and permeant properties on the permeation, leading to insight how to change the film in order to modify the permeation properties.

The solubility of diacety/carvone in starch films is low (Table 2). An increase in water activity in the mixture however leads to swelling of the matrix and consequently to an increment in the permeation of the volatile molecules through the swollen polymer. As was previously shown, the steady state flux of diacetyl is higher than the flux of carvone. This can be ascribed to the higher diffusion coefficient as well as the higher solubility of diacetyl as compared with carvone (e.g., Films 1-7 for diacetyl have a solubility almost four times higher than films 8a-10 - for carvone - see Table 2). Figure 5 shows three different calculations carried out by changing the solubility of diacetyl and water in comparison with the original calculations, referred as base case.

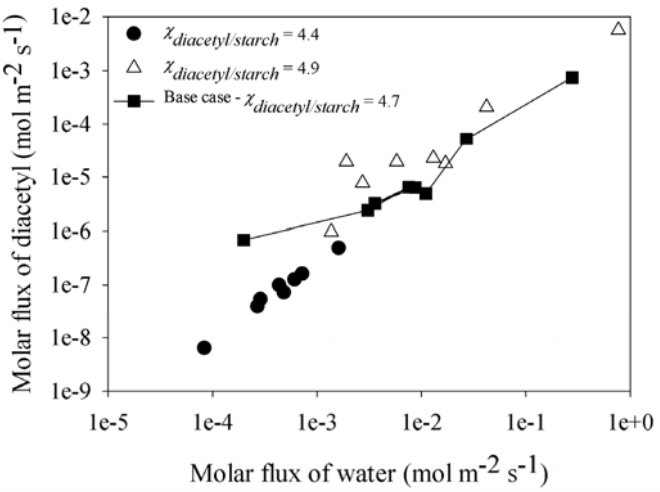

Figure 5. *Solubility effect on flux estimations.*

If the starch films are modified to be more hydrophobic (i.e., solubility of water decreases and solubility of hydrophobic compound increases), the resulting FH interaction

parameter for diacetyl decreases (simulation refers as χ_{1M} = 4.4) and the flux of water and diacetyl also decreases. In contrast, if the films are more hydrophilic (i.e., solubility of water increases and solubility of hydrophobic compound decreases), resulting in a higher FH interaction (i.e., χ_{1M} = 4.9), the flux of water and diacetyl increase. Therefore, the hydrophobicity of the film determines the degree of swelling, which has a direct influence on the flux of the diffusive species. Starch-based films are very hydrophilic and have a sorption capacity that increases with the water concentration. This sorption capacity is observed with the proportional increase of the diacetyl/carvone flux with the water concentration. As a result, the increment in the flux of the volatile component is the direct result of sorption effects, not by the flux coupling as their concentration are very low. This explanation is consistent with the assumption of negligible flux coupling between the species in their diffusion through the films. It should be noticed that having no coupling does not mean that a component in the mixture does not affect the flux of the other components. A component can affect the flux of the other components through sorption effects (Schaetzel et al., 2004).

In brief, the contra intuitive results obtained after change the hydrophobicity of the films show that swelling is more important that solubility. Therefore, to reduce the permeability, one should decrease the hydrophilicity of the matrix; even thought this will somewhat increase the sorption of the permeant species; it will reduce the swelling of the matrix.

In the case it is not possible to modify the starch, the inclusion of an additional phase with for example a more hydrophobic character, might be an option to influence the rate of permeation.

7. Conclusion

The present model coupling FV, FH and MS, was found to be adequate for the quantitative description of permeation fluxes of volatile trace components (diacetyl and carvone) and water through polymeric films. The permeation of diacetyl and carvone through starch films is dominated by swelling, i.e., permeability is mostly easily changed by changing the interaction with water. In consequence, the diffusion process of a particular volatile compound in trace concentration can be manipulated decreasing the degree of plastization of the film or via chemical or physical reduction of the hydrophilicity of starch. Even thought the absolute sorption of the trace component will be larger, the lower (equilibrium) moisture contain will result in a significantly lower permeation rate of the trace component.

Acknowledgements

The authors would like to thank the Carbohydrate Research Center Wageningen for financial support.

Nomenclature

List of symbols

A	Avogadro constant	mol^{-1}
a	activity	-
c_T	total molar concentration	$mol\ m^{-3}$
d	molecular diameter	m
$Đ$	Maxwell-Stefan diffusivity	$m^2\ s^{-1}$
G	Gibbs free energy	$J\ mol^{-1}$
k	Boltzmann constant	$J\ K^{-1}$
MW	molecular weight	$kg\ mol^{-1}$
N	molar flux	$mol\ m^{-2}\ s^{-1}$
n	number of moles	-
P	pressure	Pa
R	gas constant	$J\ mol^{-1}\ K^{-1}$
T	temperature	K
V	volume of pure component	$m^3\ mol^{-1}$
$V^\bullet$	minimum (compressed) volume	$m^3\ mol^{-1}$
V_c	critical volume	$m^3\ mol^{-1}$
V_F	free volume	m^3
χ	Flory-Huggins interaction parameter	-
x	molar fraction	-
x^m	mass fraction	-

Greek letter

ϕ	volume fraction	-
η	viscosity	Pa s
σ	surface fraction	-
$\rho^\bullet$	maximum (compressed) density	$kg\ m^{-3}$
ξ	friction coefficients	$(N\ mol^{-1})/(m\ s^{-1})$
μ	chemical potential	$J\ mol^{-1}$

Subscripts

i, j, k	numbering of components (general)
1, 2, 3, *M*	numbering of components (specific)
eff	effective value
0	initial side of the film
e	final side of the film

References

1. Fornasiero, F., Krull, F., Prausnitz, J.M., & Radke, C.J. (2005a). Steady-state diffusion of water through soft-contact-lens materials. *Biomaterials*, 26(28), 5704-5716.
2. Fornasiero, F., Prausnitz, J.M., & Radke, C.J. (2005b). Multicomponent diffusion in highly asymmetric systems. An extended maxwell-stefan model for starkly different-sized, segment-accessible chain molecules. *Macromolecules*, 38(4), 1364-1370.
3. Heintz, A. & Stephan, W. (1994). A generalized solution-diffusion model of the pervaporation process through composite membranes part II. Concentration polarization, coupled diffusion and the influence of the porous support layer. *Journal of Membrane Science*, 89(1-2), 153-169.
4. Kumar, M.N.V.R. & Kumar, N. (2001). Polymeric controlled drug-delivery systems: Perspective issues and opportunities. *Drug Development and Industrial Pharmacy*, 27 (1), 1-30.
5. Paul, D.R. (2004). Reformulation of the solution-diffusion theory of reverse osmosis. *Journal of Membrane Science*, 241(2), 371-386.
6. Schaetzel, P., Bendjama, Z., Vauclair, C., & Nguyen, Q.T. (2001). Ideal and non-ideal diffusion through polymers: Application to pervaporation. *Journal of Membrane Science*, 191(1-2), 95-102.
7. Schaetzel, P., Vauclair, C., Nguyen, Q.T., & Bouzerar, R. (2004). A simplified solution-diffusion theory in pervaporation: the total solvent volume fraction model. *Journal of Membrane Science*, 244(1-2), 117-127.
8. Seuvre, A.M., Philippe, E., Rochard, S., & Voilley, A. (2006). Retention of aroma compounds in food matrices of similar rheological behaviour and different compositions. *Food Chemistry*, 96(1), 104-114.

9. Stading, M., Rindlav-Westling, A., & Gatenholm, P. (2001). Humidity-induced structural transitions in amylose and amylopectin films. *Carbohydrate Polymers*, 45(3), 209-217.
10. Taylor, R. & Krishna, R. (1993). *Multicomponent mass transfer*. New York, USA: John Wiley & Sons.
11. Van den Berg, C. (1981). *Vapor sorption equilibria and other water-starch interactions: A physicochemical approach*. PhD thesis, Agricultural University of Wageningen, Wageningen, The Netherlands.
12. Wang, B.G., Yamaguchi, T., & Nakao, S.I. (2001). Prediction of solvent solubility, diffusivity and permeability in glassy polymeric membranes. *Polymer*, 42(12), 5225-5232.
13. Weast, R.C. (1973). *CRC handbook of chemistry and physics* (54th edition). Cleveland, OH: CRC Press.
14. Wesselingh, J.A. & Bollen, A.M. (1997). Multicomponent diffusivities from the free volume theory. *Chemical Engineering Research and Design*, 75(6), 590-602.
15. Wesselingh, J.A. & Krishna, R. (2000). *Mass transfer in multicomponent mixtures*. Delft, The Netherlands: Delft University Press.
16. Yilmaz, G., Van Dijk, C., Jongboom, R.O.J., Feil, H., & Hennink, W.E. (2004). Permeation of volatile compounds through starch films. *Biomacromolecules*, 5(2), 650-656.

On the applicability of Flory-Huggins theory to ternary starch-water-solute systems

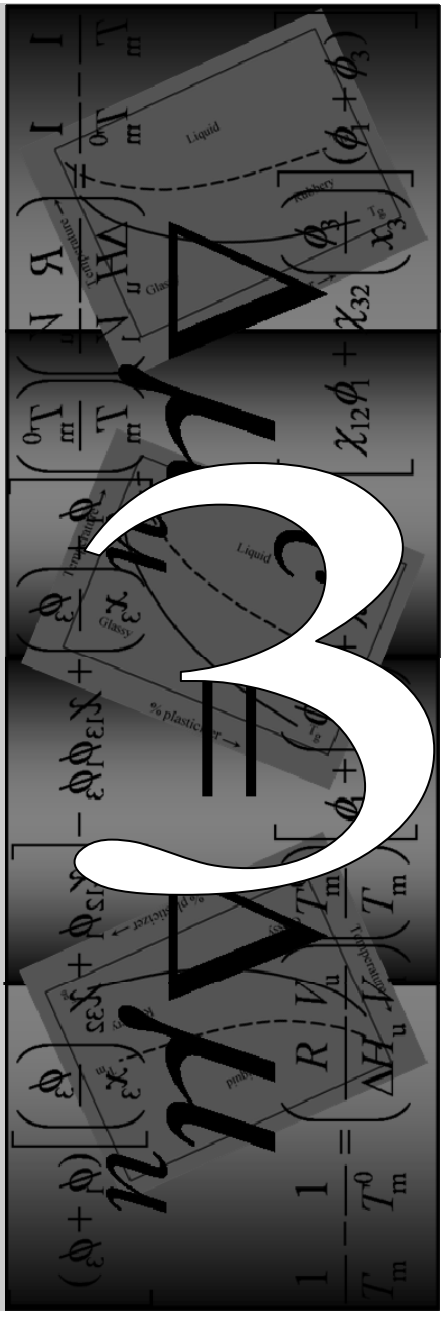

This chapter has been published as: Habeych, E., Guo, X., Van Soest, J.J.G., Van der Goot, A.J., & Boom, R. **(2009)**. On the applicability of Flory-Huggins theory to ternary starch-water-solute systems. *Carbohydrate Polymers*, 77(4), 703-712.

Abstract

The effects of glucose and glycerol on gelatinization of highly concentrated starch mixtures were investigated with wide-angle X-ray scattering and differential scanning calorimetry. The gelatinization/melting of starch was found to be a two step process. In the first step the granule swells at low temperatures (i.e., 30-50 °C), which is followed by a solvent-temperature cooperative step that induces loss of crystallinity. The results were interpreted with an extended form of the adapted Flory equation. The values of the model parameters (T_m^0, ΔH_u, χ_{12}, χ_{13}, and χ_{32}) obtained were similar to the values reported in the literature. Ternary phase diagrams were constructed with melting lines representing fully gelatinized starch. The crystalline region of starch with glucose was larger than with glycerol. This could be understood from the differences in χ_{13} (solute-solvent interaction). The extended form of Flory-Huggins model somewhat under predicts the experimental values of the gelatinization process. Comparing the Flory-Huggins model with experiments led to the conclusion that Flory equation is a useful tool to interpret and predict the gelatinization and melting behaviour of ternary starch-based systems. But the experiments are complex, the systems are often not in true equilibrium and other disturbing effects are easily encountered. Therefore, one should be cautious in the translation of experimental results to the thermodynamics of gelatinization in multicomponent systems.

1. Introduction

Starch is one of the most common and available biopolymers. Starch is used as a food ingredient and as raw material for biodegradable plastics (Rouilly & Rigal, 2002). Granular starch is a partially crystalline, granular solid (i.e., 15–39% crystallinity) (Jenkins & Donald, 1998; Slade & Levine, 1987). It consists of approximately 25% w/w linear amylose and 75% w/w branched amylopectin, which are based on chains of (1→4)-linked α-D-glucose (Imberty et al., 1991). When starch is heated above a certain temperature in the presence of excess water (>66% w/w), it undergoes an irreversible order–disorder transition, which is identified as gelatinization (Ratnayake & Jackson, 2007). On the other hand, this transition is known as melting of starch in case of low water conditions. During gelatinization or melting, various changes occur in the starch granules: loss of order, swelling, exudation of amylose, granule disruption, and increased viscosity (Ratnayake & Jackson, 2007; Sopade, Halley & Junming, 2004).

Gelatinization and melting often take place in mixtures containing low-molecular-weight solutes. For example, starch-based plastic materials, known as thermoplastic starch (TPS), are usually produced below the excess of water in the presence of plasticizers such as glycerol using heat and shear (Van Soest et al., 1996a). In the food industry, starch is often gelatinized in mixtures containing sugars, for example in the production of candies, snacks, breakfast cereals, baked goods, and ready-to-eat foods (Eliasson, 2004). Many authors have shown the strong influence of low-molecular-weight solutes on depressing the glass transition temperature, plasticizing the material, and modifying its mechanical properties (Myllarinen, et al., 2002; Nashed et al., 2003; Rodriguez-Gonzalez et al., 2004; Sopade et al., 2004). Moreover, low-molecular-weight solutes affect the melting and gelatinization temperatures (Lelievre, 1976; Nashed et al., 2003; Perry & Donald, 2002; Smits et al., 2003; Tan et al., 2004; Van Soest et al., 1994; 1996b; Van Soest & Knooren, 1997).

To understand and quantify the effect of the plasticizer on the gelatinization and melting of starch from a theoretical point of view, we propose to explore the use of an approach introduced earlier and inspired by (synthetic) polymer science. The analogies between synthetic polymers and biopolymers can be used to predict the functional properties of biopolymers during processing and storage with well-established theories from the field of synthetic polymers. For example, the structure of starch granules shows some similarities to that of the spherulites formed in crystalline synthetic polymers. The Flory-Huggins theory is often used to describe crystalline-amorphous phase transitions in polymer–diluent mixtures, and to study the effect of water and solutes on gelatinization and melting of starch

granules (Baks et al., 2007; Donovan, 1979; Donovan & Mapes 1980; Donovan et al., 1983; Farhat & Blanshard, 1998; Lelievre, 1976; Moates et al., 1998; Parker & Ring, 2001; Russell, 1987; Van den Berg, 1981; Whittam et al., 1990). In spite of the non-equilibrium nature of starch gelatinization (Slade & Levine, 1987), the Flory-Huggins theory applied to the crystalline melting of starch seems important as a means to describe and quantify the effect of low-molecular-weight components in starch gelatinization (Farhat & Blanshard, 1998). Several authors have used the Flory-Huggins theory to model phase diagrams in ternary systems: acetone-cellulose acetate-water (Altena & Smolders, 1982), dioxane-cellulose acetate-water (Altena et al., 1986), water-dextran-ethanol (Neuchl & Mersmann, 1995), water-dextran-agarose (Clark, 2000), among others.

Most literature uses the standard form of the Flory-Huggins theory developed for semi-crystalline polymers. However, a number of starch properties differ from those crystalline polymers; for example, starch contains a large fraction of amorphous material in addition to the crystalline component. Therefore, a distinction between the original amorphous and crystalline fractions is suggested (Whittam et al., 1990). In addition, inclusion of the temperature dependency of the heat of fusion of the polymer repeat unit and the Flory-Huggins interaction parameters improves the predictions. Recently, Baks et al. (2007) reported a first attempt with some of these modifications included. The authors adapted the Flory-Huggins equation to provide a quantitative description of the degree of starch gelatinization in the binary water–starch system as a function of the starch–water ratio and the temperature.

This chapter extends the approach of Baks et al. (2007) to three-component systems (water–starch–solute). An extended form of the Flory-Huggins theory is used to analyze the effect of a low-molecular-weight solute on the gelatinization and the melting of starch mixture, to provide a quantitative description of the dependence of the degree of starch gelatinization on the starch–water–solute composition and the temperature. Since the purpose of this study is to monitor the extent of the gelatinization process at different stages, we made use of offline measurements. The advantages of this approach are that different techniques (i.e., DSC, WAXS, etc) can be applied to stable materials and kinetics effects can be suppressed.

2. Flory-Huggins theory of melting in polymers

The Flory-Huggins model can be used to describe the equilibrium between a crystalline polymer and a solution of polymer in solvent at temperature T (Flory, 1964). Defining water as component 1, the polymer as component 2, and the low-molecular-weight solute as component 3, the Flory-Huggins model applied to a tertiary system in equilibrium can be expressed as follows:

$$\frac{1}{T_{\mathrm{m}}}-\frac{1}{T_{\mathrm{m}}^{0}}=\left(\frac{R}{\Delta H_{\mathrm{u}}}\frac{V_{\mathrm{u}}}{V_{1}}\right)\left[\phi_{1}+\left(\frac{\phi_{3}}{x_{3}}\right)+\chi_{13}\phi_{1}\phi_{3}-\left[\chi_{12}\phi_{1}+\chi_{32}\left(\frac{\phi_{3}}{x_{3}}\right)\right](\phi_{1}+\phi_{3})\right], \qquad (1)$$

where ΔH_{u} is the heat of fusion of a polymer repeat unit, T is the absolute temperature, T_{m}^{0} is the melting temperature of pure polymer, R is the gas constant, V_1 and V_{u} are the molar volumes of the diluents and the repeating unit of the polymer; ϕ_1, ϕ_2, and ϕ_3 are the volume fractions; x_3 is the number of segments per molecule of solute, and χ_{12}, χ_{13}, and χ_{32} are the (enthalpic) interaction parameters. The values of the interaction parameters are assumed to be independent of the composition. Eq. (1) was derived assuming that ΔH and ΔS, in the thermodynamic relation $\Delta G=\Delta H-T\Delta S$, are constant with temperature, and equal to ΔH_{u} and $\Delta H_{\mathrm{u}}/T_{\mathrm{m}}^{0}$, respectively. However, ΔH and ΔS are expected to depend on temperature (Hoffman, 1958). Therefore, we included a correction based on Hoffman's approximation (Hoffman, 1958):

$$\frac{1}{T_{\mathrm{m}}}-\frac{1}{T_{\mathrm{m}}^{0}}=\left(\frac{R}{\Delta H_{\mathrm{u}}}\frac{V_{\mathrm{u}}}{V_{1}}\right)\left(\frac{T_{\mathrm{m}}^{0}}{T_{\mathrm{m}}}\right)\left[\phi_{1}+\left(\frac{\phi_{3}}{x_{3}}\right)+\chi_{13}\phi_{1}\phi_{3}-\left[\chi_{12}\phi_{1}+\chi_{32}\left(\frac{\phi_{3}}{x_{3}}\right)\right](\phi_{1}+\phi_{3})\right], \qquad (2)$$

The resulting expression relates the melting temperature to the composition of the liquid surrounding the crystals. This can be rewritten as:

$$T_{\mathrm{m}}=T_{\mathrm{m}}^{0}-\left(\frac{R}{\Delta H_{\mathrm{u}}}\frac{V_{\mathrm{u}}}{V_{1}}\right)(T_{\mathrm{m}}^{0})^{2}\left[\phi_{1}+\left(\frac{\phi_{3}}{x_{3}}\right)+\chi_{13}\phi_{1}\phi_{3}-\left[\chi_{12}\phi_{1}+\chi_{32}\left(\frac{\phi_{3}}{x_{3}}\right)\right](\phi_{1}+\phi_{3})\right], \qquad (3)$$

We can now derive a relation for the dependence of the degree of crystallization as a function of the temperature. Following a similar procedure to that proposed earlier by Baks et al. (2007) but extended to three components, we define:

- The degree of starch crystallinity (α_{c}):

$$\alpha_{\mathrm{c}}=\frac{v_{2}^{\mathrm{c}}}{v_{2}^{\mathrm{a}}+v_{2}^{\mathrm{c}}} \quad \text{or} \quad v_{2}^{\mathrm{a}}=(v_{2}^{\mathrm{a}}+v_{2}^{\mathrm{c}})(1-\alpha_{\mathrm{c}}), \qquad (4)$$

where v_2^a and v_2^c are the volume of the amorphous and crystalline parts of starch, respectively.

- The volume fractions of the solvent (1) and solute (3) in the amorphous part of the system (ϕ_1, ϕ_3) are:

$$\phi_1 = \frac{v_1}{v_1 + v_2^a + v_3}, \tag{5a}$$

$$\phi_3 = \frac{v_3}{v_1 + v_2^a + v_3}, \tag{5b}$$

where v_1 and v_3 are the volume occupied by the solvent and solute, respectively.

- The overall volume fraction of the solvent and solute (ϕ_1^T , ϕ_3^T) are:

$$\phi_1^T = \frac{v_1}{v_1 + v_2^a + v_2^c + v_3}, \tag{6a}$$

$$\phi_3^T = \frac{v_3}{v_1 + v_2^a + v_2^c + v_3}, \tag{6b}$$

By substituting Eq. (4) into Eq. (5a), dividing the denominator and numerator by $v_1 + v_2^a + v_2^c + v_3$, then substituting Eqs. (6a) and (6b), and using $\phi_3^T = 1 - \phi_1^T - \phi_2^T$, we obtain:

$$\phi_1 = \frac{\phi_1^T}{1 - \phi_2^T \alpha_c}, \tag{7a}$$

Analogously, combining Eqs. (4), (5b), (6a), and (6b), gives:

$$\phi_3 = \frac{1 - \phi_1^T - \phi_2^T}{1 - \phi_2^T \alpha_c}, \tag{7b}$$

Substituting Eqs. (7a) and (7b) into (Eq. 3) gives:

$$T_m = T_m^0 - \left(\frac{R}{\Delta H_u}\frac{V_u}{V_1}\right)\left(T_m^0\right)^2\left(\left(\frac{\phi_1^T}{1-\phi_2^T\alpha_c}\right) + \left(\frac{1}{x_3}\right)\left(\frac{1-\phi_1^T-\phi_2^T}{1-\phi_2^T\alpha_c}\right) + \chi_{13}\left(\frac{\phi_1^T}{1-\phi_2^T\alpha_c}\right)\left(\frac{1-\phi_1^T-\phi_2^T}{1-\phi_2^T\alpha_c}\right) - \ldots \right.$$
$$\left. \ldots - \left[\chi_{12}\left(\frac{\phi_1^T}{1-\phi_2^T\alpha_c}\right) + \frac{\chi_{32}}{x_3}\left(\frac{1-\phi_1^T-\phi_2^T}{1-\phi_2^T\alpha_c}\right)\right]\left(\frac{\phi_1^T}{1-\phi_2^T\alpha_c} + \frac{1-\phi_1^T-\phi_2^T}{1-\phi_2^T\alpha_c}\right)\right), \tag{8}$$

If we assume that the non-crystalline fraction of starch is an inert component in the system, we can state that the amount of crystallinity far below the gelatinization/melting temperature represents 100% crystallinity. Therefore, the relative crystallinity can be used

instead of the degree of crystallinity (Baks et al., 2007). Thus, α_c can be replaced by 1-DG, where DG stands for the degree of gelatinization/melting. The resulting expression is:

$$T_m = T_m^0 - \left(\frac{R}{\Delta H_u}\frac{V_u}{V_1}\right)\left(T_m^0\right)^2 \cdot \ldots$$
$$\ldots \cdot \left(\left(\frac{\phi_1^T}{1-\phi_2^T(1-DG)}\right) + \left(\frac{1}{x_3}\right)\left(\frac{1-\phi_1^T-\phi_2^T}{1-\phi_2^T(1-DG)}\right) + \chi_{13}\left(\frac{\phi_1^T}{1-\phi_2^T(1-DG)}\right)\left(\frac{1-\phi_1^T-\phi_2^T}{1-\phi_2^T(1-DG)}\right) - \ldots \right. \quad (9)$$
$$\left. \ldots - \left[\chi_{12}\left(\frac{\phi_1^T}{1-\phi_2^T(1-DG)}\right) + \frac{\chi_{32}}{x_3}\left(\frac{1-\phi_1^T-\phi_2^T}{1-\phi_2^T(1-DG)}\right)\right]\left(\frac{\phi_1^T}{1-\phi_2^T(1-DG)} + \frac{1-\phi_1^T-\phi_2^T}{1-\phi_2^T(1-DG)}\right)\right)$$

Eq. (9) describes the relationship between the melting temperature, the total concentration of plasticizer, and the degree of gelatinization of starch in a starch-water-solute system.

3. Experimental section

3.1 Materials

Native wheat starch (<12% H_2O) (S5127) and D-glucose (<0.5% H_2O) (G7528) were purchased from Sigma-Aldrich (Steinheim, Germany). Glycerol (<0.1% H_2O) was obtained from Acros Organics (Geel, Belgium). The moisture content of the most important powder materials was determined using an infrared heating balance (Sartorius MA30 Moisture Balance) heated to 130 °C. The water content of the starch, glucose, and glycerol was taken into account in all experiments.

Known amounts of native wheat starch, water, and solute (i.e., glycerol or glucose) were prepared and thoroughly mixed manually with a spatula before equilibration for at least 12 h at room temperature. The composition of the mixtures and the range of the treatment temperature are presented in Table 1. In addition, a 60% w/w starch-water mixture was prepared to compare with the ternary mixtures and the literature data.

3.2 Compression molding

Compression molding was used to investigate the effect of the solute during the gelatinization of starch, which leads to a reduction in starch crystallinity according to the compression molding conditions. To obtain the heat-treated sample, 30 g of the starch-water-solute mixture were put into the mold, which consisted of three stainless steel plates (300×350 mm^2). The upper and lower plates were 4 mm thick. The middle plate had a

rectangular hole (150×100×1 mm^3), into which the mixture was placed. The samples were covered with plastic overhead transparencies (printable grade) on both sides of the middle plate to facilitate removal of the sample from the mold. The mold was then placed in a hydraulic PHI press (City of Industry, California). The mold was heated to the desired temperature at a rate of 10 °C min^{-1}, and a pressure of 0.86 MPa was applied. After heating, the starch mixture was compressed at the set temperature for an additional 45 minutes. The mold was cooled to room temperature at a cooling rate of 10–15 °C min^{-1}, and the material was then released from the mold.

Table 1. *Summary of thermal treatment and composition of the water, starch, and solute mixtures*

Starch:water ratio	Water (% w/w)	Starch (% w/w)	Glucose (% w/w)	Glycerol (% w/w)	Thermal treatment (°C)
3:2	40	60	-	-	30, 40, 50, 60, 70, 80,90,100, 110, 120
2:1	30	60	10	-	30, 40, 50, 70, 83, 90,100, 110, 120, 130, 140, 150
	26	50	24	-	30, 40, 50, 70, 83, 100, 120, 130, 140, 150
	20	40	40	-	70, 83, 90, 100, 110, 120, 130, 140, 150
3:1	17	60	-	23	30, 40, 50, 60, 70, 80, 83, 90, 100, 110, 120, 130, 140, 150
2:1	26	50	-	24	30, 40, 50, 60, 70, 80, 83, 90, 100, 110, 120, 130, 140, 150
	20	40	-	40	70, 83, 100, 120, 130, 140,150

3.3 Handling of samples

To minimize re-crystallization, samples taken from the compression molder were immediately transferred to a vessel containing liquid nitrogen and stored at –80 °C until further use.

After storage, the samples were freeze-dried in a Christ Epsilon 2-6D freeze-dryer (Osterode am Harz, Germany) prior to analysis. Freeze-drying was started at –20 °C and 1.03 mbar for 20 h followed by a second drying stage at –20 °C and 0.05 mbar for 20.5 h,

and a third drying stage –5 °C and 0.001 mbar for 29.5 h. The freeze-dried samples were ground in an analytical mill (type A10) from IKA (Staufen, Germany) to obtain a fine powder that dissolved easily. For comparison, each unprocessed starch-water-solute mixture was freeze-dried and ground under the same conditions described above.

3.4 Wide-angle X-ray scattering (WAXS)

Diffractograms were recorded with a Philips PC-APD diffractometer. The scattered X-ray radiation was recorded by a proportional moving detector over a 4° and 40° (2θ) angular range with an angular scanning velocity of 1.2° min^{-1} and with a measurement frequency of 1 s^{-1}. The Cu Ka radiation from the anode operating at 40 kV and 50 mA was monochromated using a 15-mm thick Ni foil. The diffractograms were smoothed with the computer program Table Curve 2D (Jandel Scientific, 1994, version 2.0, San Rafael, USA) by applying Savitsky-Golay data smoothing (5% smoothing). The procedure of (Van Soest et al., 1995) was used to determine the relative crystallinity. For wheat starch, the characteristic peak at 2θ=22.9° was selected. A straight line was used to approach the baseline below the characteristic peak. Following the procedure described by Baks et al. (2007), the height of the characteristic peak (H_t), and the total height of the characteristic peak minus the height of the baseline at the diffraction angle at 2θ=22.9° (H_c) were measured. The ratio $R_H=H_c/H_t$ was obtained for native wheat starch (100% relative crystallinity). The relative crystallinity of a sample based on peak heights (X_{rH}) was determined using the following equation:

$$X_{\mathrm{rH}} = \frac{(R_{\mathrm{H}})_{\mathrm{s}}}{(R_{\mathrm{H}})_{\mathrm{n}}}, \tag{10}$$

where the indices s and n indicate sample and native wheat starch, respectively. The relative crystallinity was used as a measure for the degree of gelatinization/melting by applying the following equation:

$$\mathrm{DG} = 1 - X_{\mathrm{rH}}, \tag{11}$$

3.5 Differential scanning calorimetry (DSC)

Freeze-dried starch samples (5 mg) with 50 µl of Milli-Q water (i.e., ≈10% w/w starch–solute mixture) were hermetically sealed in stainless steel DSC pans (60 µl). The mixtures were left overnight to equilibrate the starch–water–solute mixture. Next, the samples were scanned against a blank (empty pan) using a Perkin Elmer Diamond DSC (Perkin-Elmer Co., Norwalk, CT). Before the actual measurement, the samples were held at 0 °C for 5 min

in the DSC measuring cell. Subsequently, the sample was heated at 10 °C min^{-1} from 0 °C to 150 °C. The raw data were processed with Pyris version 8.0 (Perkin-Elmer Co., Norwalk, CT) to obtain the enthalpy changes needed to gelatinize the crystalline part of the starch in the sample (ΔH_s). For simplicity we will use enthalpy to refer to the change of enthalpy. The characteristic gelatinization endotherms obtained were corrected for the amount of solvent and solute present in the sample after the freeze-drying step. Using the gelatinization enthalpy of dried native wheat starch (ΔH_n), the degree of gelatinization/melting of the sample was determined:

$$DG = 1 - \frac{\Delta H_s}{\Delta H_n}, \tag{12}$$

To eliminate any thermal effect on the gelatinization enthalpy of native wheat, untreated starch-water-solute mixtures were freeze-dried, re-suspended in approximately 10% w/w water, and analyzed. For each starch–water–solute mixture at least two independent DSC traces were recorded. The average DSC enthalpies of each starch-water-solute mixtures were used as reference for the estimation of DG.

3.6 Finding model parameter values

Eq. (9) was used to calculate the melting temperature as a function of the degree of gelatinization/melting, starch concentration, and the total concentration of plasticizers. The results from the model were compared to the experimental data in the temperature range 60–140 °C using Mathcad (Parametric Technology Corporation, version 14.0, USA). The partial molar volumes were 18.1 cm^3 mol^{-1} for water (Baks et al., 2007), 97.5 cm^3 mol^{-1} for wheat starch (Shahidi et al., 1976), 112.2 cm^3 mol^{-1} for glucose (Shahidi et al., 1976), and 73.0 cm^3 mol^{-1} for glycerol (Habeych et al., 2007), respectively. It was assumed that these partial molar volumes are constant and do not depend on temperature. In addition, it was assumed that the densities of the crystalline and the amorphous wheat starch are equal. Two interaction parameters (χ_{13} and χ_{23}) were determined by minimizing the sum of the squared residuals.

4. Results

The gelatinization enthalpies obtained for each untreated starch-water-solute mixture are given in Table 2. The gelatinization enthalpy obtained for freeze-dried native wheat starch: 13.4±0.6 J g^{-1} (95% confidence interval) is in good agreement with the value reported elsewhere (Baks et al., 2007; Chiotelli & Le Meste, 2002; Ratnayake & Jackson, 2007). Moreover, average DSC enthalpies of the binary starch-water system treated at low

temperature (i.e., 30–50 ºC) increased from ~16.2 J g^{-1} at 30 °C to 18.1 J g^{-1} at 50 °C. Ratnayake and Jackson (2007) observed similar results in starch-water system. The authors explained this phenomenon due to the rearrangement of amylose in the amorphous domains of the starch granules. During the first part of the starch gelatinization/melting process, the water absorbed by the granules increases the mobility, especially of amylose, in the amorphous domains, leading to realignment and formation of new intermolecular bonds (Ratnayake & Jackson, 2007). Overall, it leads to an additional enthalpy bonus, which however is not directly related to crystallinity. We therefore took zero values for DG at low temperature in the fitting estimations. Furthermore, the addition of glycerol decreases the average DSC enthalpy of untreated samples especially for mixtures containing a high glycerol concentration (i.e., 40% w/w glycerol) (Table 2). Mixtures containing glucose did not show a statistically significant difference with only starch in water.

Table 2. *Enthalpy (ΔH) of the gelatinization or melting for different untreated freeze-dried water-starch-solute mixtures (i.e., 10% w/w starch-solute) determined by DSC measurements with a heating rate of 10 ºC* min^{-1} *(native wheat starch 13.4±0.6 J* g^{-1}*)*

Starch:water ratio	Glucose (% w/w)	Glycerol (% w/w)	ΔH (J g^{-1})[a]
2:1	10	-	13.4 ± 1.0[b]
	24	-	14.9 ± 0.9[b]
	40	-	12.4 ± 1.1[b]
3:1	-	23	12.8 ± 0.8[b]
2:1	-	24	11.2 ± 0.3[b]
	-	40	8.6 ± 1.9[b]

[a]Gelatinization enthalpy in J g^{-1} dry starch.

[b]95% confidence interval.

Figure 1 shows the most characteristic WAXS diffractograms obtained from each starch–water–solute mixture. WAXS data showed three crystal structures depending on the processing conditions and composition. The V_H ($2\theta \approx 19.8°$) and E_H ($2\theta \approx 18.5°$) type peaks are generally associated with the single helical amylose during processing and have been reported to appear after compression molding of wheat starch containing water and glycerol (Van Soest et al., 1996c). The relative crystallinity of wheat starch gradually decreased with the heat treatment starting at 30 ºC (see Figure 1). Similar results were reported by Ratnayake and Jackson (2007) for 6% w/v mixture of different starches heated in the range of 35 to 85 °C at 5 °C intervals for 30 min. In contrast, 26:50:24 water:starch:glycerol sample showed an opposite trend that agree with the DSC data collected for low temperate

treated samples (Figure 1-BII). Furthermore, WAXS for mixtures with 40% w/w glucose shown a overlapped signal with glucose and were therefore not use in the fitting procedure.

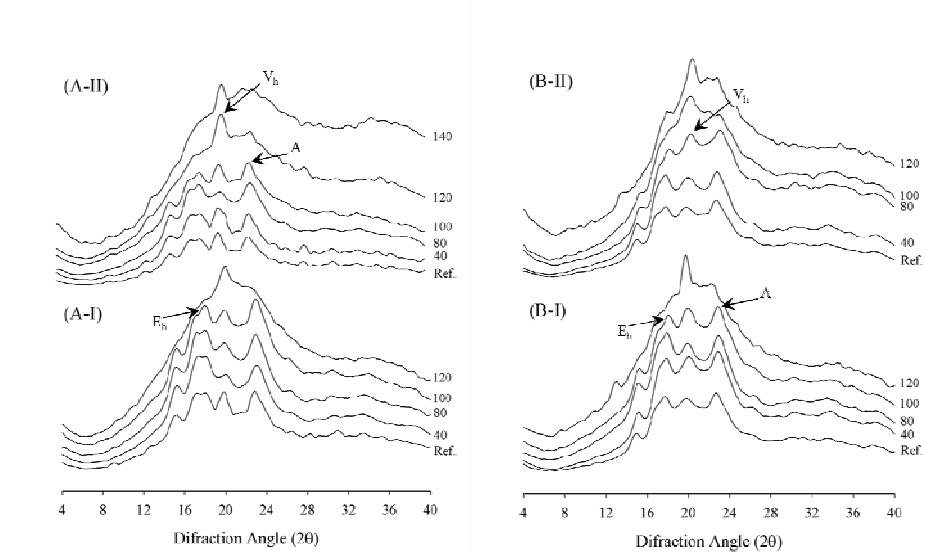

Figure 1. *WAXS from starch-water-solute samples treated at different temperatures. Water:starch:glucose: (A-I) 30:60:10, (A-II) 26:50:24. Water:starch:glycerol: (B-I) 17:60:23, (B-II) 26:50:24. Bottom: untreated native wheat starch. Numbers to the right of each profile represent the corresponding treatment temperature (°C).*

Figure 2 shows the degree of gelatinization of a starch-water-solute mixture obtained from WAXS and DSC measurements after various treatments at constant temperature for 45 min. The start and the end of the gelatinization/melting process used in the fitting procedure are marked with vertical lines. Within this range the DSC measurements yield a higher estimation of the gelatinization temperature than WAXS for mixtures containing glucose; for mixtures containing glycerol, DSC gave comparable results as WAXS. Furthermore, the temperature span of the gelatinization process (i.e., start to end) decreases by increasing the total amount of plasticizer.

Figure 2 compares the experimental values with those predicted by the model. The predicted and experimental values are close although there are some deviations at relatively large quantities of solute.

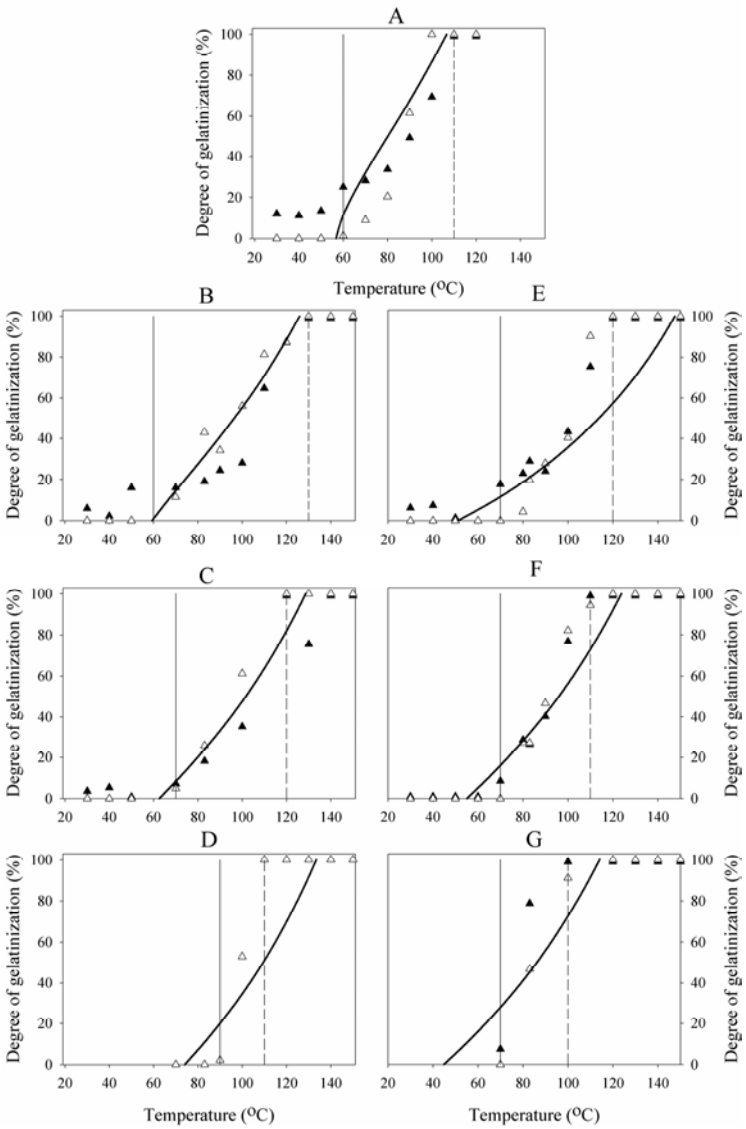

Figure 2. *Degree of gelatinization of starch as a function of the treatment temperature (treatment time 45 min). Solid line represents the model prediction, DSC data (Δ), and X-ray data (▲). (A) 60% w/w wheat starch-water mixture. Water:starch:glucose: (B) 30:60:10, (C) 26:50:24, (D) 20:40:40. Water:starch:glycerol: (E) 17:60:23, (F) 26:50:24, (G) 20:40:40. Vertical solid and dash line represent the onset and the end of the gelatinization process obtained during the isolation of the samples.*

In general, the modified Flory-Huggins equation used here somewhat under predicts the degree of gelatinization process and gave more accurate results when the solute concentrations were relatively low. Relative to the values obtained for the binary system (Figure 2A), the addition of solute at constant starch concentration shifted the end of the gelatinization curve (i.e., DG=100 %) upwards in temperature (see dash line Figures 2A, B, and E). This situation is observed for every starch:water ratio and has a direct relation with the molecular weight of the solute. The presence of glucose seems to shift the onset of the gelatinization/melting process (i.e., DG=0 %) to a higher temperature (see straight line Figures 2B–D), glycerol had a different effect: the onset gelatinization temperature now remains approximately constant at 70 °C (cf. Figures 2E-G).

Table 3 presents the predicted Flory-Huggins parameters obtained using the DSC and WAXS values. The starch-water interaction parameter (χ_{12}), the heat of fusion of the starch repeat unit (ΔH_u), and the melting temperature of pure polymer (T_m^0) were derived from the results obtained for the binary system (60% starch) in combination with data reported earlier (Baks et al., 2007). The values are within the confidence interval of those reported earlier. χ_{12} is in agreement with the value obtained by others using different methods of measurement (Lelievre, 1976; Moates et al., 1997), ΔH_u is quite close to the enthalpy of fusion of D-glucose, which has been reported to be around 30 kJ mol^{-1} (Moates et al., 1997). The value of T_m^0 is close to the value of 259.85 °C obtained by van den Berg (Van den Berg, 1981).

Table 3. *Flory-Huggins parameter relevant to water-starch-solute used by different authors*

System	ΔH_u (kJ mol^{-1})	T_m^0 (°C)	χ_{12} (–)	χ_{13} (–)	χ_{23} (–)	Reference
Water:starch	32.83	258.20	0.48	–	–	This article
Water:starch:glycerol	32.83	258.20	0.48	–0.21	–1.64	This article
Water:starch:glucose	32.83	258.20	0.48	0.30	–1.00	This article
Water:starch:glucose	25.12	221.85	0.50	0.50	0.00	(Lelievre, 1976)
Water:starch:glucose	22.00	262.85	0.57	0.74	–1.63	(Moates et al., 1998)
Water:starch:D-glucitol	22.00	262.85	0.57	0.74	–1.42	(Moates et al., 1998)

The interaction parameter between starch and the solute (χ_{23}) was found to be negative in both cases, indicating strong enthalpic interaction. Similar results were reported earlier for starch-glucose and starch-D-glucitol (polyol) (Moates et al., 1998). The interaction parameter between water and glucose (χ_{13}≈0.30) appeared to be slightly lower than the value obtained for starch-water (χ_{12}≈0.48) and the values reported earlier (χ_{13}≈0.5) (Baks et al., 2007; Lelievre, 1976; Van den Berg, 1981).

In order to evaluate the plasticizing capability of water, glycerol, and glucose; Eq. (3) can be rearranged to estimate the effect of each plasticizer on the change in melting temperature of starch (i.e., $T_m^0 - T_m$) as a function of the volume fraction of the plasticizers, as follows:

$$T_m^0 - T_m = \left[\left(T_m^0\right)^2 \frac{R}{\Delta H_u}\frac{V_u}{V_1}\right]\left[\phi_1 + \left(\frac{\phi_3}{x_3}\right) + \chi_{13}\phi_1\phi_3 - \chi_{32}\left(\frac{\phi_3}{x_3}\right)\left(\phi_1+\phi_3\right) - \chi_{12}\phi_1\left(\phi_1+\phi_3\right)\right], \quad (13)$$

Figure 3 shows the results of the simulation for the onset of melting (i.e., DG is 100%), which can be seen as a measure of the effectiveness as plasticizer of each molecule.

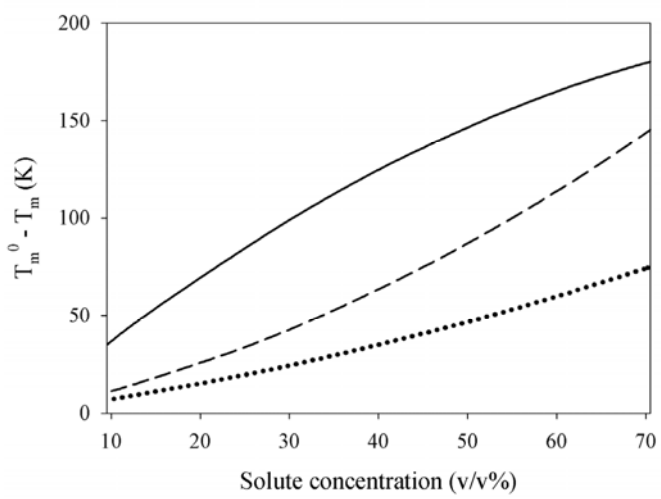

Figure 3. *Theoretical prediction of the effect of plasticizer concentration on the change in melting temperature. Solid line: water, dash line: glycerol, and dot line: glucose.*

From this figure one can see that water has the highest effectiveness in terms of change in melting temperature compared to glycerol and glucose with glycerol being more effective than glucose. The contributions of each term in the second bracket at the right side of the

Eq. (13) can be analyzed as well. In this equation the first and second terms arise from the entropy of mixing and the other three terms are related to the enthalpy of mixing and depend of the interaction parameters χ_{13}, χ_{32}, and χ_{12} (Lelievre, 1976; Moates et al., 1997).

Figure 4 shows the change in the magnitude of each term when 10% of the volume fraction of water is replaced by either glycerol or glucose. In both cases, the main contributions to the change in melting of starch come from Term 1 and Term 5, meaning that waters plays a major role in the equation because the entropy of mixing is given by water and the interaction between starch-water mainly. Replacing water for a larger molecule (i.e., glycerol or glucose) results in a lower entropy of mixing and hence, (as can be seen with the reduction in Term 1), leading to a smaller change in melting temperature of starch (Figure 3). In summary, the depression of starch gelatinization is mainly affected by the entropic (Term 1) and enthalpic (Term 5) contribution of water with little influence of the other terms.

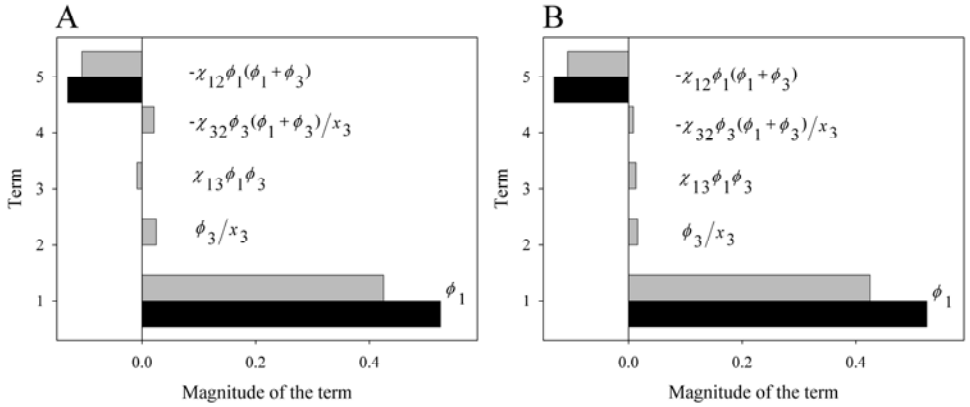

Figure 4. *Contributions of the four composition terms in Eq. (13) to the change in melting temperature in a 60% w/w starch-water mixture due to replacement of 10% v/v water by solute as predicted by the extended Flory-Huggins's theory. (A) Effect on glycerol addition. (B) Effect on glucose addition.*

5. Discussion

To study the gelatinization/melting process one can follow an on-line or an off-line approach (Cooke & Gidley, 1992). The on-line approach implies an on-line direct registration of the physical-chemical changes during gelatinization/melting by for example DSC, light scattering, and/or optical microscopy. In this study, we have used off-line

analysis to obtain detailed information on the crystalline order at different temperatures and water-starch-solute concentrations. During the off-line approach samples were isolated during gelatinization/melting and analyzed afterwards. The principal disadvantage of this approach is the possibility of structural changes during the isolation process, which probably explains a relatively large spread in WAXS and DSC data (Figure 2) but it allows much more extensive analysis. Nevertheless, an offline approach is the most appropriate to one obtained data where kinetic effects can be suppressed.

The DSC endothermic enthalpy values reflect both the loss of double-helical order and crystallinity. WAXS however only detects crystallinity (Cooke & Gidley, 1992). Cooke and Gidley (1992) found that the total amount of ordering is almost twice as large as the amount of crystallinity. This explains why DSC gives higher values for the loss of crystallinity compared to WAXS.

The results presented above show that the start and the end of the gelatinization/melting process depend on the amount and type of plasticizers. Compared to systems with only water, the presence of another solute during the gelatinization/melting process shifts the end of the gelatinization curve (i.e., DG=100 %) upwards in temperature. An increase in the total amount of plasticizers reduced the temperature span of gelatinization process. Therefore, this reduction of the temperature span of the gelatinization process gives a probe that what fundamentally matters is the properties of the mixture as a whole. Similar findings were reported earlier (Perry & Donald, 2000; 2002), who proposed a *solvent-temperature-time superposition* model envisaged in two steps. The first step was referred to as a swelling-driven step in which a minimum degree of plasticization is required to induce mobility in the granule. Thereafter, the combined action of solvent and temperature prompts the loss of crystallinity. Our results agree with this model: changes occurred prior to the gelatinization, as was observed with increase in enthalpy changes at low temperature. Furthermore, at higher temperatures the crystalline regions are disrupted due to the cooperative action of solvent and heat.

Strong enthalpic interactions were found between starch and the solutes glucose and glycerol ($\chi_{23}<0$). Previous work showed a strong exothermic peak during DSC measurements of dry starch in the presence of glycerol and sugars (Perry & Donald, 2000; Van Soest et al., 1996b). Van Soest et al. (1996b) attributed the exothermic peak to the stronger interaction between starch-glycerol compared to the starch-water interaction. Perry and Donald (2000) gave this a physical interpretation by suggesting that the exothermic

peak is indicative of reorganization in the crystalline lamellae. Before the ingress of the solvent, the lamellar and crystalline organization is imperfect. Due to solvent absorption, rearrangement of the crystalline lamella can occur giving an enthalpic bonus derived from crystallization. In addition, the diffusion of the solute in between the starch molecules takes time, but will be faster at higher temperatures. Therefore, at high solute concentration, the temperature to which the starch-solute mixture must be heated to obtain plasticization increases. In addition, higher molecular weight solutes will need much more time to penetrate into the starch granule, because they diffuse much more slowly in the granule matrix, and are less effective plasticizers due to their lower contribution to the entropy of mixing. In consequence, when only water acts as the solvent, it is proposed that hydration, plasticization and resulting lamellar arrangement crystallization occurs faster, while the effects of glucose and glycerol are slower and smaller (see Figure 2).

The Flory-Huggins model was developed for concentrated polymer mixtures (Lelievre, 1976; Moates et al., 1998). Therefore, it is not surprising that the (modified) Flory-Huggins equation shows some deviation at high solute concentration. Moreover, starch contains other components, such as lipids, which influence the behavior of the amylose and amylopectin by complex formation. A further additional problem is that starch is only partially crystalline; situation that is not included in the model. Finally, the initial plasticizing step previous to gelatinization is not taken into account in the model.

The applicability of the extended Flory-Huggins equations has pros and cons that should be taken into account before using it as a predictive tool. Figure 5 compares the binary model with the extended form for ternary systems. The extended form gives closer predictions even in the case of assuming a higher starch concentration as a result of the lower water availability due to the presence of the solute.

One can thus see from Figure 5 that the binary model does not improve the prediction and gives significant over prediction the onset (start) of the process. In addition, in spite of the many assumptions and simplifications made, the extended form can be interpreted physically, which has been proven to work well in ternary mixtures (Clark, 2000). Finally, the validity of the extended form of the Flory-Huggins equation allows to reduce the amount of experimental work, which is not possible with the binary model. However, the extended form of the model does require the finding of two additional parameters (i.e., χ_{13} and χ_{32}), which however do not contribute strongly to the prediction (Figure 4), and therefore might be estimated. The predictability decreases specially at high solute

concentration, so its applicability seems mainly in systems that are more concentrated in starch. In summary, the use of the extended form has some advantages that make it fair to consider in spite of the deviation obtained.

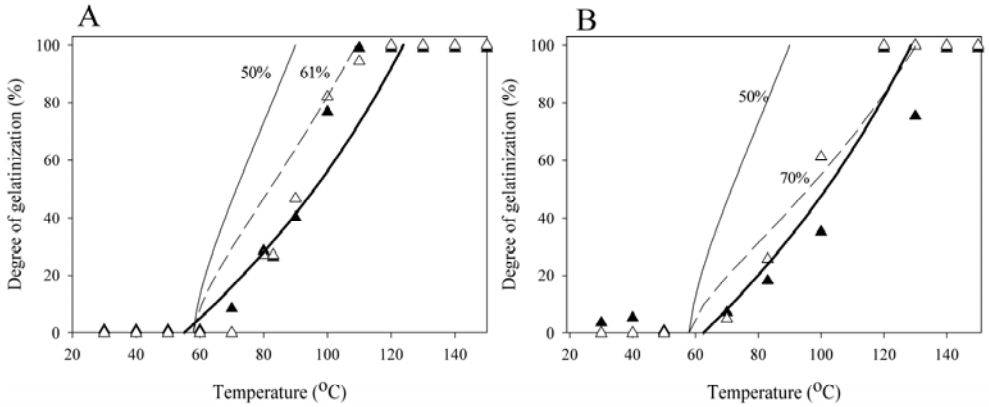

Figure 5. *Degree of gelatinization of starch as a function of the treatment temperature (treatment time 45 min). Solid bold line represents the model prediction using the extended model, percentage indicate the predicted value using the binary model, DSC data* (Δ)*, and X-ray data* (▲)*. (A) 26:50:24 water:starch:glycerol. (B) 26:50:24 water:starch:glucose.*

The Flory-Huggins theory applied to starch has a number of shortcomings. In the original theory, a solvent molecule was assumed to occupy the same volume as a monomer unit of the polymer. In the case of molecules with large size differences such as starch and water, this assumption is not true (Gustafsson et al., 1986). For polymers capable of hydrogen bonding with water, the inter-polymer H-bonds may be disrupted by replacement of these bonds by polymer-water H-bonds (Slade & Levine, 1987), leading to a large increase in molecular mobility. Many solvent molecules will interact with the monomeric unit making this interaction more complex than the pair-wise nearest-neighbor interactions assumed in the Flory-Huggins theory (Flory, 1964). Nevertheless, the application of this theory to uncharged biopolymer-water systems for the description of ternary diagrams has proven to be no worse than for synthetic polymer-solvent systems, and is sometimes even better (Clark, 2000). Obtaining the correct experimental equilibrium conditions and thereby the correct analytical data is difficult. For the case of stiff, high molecular weight polysaccharides, Clark (2000) stated that this is of greater importance than incorrect assumptions in the model.

In spite of the limitations outlined above, the Flory-Huggins theory can be used to derive ternary phase diagrams using the set of parameters obtained for the starch-water-solute system (see Table 3), and setting DG=100%, and Eqs. (7) and (9). Figures 6 and 7 show the solid–liquid transition phase diagrams for the starch-water-solute systems.

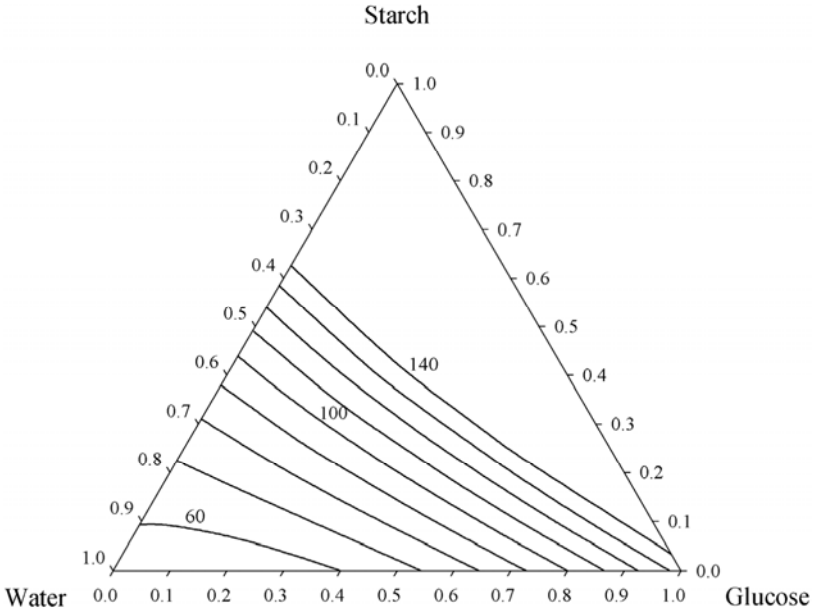

Figure 6. *Volumetric ternary phase diagram for the gelatinization/melting of the starch-water-glucose system. The solid lines refer to the corresponding predicted equilibrium gelatinization/melting isotherm. Numbers in the graph represent the corresponding isotherm in ascending order starting from T=60 ℃ to T=140 ℃.*

The curves represent the compositions at equilibrium with (pure starch) crystals at specific, indicated temperatures. Comparing Figure 6 with Figure 7, it can be seen that the starch-water-glycerol system shows a smaller crystallization region than starch-water-glucose, due to the stronger water-glycerol interaction and lower molar volume relative to water-glucose (see χ_{13} in Table 3). Since the extended form of the Flory-Huggins model under predicts the experimental values of the gelatinization process, the values reported in Figures 6 and 7 give a reasonable estimation of the amount of plasticizer and heat treatment required to obtain a fully gelatinized starch.

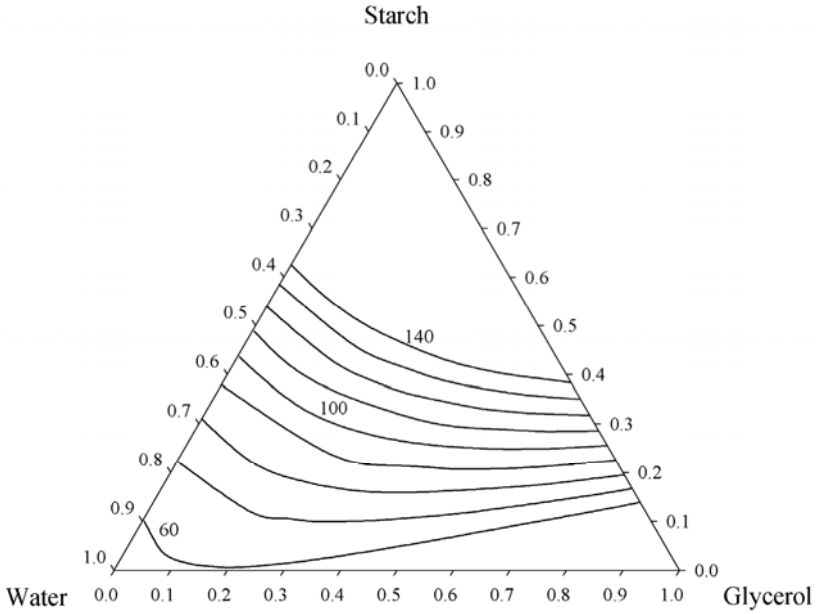

Figure 7. *Volumetric ternary phase diagram for the gelatinization/melting of the starch-water-glycerol system. The solid lines refer to the corresponding predicted equilibrium gelatinization/melting isotherm. Numbers in the graph represent the corresponding isotherm in ascending order starting from T=60 ℃ to T=140 ℃.*

6. Conclusion

The effects of glucose and glycerol on gelatinization/melting of highly concentrated starch mixtures were investigated with WAXS and DSC. The results suggest that the gelatinization/melting of starch can be envisaged in two steps, similar to the solvent-temperature-time superposition model proposed earlier (Perry & Donald, 2000; 2002). An adapted version of the Flory equation provided a quantitative description of the degree of starch gelatinization/melting as a function of the starch-water-solute ratio and temperature. The applicability of this extended model showed that it is useful to consider the theory as a mean to interpret and predict the gelatinization/melting behaviour of ternary starch-based systems. However, the theory does not capture all changes occurring in the ternary starch system.

Fitting the model to experimental data resulted in T_m^0, ΔH_u, χ_{12}, χ_{13}, and χ_{23} values that are reasonable and in agreement with values reported in the literature. The adapted Flory

equation can be used as a means to estimate the temperature that is needed to completely gelatinize starch in a starch-water mixture over the whole concentration range. Ternary phase diagrams were constructed with crystallization lines representing fully gelatinized starch. The crystalline region with glucose was larger than with glycerol. This could be understood from the differences in χ_{13} (solute-solvent interaction) and molar volumes.

Acknowledgments

The authors wish to thank Frans Kappen for his assistance with the compression molder, Dr. Guus Frissen for assistance with the X-ray measurements, Herman de Beukelaer for his assistance with the DSC measurements (all from the Agrotechnology and Food Sciences Group in Wageningen), and Dr. Tim Baks for the stimulating conversations over Flory-Huggins' model. This research was conducted within the framework of the Carbohydrate Research Centre at Wageningen.

References

1. Altena, F.W., Schroder, J.S., Van de Huls, R., & Smolders, C.A. (1986). Thermoreversible gelation of cellulose acetate solutions studied by differential scanning calorimetry. *Journal of Polymer Science, Part B: Polymer Physics, 24(8)*, 1725-1734.
2. Altena, F.W., & Smolders, C.A. (1982). Calculation of liquid-liquid phase separation in a ternary system of a polymer in a mixture of a solvent and a nonsolvent. *Macromolecules, 15(6)*, 1491-1497.
3. Baks, T., Ngene, I.S., Van Soest, J.J.G., Janssen, A.E.M., & Boom, R. M. (2007). Comparison of methods to determine the degree of gelatinisation for both high and low starch concentrations. *Carbohydrate Polymers, 67(4)*, 481-490.
4. Chiotelli, E. & Le Meste, M. (2002). Effect of small and large wheat starch granules on thermomechanical behavior of starch. *Cereal Chemistry, 79(2)*, 286-293.
5. Clark, A.H. (2000). Direct analysis of experimental tie line data (two polymer-one solvent systems) using Flory-Huggins theory. *Carbohydrate Polymers, 42(4)*, 337-351.
6. Cooke, D. & Gidley, M.J. (1992). Loss of crystalline and molecular order during starch gelatinisation: origin of the enthalpic transition. *Carbohydrate Research, 227*, 103-112.

7. Donovan, J.W. (1979). Phase transitions of the starch-water system. *Biopolymers*, *18(2)*, 263-275.
8. Donovan, J.W., Lorenz, K., & Kulp, K. (1983). Differential scanning calorimetry of heat-moisture treatment of starches. *Cereal Chemistry*, *60*, 381-387.
9. Donovan, J.W. & Mapes, C.J. (1980). Multiple phase transitions of starches and Nägeli amylodextrins. *Starch - Stärke*, *32(6)*, 190-193.
10. Eliasson, A.C. (2004). *Starch in food: Structure, function and applications*. Cambridge, England: Woodhead Publishing Ltd.
11. Farhat, I.A. & Blanshard, J.M.V. (1998). On the extrapolation of the melting temperature of dry starch from starch-water data using the Flory-Huggins equation. *Carbohydrate Polymers*, *34(4)*, 263-265.
12. Flory, P.J. (1964). *Principles of Polymer Chemistry*. Ithaca: Cornell University Press.
13. Gustafsson, A., Wennerstrom, H., & Tjerneld, F. (1986). The nature of phase separation in aqueous two-polymer systems. *Polymer*, *27(11)*, 1768-1770.
14. Habeych, E., Van der Goot, A., & Boom, R. (2007). Prediction of permeation fluxes of small volatile components through starch-based films. *Carbohydrate Polymers*, *68(3)*, 528-536.
15. Hoffman, J.D. (1958). Thermodynamic driving force in nucleation and growth processes. *Journal of Chemical Physics*, *29*, 1192-1193.
16. Imberty, A., Buleon, A., Tran, V., & Perez, S. (1991). Recent advances in knowledge of starch structure. *Starch - Stärke*, *43(10)*, 375-384.
17. Jenkins, P.J. & Donald, A.M. (1998). Gelatinisation of starch: a combined SAXS/WAXS/DSC and SANS study. *Carbohydrate Research*, *308(1-2)*, 133-147.
18. Lelievre, J. (1976). Theory of gelatinization in a starch-water-solute system. *Polymer*, *17(10)*, 854-858.
19. Moates, G.K., Noel, T.R., Parker, R., & Ring, S.G. (1997). The effect of chain length and solvent interactions on the dissolution of the B-type crystalline polymorph of amylose in water. *Carbohydrate Research*, *298(4)*, 327-333.
20. Moates, G.K., Parker, R., & Ring, S.G. (1998). Preferential solvent interactions and the dissolution of the B-type crystalline polymorph of starch in aqueous solutions. *Carbohydrate Research*, *313(3-4)*, 225-234.
21. Myllarinen, P., Partanen, R., Seppälä, J., & Forssell, P. (2002). Effect of glycerol on behaviour of amylose and amylopectin films. *Carbohydrate Polymers*, *50(4)*, 355-361.

22. Nashed, G., Rutgers, R.P.G., & Sopade, P.A. (2003). The plasticisation effect of glycerol and water on the gelatinisation of wheat starch. *Starch - Stärke, 55(3-4)*, 131-137.
23. Neuchl, C., & Mersmann, A. (1995). Fractionation of polydisperse dextran using ethanol. *Chemical Engineering Science, 50(6)*, 951-958.
24. Parker, R. & Ring, S.G. (2001). Aspects of the physical chemistry of starch. *Journal of Cereal Science, 34(1)*, 1-17.
25. Perry, P.A. & Donald, A.M. (2000). The role of plasticization in starch granule assembly. *Biomacromolecules, 1(3)*, 424-432.
26. Perry, P.A. & Donald, A.M. (2002). The effect of sugars on the gelatinisation of starch. *Carbohydrate Polymers, 49(2)*, 155-165.
27. Ratnayake, W.S. & Jackson, D.S. (2007). A new insight into the gelatinization process of native starches. *Carbohydrate Polymers, 67(4)*, 511-529.
28. Rodriguez-Gonzalez, F. J., Ramsay, B. A., & Favis, B. D. (2004). Rheological and thermal properties of thermoplastic starch with high glycerol content. *Carbohydrate Polymers, 58(2)*, 139-147.
29. Rouilly, A. & Rigal, L. (2002). Agro-materials: A bibliographic review. *Journal of Macromolecular Science - Polymer Reviews, 42(4)*, 441-479.
30. Russell, P.L. (1987). Gelatinization of starches of different amylose/amylopectin content. A study by differential scanning calorimetry. *Journal of Cereal Science, 6(2)*, 133-145.
31. Shahidi, F., Farrell, P.G., & Edward, J.T. (1976). Partial molar volumes of organic compounds in water. III. Carbohydrates. *Journal of Solution Chemistry, 5(12)*, 807-816.
32. Slade, L. & Levine, H. (1987). Recent advances in starch retrogradation. *Industrial Polysaccharides*, 387-430.
33. Smits, A.L.M., Kruiskamp, P.H., Van Soest, J.J.G., & Vliegenthart, J.F.G. (2003). Interaction between dry starch and plasticisers glycerol or ethylene glycol, measured by differential scanning calorimetry and solid state NMR spectroscopy. *Carbohydrate Polymers, 53(4)*, 409-416.
34. Sopade, P.A., Halley, P.J., & Junming, L.L. (2004). Gelatinisation of starch in mixtures of sugars. II. Application of differential scanning calorimetry. *Carbohydrate Polymers, 58(3)*, 311-321.
35. Tan, I., Wee, C.C., Sopade, P.A., & Halley, P.J. (2004). Investigation of the starch gelatinisation phenomena in water-glycerol systems: application of modulated

temperature differential scanning calorimetry. *Carbohydrate Polymers*, *58(2)*, 191-204.

36. Van den Berg, C. (1981). *Vapor sorption equilibria and other water-starch interactions: A physicochemical approach*. Wageningen, The Netherlands: Agricultural University of Wageningen.
37. Van Soest, J.J.G., Benes, K., De Wit, D., & Vliegenthart, J.F.G. (1996a). The influence of starch molecular mass on the properties of extruded thermoplastic starch. Polymer, 37(16), 3543-3552.
38. Van Soest, J.J.G., Bezemer, R.C., De Wit, D., & Vliegenthart, J.F.G. (1996b). Influence of glycerol on the melting of potato starch. *Industrial Crops and Products*, *5(1)*, 1-9.
39. Van Soest, J.J.G., de Wit, D., Tournois, H., & Vliegenthart, J.F.G. (1994). Influence of glycerol on structural changes in waxy maize starch as studied by Fourier transform infra-red spectroscopy. *Polymer*, *35(22)*, 4722-4727.
40. Van Soest, J.J.G., Hulleman, S.H.D., De Wit, D., & Vliegenthart, J.F.G. (1996c). Crystallinity in starch bioplastics. *Industrial Crops and Products*, *5(1)*, 11-22.
41. Van Soest, J.J.G., & Knooren, N. (1997). Influence of glycerol and water content on the structure and properties of extruded starch plastic sheets during aging. *Journal of Applied Polymer Science*, *64(7)*, 1411-1422.
42. Van Soest, J.J.G., Tournois, H., De Wit, D., & Vliegenthart, J.F.G. (1995). Short-range structure in (partially) crystalline potato starch determined with attenuated total reflectance Fourier-transform IR spectroscopy. *Carbohydrate Research*, *279*, 201-214.
43. Whittam, M.A., Noel, T.R., & Ring, S.G. (1990). Melting behaviour of A- and B-type crystalline starch. *International Journal of Biological Macromolecules*, *12(6)*, 359-362.

Starch-zein blends formed by shear flow

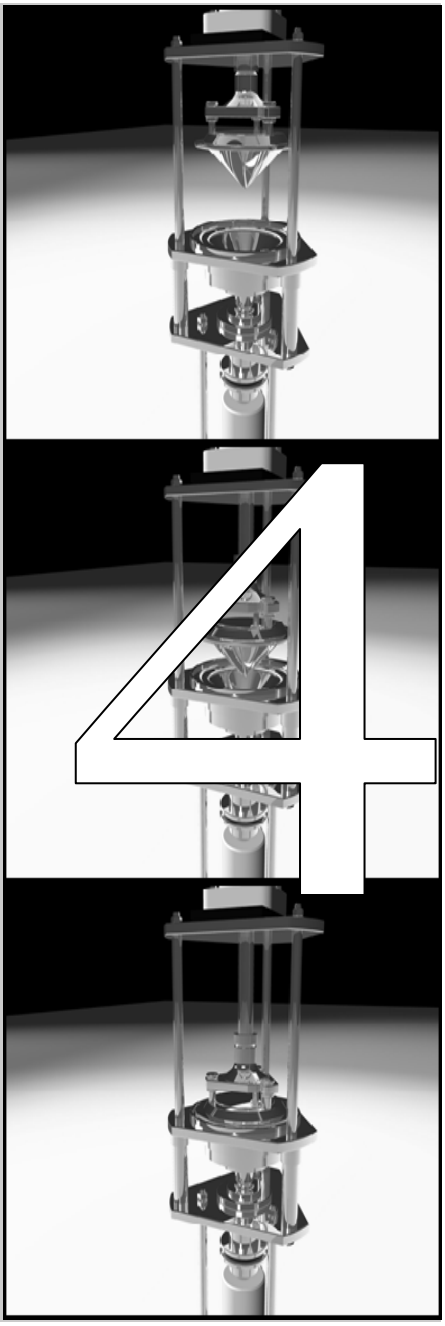

This chapter has been published as: Habeych, E., Dekkers, B., Van der Goot, A.J., & Boom, R. (**2008**). Starch-zein blends formed by shear flow. *Chemical Engineering Science*, 63(21), 5229-5238.

Abstract

A newly in-house developed shearing device was used to explore the formation of new types of microstructures in concentrated starch-zein blends. The device allowed processing of the biopolymer blends under homogeneous, simple shear flow conditions. Water and glycerol were added as plasticizers. Different ratios (0–20% zein, dry basis) were used to study the influence of the matrix composition and processing conditions on the properties of the final material. The properties at large deformation were examined by tensile tests in two different directions (i.e., along the flow (∥) and in the vorticity (⊥) directions). The morphology of the blends observed by confocal scanning laser microscopy and field emission electron microscopy showed that under shearless conditions, starch-zein formed a co-continuous blend. The application of shear transformed this structure into a dispersion, with zein as the dispersed phase. The size of the zein aggregates increased with zein concentration. A certain degree of anisotropy was found with the 10% zein blend at the highest shear rate applied ($\dot{\gamma}$=120 s^{-1}). Here, the zein aggregates were slightly deformed along the shear flow (∥). Both microscopy and tensile tests indicated that the blends have no or weak adhesion between the zein and starch phases. The effect of zein particles on the mechanical properties followed a modified model used for particle-matrix materials with weak adhesion between the phases.

1. Introduction

Biodegradable materials such as starch have been proposed for many types of applications. However, the properties of the available materials often do not match the requirements for the applications. Chemical modification of the material is an option, but this is costly and time consuming. Another option often used to fine tune the properties is blending one material with another (Avérons, 2004; Tao et al., 2005); this is more cost effective, and the resulting properties can be better predicted.

Starch can be processed into thermoplastic materials in the presence of plasticizers using heat and shear (Averous & Boquillon, 2004; Gross & Kalra, 2002). Unfortunately, plasticized (or thermoplastic) starch swells or even dissolves in water and has rather poor mechanical properties compared to synthetic polymers (Averous & Boquillon, 2004; Follain, 2005; Van Soest & Vliegenthart, 1997). To overcome this limitation while maintaining its biodegradability, plasticized starch can be blended with hydrophobic, biodegradable polymers (Gross & Kalra, 2002; Habeych et al., 2007; Park et al., 2000).

Starch has already been blended with synthetic polymers such as aliphatic polyesters, e.g., polycaprolactone, polyesteramide, polylactic acid and poly-(hydroxybutyrate-co-valerate) (Avérous et al., 2004), and also with other biopolymers, e.g., proteins (Corradini et al., 2006; Lawton, 2002; Shukla & Cheryan, 2001).

Blending starch with proteins reduces its sensitivity to water. Zein seems an interesting option for this. It comprises approximately 45-50% of the protein present in corn, and is particularly rich in glutamic acid (21-26%), leucine (20%), alanine (10%), and proline (10%) (Shukla & Cheryan, 2001), which explains its high hydrophobicity (Paulis, 1982). In addition, zein can form tough, glossy, hydrophobic and greaseproof coatings with excellent flexibility and compressibility (Shukla & Cheryan, 2001).

Recently, several studies have used a starch-zein blend as a model system to understand the behavior of corn flour under extrusion conditions (Batterman-Azcona et al., 1999; Chanvrier et al., 2005; Chanvrier et al., 2006). Batterman-Azcona et al. (1999) showed the formation of zein aggregates during thermomechanical treatment, which was attributed to the creation of disulfide bonds. Chanvrier et al. (2005) highlighted the influence of blend morphology on the mechanical properties. Chanvrier et al. (2006) showed that blends in a glassy state exhibit weak adhesion between the two phases; dispersed zein particles behaved like solid filler particles, with a large influence on the mechanical properties of the

blend. Furthermore, Liu et al. (2007) applied zein-carbohydrate blends as a drug delivery system for delivery of drugs to a specific gastrointestinal segment at designed time points.

Most blends were prepared using a mixer or extruder. However, the conditions in an extruder are not homogeneous; the material is therefore subjected to extremely high stresses at some locations, while it is not sufficiently processed at other locations. This can lead to severe thermomechanical degradation of some of the material, and an underdeveloped blend structure in another part (Van den Einde et al., 2005). In addition, the temperature in an extruder cannot be well controlled, which may induce denaturation and other unwanted chemical reactions (McClements, 2007). These inhomogeneities can be avoided by only applying simple shear flow which may yield better defined composites, and even new types of structured composites (Manski et al., 2007).

In this chapter, we report on the use of a new device that can be used to prepare starch-zein blends under simple shear flow. Compared to the previous shearing devices (Van den Einde et al., 2004; Manski et al., 2007), the new device allows even higher shear stresses, which makes it more suitable to process extreme viscous materials. The main goal is therefore to explore the influence of process conditions and matrix composition on the morphology of the starch-zein blend, using simple shear flow. Starch-zein blends with different protein concentrations were prepared under shear and shearless conditions at 95 °C. The morphology of the starch-zein blends was investigated with confocal scanning laser microscopy (CSLM) and field emission electron microscopy (FESEM). Large deformation tests were carried out to elucidate the tensile properties of the starch-zein blends.

2. Materials and methods

2.1 Materials

Native wheat starch was purchased from Latenstein BV (The Netherlands). The moisture content was 11.7±0.1% w/w. Corn zein (Z3625) was obtained from Sigma-Aldrich (Zwijndrecht, The Netherlands), with a moisture content of 5.8±0.1% w/w. Glycerol (<0.1% H_2O) was obtained from Acros Organics (Geel, Belgium) and ethanol (<0.05% H_2O) from Merck Chemicals (Germany). The moisture content of the most important powder materials was determined using a vacuum drying oven (minimum 16 h) at 105 °C (according to ISO1741). The water content of the starch was taken into account in all experiments. Acetic acid (Merck), dimethylsulfoxide (DMSO), and fuchsin acid (Sigma-

Aldrich), used for the preparation of samples for FESEM and CSLM, were of analytical grade.

2.2 Sample preparation

Prior to shear processing, the starch-zein-plasticizer premix was prepared using the protocol described by (Lim & Jane, 1993). The mixtures were freeze-dried in a Christ Epsilon 2-6D freeze dryer (Osterode am Harz, Germany) before processing. The freeze-dried samples were cryo-grinded in an analytical mill (type A10) from IKA (Staufen, Germany). The resulting fine powder then was stored at –20 °C. Finally, a homogenous mixture with dough-like consistency was prepared by adding water and glycerol (plasticizers) 1 h before processing. The final starch-plasticizer mixture had the following composition: 50% wheat starch, 20% glycerol, and 30% w/w water (wb). Table 1 shows the compositions used in this study.

Table 1. *Treatment conditions and SME results for starch-zein blends processed in the shear cell at 95 °C for 40 min*

Starch:zein ratio (db)	Maximum shear rate (s^{-1})	SME (kJ kg^{-1})
100:0	72	1022
	120	1594
95:05	72	801
90:10	36	307
	72	728
	120	1310
85:15	72	974
80:20	72	964
	120	1558

2.3 Shear cell processing

The starch-zein blends were thermomechanically treated in a newly developed shearing device. The new shear cell is an improved version of previous device developed in-house (Wageningen University, The Netherlands). The main additional features are the higher maximum shear stresses that can be applied up to 200 kPa, an improved temperature control, and an improved torque registration. It was designed and sized at pilot scale, based on an upscale rheometer concept (Peighambardoust et al., 2004; Van den Einde et al., 2004). The maximum gap size between the cone and the plate (i.e., the bottom cone) was small compared with the diameter of the cone (i.e., angle α_{plate}=105°, α_{cone}=100°) leading to

a linear shear profile. The thickness of the blend was kept small compared to the diameter of the cone, in order to apply the desired shear rates at a relatively low rotation speed to avoiding circular flow and guarantee ideal flow conditions. Furthermore, the contact surface of both cone and plate (moving bottom cone) was roughened (serrated) to avoid slippage of the material during shear processing. A schematic configuration of the shear cell is shown in Figure 1.

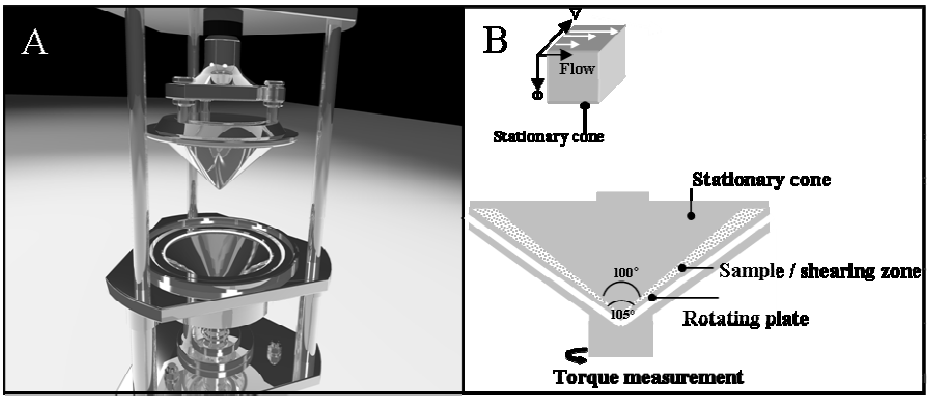

Figure 1. *An new, improved version of the shear cell device. (A) Animation and (B) schematic overview of the shear cell device. Cone angle=100°, angle between cone and plate (shearing zone), θ=2.5°.*

In the shear cell device (V=190 ml), the stationary cone and rotating plate are electrically heated and can be cooled with water. The temperature of the material is measured with a set of thermocouples located in the upper cone. The device is attached to a Brabender Do-Corder 330 (Brabender OHG, Duisburg, Germany) to enable shear rate control, and torque and temperature readings. After filling the shearing zone with starch-zein mixture, the cone-plate cell was closed. A vertical pressure (250 kPa) was applied and kept constant during the experiments.

To obtain reproducible initial conditions, the samples were heated from room temperature to 95 °C, then annealed for 30 min. The sample was then sheared between the stationary cone and the rotating plate. Blends were treated for 40 min with an increasing shear rate starting from 24 s^{-1} (10 rpm), and increased to a maximum final shear rate set at three different levels ($\dot{\gamma}$ =36, 72, 120 s^{-1}), corresponding to a rotation speed of 15, 30, and 50 rpm (see Table 1). The shear rate ($\dot{\gamma}$ in s^{-1}), shear stress (τ in kPa), and specific

mechanical energy input (SME in kJ kg^{-1}) into the material were calculated following the method described previously (Peighambardoust et al., 2004; Van den Einde et al., 2004). After processing, the shear was stopped and the material was cooled in the cell to room temperature at a rate of about 1.2 °C min^{-1}. The processed blends were then quickly stored at –40 °C prior to further analysis.

After shearing the starch-zein blends, a visual observation of a homogenous surface with the presence of lines in the blends originated by the grooves in the cone and plate geometry were used as a signal of good shearing process without slippage (see Figure 2). The results presented in this study are mostly a single experiment; however, three blends were (80:20 at $\dot{\gamma}$ =72 and 120 s^{-1}, and 90:10 at $\dot{\gamma}$ =72 s^{-1}) were reproduced showing a standard deviation lower than 6% of the recorded shear stress values.

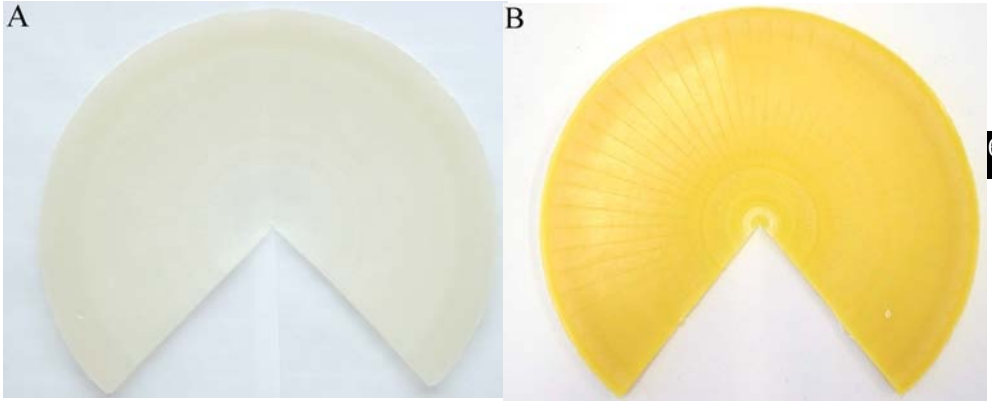

Figure 2. *(A) Thermoplastic starch sheared at $\dot{\gamma}$ =72 s^{-1} for 40 min; (B) 90:10 starch-zein blend sheared at $\dot{\gamma}$ =72 s^{-1} for 40 min.*

2.4 Compression molding

Compression molding was used to investigate the effect of heat treatment under shearless conditions. To obtain the compressed blend, 30 g of the starch-zein-glycerol-water mixture were put into the mold, which consisted of three stainless steel plates (300×350 mm^2). The upper and lower plate had a thickness of 4 mm. The middle plate had a rectangular hole (150×100×1 mm^3), into which the blend was placed. The samples were covered with plastic overhead transparencies (printable grade) on both sides of the middle plate to facilitate removal of the sample from the mold. The mold was then placed in a hydraulic PHI press (City of Industry, California). The mold was heated to 95 °C at a rate of 10 °C min^{-1}, and a

pressure of 0.86 MPa was applied, which minimized the water loss due to evaporation. During the molding experiments, the starch-zein mixture was first heated to the desired temperature, annealed for 30 min, and pressed for 40 min as in the shear experiments. Subsequently, the mold was cooled to room temperature at 10–15 °C min^{-1}, and the material was released from the mold.

2.5 Confocal scanning laser microscopy

CSLM was used to examine the distribution of the protein in the blends. For each sample, 20 μm thick slices of the processed starch-zein blends were prepared using a cryomicrotome at –20°C. The sections were placed on a flat glass slide and defrosted. Protein staining was performed with 0.01% (w/v) fuchsin acid dissolved in 1% acetic acid (v/v) for 5 min, following (Chanvrier et al., 2005). The slices were extensively washed with distilled water, placed on a microscope slide, covered with a cover slide and sealed with nail varnish to avoid drying out.

The samples were analyzed using an inverted Zeiss Pascal CSLM (Zeiss, Oberkochen, Germany). The CSLM consisted of an Aviovert 200M inverted microscope, using a He/Ne laser with 543 nm wavelength. The light was filtered using a 560-nm long-pass filter. Z stacks of 2-μm optical sections were made through the whole *Z*-axis of the sample, using a 20× Plan-Neofluar objective with a zoom factor of 1. Each presented image corresponds to a flat projection of the *Z* stack (636.4×636.4 μm^2) excluding 80:20 starch-zein blends (225×225 μm^2). The images were analyzed on a computer using Scion imaging software available online at http://www.scioncorp.com/. The binarization threshold, defined from the histograms of the grey levels, was set at a grey level value of 50 for each image. The zein surface ratio (ZSR) is defined as the ratio between the surface covered by zein and the total surface of an image. The ZSR and the number of particles were calculated based on image analysis done for at least two flat projections images (obtained by observing about 10 planes of 2 μm) of different spots in the blends.

2.6 Scanning electron microscopy

Microstructural aspects of the starch-zein blends were observed with a field emission scanning electron microscope (FESEM) at ambient temperature. Dry samples were prepared according to the modified method described by (Manski et al., 2007) to observe the blend without interference from a water phase.

Freeze fracturing was performed before the samples were glued to a sample holder using conductive carbon cement (Leit-C, Neubauer Chemicalien, Germany) and subsequently sputter coated with 20 nm platinum (JFC 1200, JEOL, Japan). The fractured surfaces were analyzed with a FESEM (JEOL 6300 F, Tokyo, Japan) at room temperature using a working distance of 8 mm, with SE detection at 3.5–5 kV. All images were recorded digitally (Orion, 6 E.L.I. sprl., Belgium) at a scan rate of 100 s (full frame) at a size of 2528×2030, 8 bit. Noise reduction and resizing of the images were done using Adobe Photoshop CS.

2.7 Large-scale deformations

A Texture Analyzer T2 (Stable Micro Systems Ltd., Surrey, UK) was used for large deformation tests. Before the measurement, starch-zein blends were defrosted at room temperature. The samples were cut into a dog-bone shape with a custom-made mold, according to ASTM D638 type IV. The thickness (e≈4 mm), was measured precisely with a micrometer model 7305 (Mitutoyo, Japan) for each specimen. Uniaxial tensile tests were conducted with a constant crosshead speed of 3 mm min^{-1}, until sample fracture. All measurements were done at least in triplicate. Only the 80:20 starch-zein blends could not be tested due to the irregular surface of the samples after processing.

From the stress-strain (force elongation) diagram, the tensile strength (σ), tensile elongation (ε) were calculated:

$$\sigma = \frac{F}{A_0} \quad \text{(MPa)}, \tag{1}$$

where F (N) is the maximum tensile force and A_0 (mm^2) is the initial cross-section of the specimen at the start.

$$\varepsilon = \frac{L_M - L_0}{L_0}\ 100\ (\%), \tag{2}$$

where L_0 (mm) is the original length and L_M (mm) is the elongation length.

To test the anisotropy of the material, the specimens were cut along the flow ($\parallel$) and vorticity ($\perp$) directions (see Figure 1B).

3. Results

3.1 Blends processing

Before processing, starch-zein blends containing 50% w/w of the plasticizers formed a dough-like material. This is in line with previous studies that showed 90:10 starch-zein blends plasticized with water and dibutyl tartrate formed dough-like material resembling wheat flour (Lawton, 1992). The application of simple shear to starch-zein blends led to a thermoplastic material. The product was white for 100:0 starch-zein and yellow for all blends containing zein (Figure 2).

Typical changes in torque values during shearing of blends with different starch-zein ratios showed a single peak in the shear stress curves (Figure 3A), which is the result of gelatinization of the starch. The maximum shear stresses observed as a function of the zein concentration at $\dot{\gamma}$ =72 and 120 s^{-1} are presented in Figure 3B. The 90:10 starch-zein blends manifested shear thinning behavior (see inset in Figure 3B).

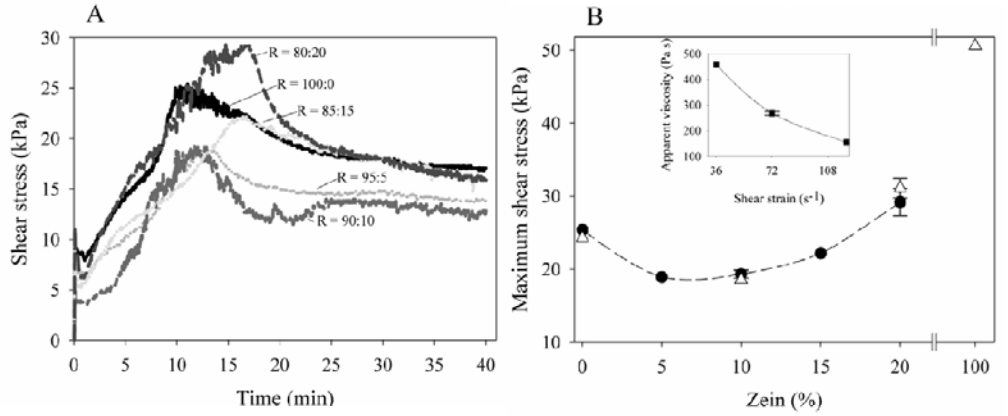

Figure 3. *(A) Shear stress profiles for starch-zein blends processed at $\dot{\gamma}$ =72 s^{-1}; (B) maximum shear stresses under simple shear flow as a function of the zein content. (●), $\dot{\gamma}$ =72 s^{-1}; (△), $\dot{\gamma}$ =120 s^{-1}. The inset shows the apparent viscosity as a function of shear rate for a starch-zein ratio of 90:10.*

3.2 Microstructure of the blends

CSLM was used to analyze the distribution, size, and orientation of the phases. In addition, the adhesion of the phases was visualized with FESEM images.

Figure 4 shows the morphological distribution of starch-zein blends with different zein concentration processed at different shear rates. The red areas depict the protein phase and green areas represent the starch phase.

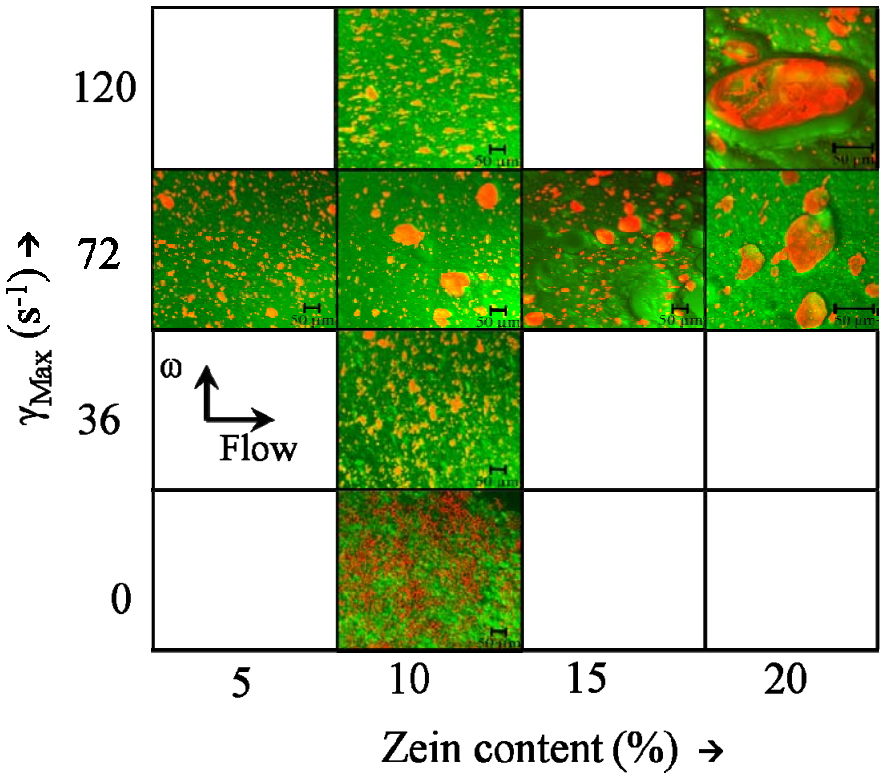

Figure 4. *Effect of shear rate and zein content on the morphology of starch-zein blends at 95 °C. (CSLM pictures). Flow direction: from left to right. Scale bar: 50 μm.*

All samples analyzed showed phase separation on a micrometer scale. In addition, the FESEM images showed the presence of voids at the interface (Figure 5).

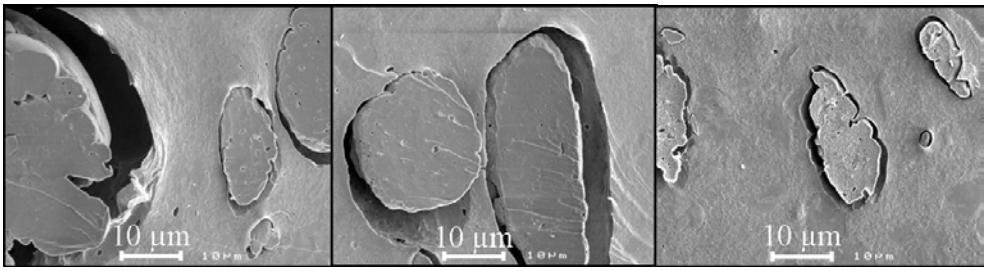

Figure 5. *Field emission electron micrograph showing the zein flocs in starch-zein blends (90:10 starch-zein ratio processed at 95 °C).*

Effect of shear rate

The effect of shear rate was studied using the 90:10 and 80:20 starch-zein blends. Under shearless conditions (compression molding experiment) the 90:10 starch-zein blend showed a co-continuous morphology (Figure 4). Under shear conditions, this co-continuity was broken down. At low shear rate ($\dot{\gamma}$ =36 s^{-1}), the flow induces the formation of small protein flocs slightly oriented along the vorticity direction ($\perp$). After increasing the shear rate ($\dot{\gamma}$ =72 s^{-1}), the flocs are larger without any specific orientation. A further increase in the shear rate ($\dot{\gamma}$ =120 s^{-1}), led to stretching of the flocs oriented along the flow ($\parallel$). On the other hand, the 80:20 starch-zein blends showed a coalescent effect due to an increased shear rate from 72 to 120 s^{-1} without orientation of the zein flocs.

Effect of protein concentration

Figure 4 shows the effect of the protein concentration on the morphology of the blends at constant shear rate ($\dot{\gamma}$ =72 s^{-1}). At a low zein concentration (5%, dry basis), zein appeared as homogeneously dispersed droplets. Upon increasing the zein concentration, the images suggest that zein aggregates into clusters (flocs) without any orientation.

The average number of zein flocs decreased for blends processed at $\dot{\gamma}$ =72 s^{-1} from 524 for the 95:5 blend to 131 for the 80:20 blend as a consequence of zein coalescence (Table 2). A similar result was observed for blends processed at a higher shear rate ($\dot{\gamma}$ =72 s^{-1}). In summary, a clear coalescence effect was observed when the zein concentration was higher.

Table 2. *Zein surface ratio (ZSR) and swelling factor (β) obtained for starch-zein blends by using CSLM image analysis*

Starch:zein ratio (db)	Maximum shear rate (s^{-1})	Zein surface ratio (ZSR)	Swelling factor (β)	Number of zein particles
95:05	72	16.9 ± 2.3	3.4 ± 0.5	524 ± 38
90:10	0	36.8 ± 10.3	3.7 ± 1.0	-
	36	22.5 ± 2.8	2.3 ± 0.3	491 ± 50
	72	14.6 ± 7.3	1.5 ± 0.7	421 ± 58
	120	20.6 ± 3.7	2.1 ± 0.4	443 ± 114
85:15	72	18.2 ± 16.9	1.2 ± 1.1	219 ± 122
80:20	72	22.7 ± 0.3	1.2 ± 0.0	131 ± 9
	120	30.2 ± 6.4	1.5 ± 0.3	75 ± 29

3.3 Mechanical properties

The mechanical properties of thermoplastic starch-zein blends are summarized in Figures 6 and 7. The effects of zein content and shear rate on the mechanical properties of the blends were evaluated along the flow ($\parallel$) and vorticity ($\perp$) directions.

Effect of shear rate

Figure 6 summarizes the effects of the shear rate on the mechanical properties (tensile strength and tensile elongation) for 90:10 starch-zein blends. Based on the tensile strength and tensile elongation measured along the flow and vorticity directions, we observed a transition from isotropic to slightly anisotropic distribution of the zein phase. The values of the tensile strength and tensile elongation are not statistically different along the flow ($\parallel$) and vorticity ($\perp$) directions for blends processed at 36 and 72 s^{-1}. Nevertheless, when a shear rate of 120 s^{-1} was applied, the tensile strength and tensile elongation showed a marked difference along the flow ($\parallel$) and vorticity ($\perp$) directions, being higher along the flow direction.

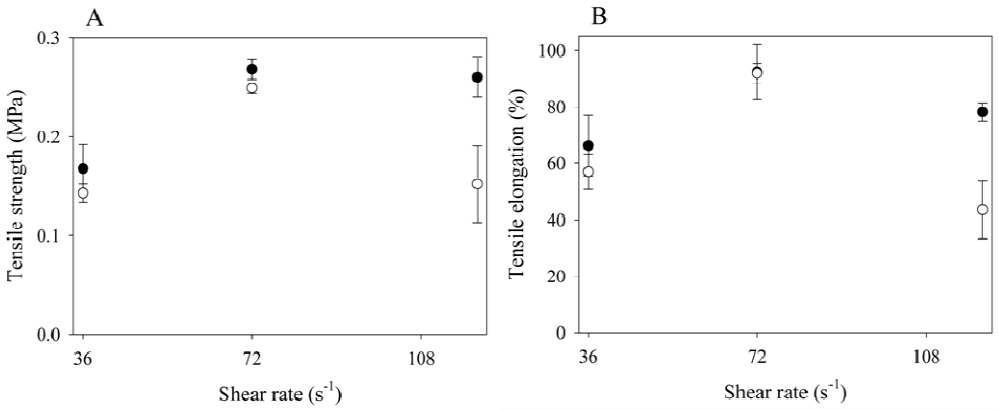

Figure 6. *Mechanical properties of starch-zein blends in two different directions as a function of the applied shear rate. (A) Tensile strength and (B) tensile elongation. The tensile properties were measured along the flow (‖) direction (•) and vorticity (⊥) direction (○) in the shear cell device. The bars indicate the mean±average standard deviation.*

Effect of protein concentration

Figure 7 depicts the mechanical properties (tensile strength and tensile elongation) as a function of the zein content for the starch-zein ratios of: 100:0, 95:5, 90:10, and 85:15. The values of the tensile strength dropped to about 75% of the initial value obtained for 100:0 starch-zein in the 85:15 starch-zein blend. On the other hand, the opposite situation is observed for the tensile elongation, which increased with zein concentration. Finally, the values of the tensile strength and tensile elongation as a function of zein content along the flow (‖) and vorticity (⊥) directions for all samples did not show a significant difference. Thus, all blends showed isotropic behavior.

An interesting observation was found when the mechanical properties along the flow (‖) and vorticity (⊥) directions between plasticized starch and the blends were compared. The addition of the zein phase changed the higher strength along the vorticity direction to the flow direction (see Figure 7A).

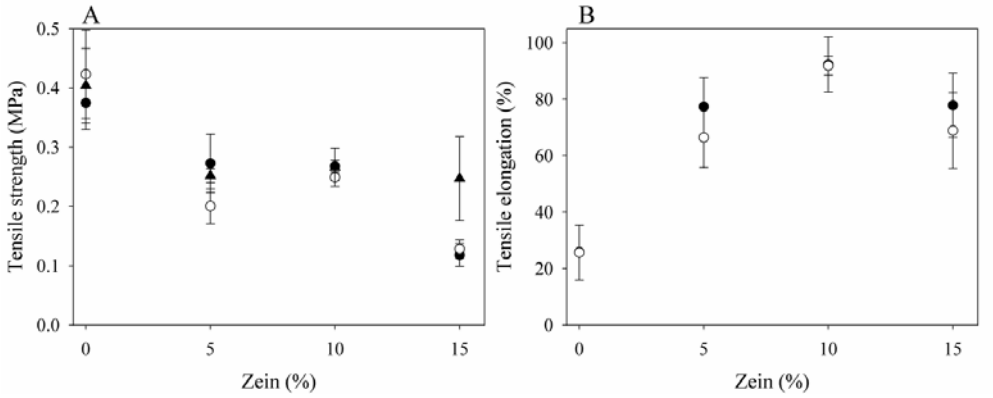

Figure 7. *Mechanical properties of starch-zein blends processed at* $\dot{\gamma}$ *=72* s^{-1} *in two different directions as a function of the zein concentration. (A) Tensile strength and (B) tensile elongation. The tensile properties were measured along the flow (*$\parallel$*) direction (•) and vorticity (*$\perp$*) direction (○) in the shear cell device. (▲), predicted values using the modified composite model with swelling factor (*β*). The bars indicate the mean±average standard deviation.*

4. Discussion

The structure of plasticized starch-zein mix prior to heating and shearing is unknown, but it can presumably be described as a continuous zein matrix with embedded starch granules. This description is based on three facts. First, the properties of starch-zein prepared above the zein glass transition temperature (T_g) have been reported to be dominated by the formed zein network (Lawton, 1992). Second, zein with a moisture content of 30% has a T_g of –30 °C (Madeka & Kokini, 1996). Third, glycerol and water do not have a plasticizing effect on starch granules prior to gelatinization (i.e., T≈55 °C) (Tan et al., 2004).

A co-continuous morphology for the 90:10 starch-zein blend was obtained under shearless conditions (compression molding experiment). Under these conditions, a large coalescence effect was observed, which indicates a high interfacial mobility between these polymers. This type of coalescence has been reported as *static coalescence*, a common mechanism observed during annealing of polymer blends that reduces the interfacial area through particle–particle fusion (Lyu et al., 2000; Sundararaj & Macosko, 1995). Under shear conditions, zein appeared dispersed, forming aggregates (flocs) in a continuous gelatinized starch matrix. These flocs have been reported previously to form during mixing or extrusion of starch-zein blends (Batterman-Azcona et al., 1999; Chanvrier et al., 2005; Corradini et al., 2006).

The drop in shear stress during processing presented in Figure 3B is related to the presence of zein. The introduction of a small amount of an immiscible second polymer (i.e., zein) is known to reduce the viscosity and elasticity of a polymer blend (Rudin & Schreiber, 1983). This effect is also evident in the reduction of the shear stress and SME values (Table 1).

The size of the clusters obtained after simple shear processing is larger than that reported in studies on similar blends obtained via extrusion and mixing (Batterman-Azcona et al., 1999; Chanvrier et al., 2005; Corradini et al., 2006). Mixing and extrusion of polymer blends generally lead to smaller aggregates compared with shear flow (Lin, 2003; Utracki, 1986). The main reason for this situation relates to the differences in the flow field. During mixing and extrusion, a polymer melt: experiences simple shear flow and elongational flow. In addition, reorientation occurs frequently during mixing. Shear flow is known to have a lower dispersing (break-up) capacity than elongational flow (Khayat et al., 2000), while, elongational flow is more efficient for generating the dispersive mixing (Grace, 1982). Therefore, the larger clusters obtained under simple shear conditions is likely due to the low dispersing capacity in the simple shear. This effect, combined with the absence of reorientation in the shearing device accounts for the formation of larger protein clusters.

Blends processed at different shear rates showed a transition from isotropic to slightly anisotropic distribution of the zein phase. This anisotropy was observed with a CSLM image for the 90:10 blend processed at $\dot{\gamma}$ =120 s^{-1} with stretched droplets oriented in the flow direction. Mechanical tests confirmed the anisotropy. Under shear conditions, zein droplets form flocs as attractive forces prevail over hydrodynamic forces. Once the hydrodynamic forces exceed the attractive forces, zein flocs are stretched and will align along the flow. According to the results observed, shear rate appears to be an essential tool to influence the creation of anisotropic structures in starch-zein blends. Similar conclusions have been made previously for other model systems (Hoekstra et al., 2003; Manski et al., 2008; Vermant et al., 1998).

4.1 Model for mechanical properties

All blends showed the presence of voids in the interfacial domain. These voids have been seen as a signal of a poorly compatibilized system (Utracki, 2002; Wu, 2003). Certainly, this lack of compatibilization influences the mechanical behavior of the materials. Mechanical tests have shown that the addition of zein to the starch matrix decreases the tensile strength (σ) of the blend and increases the elongation (Figure 7). In fact, bad

adhesion leads to high elongation as shown for uncompatibilized thermoplastic styrene–acrylonitrile copolymer filled with glass (Nicolais & Nicodemo, 1974). This situation is a consequence of the inhomogeneous deformation mechanism resulting from the formation and the propagation of crazes through the polymer matrix. This explains why zein weakened the starch matrix as a consequence of the reduction of internal friction of the polymer mass due to lower adhesion between domains of the polymer types.

The weakened effect of zein over the starch matrix can be confirmed using a model that involves particle–matrix adhesion. Nicolais and Nicodemo (Nicolais & Nicodemo, 1974) described a model that suggests that the ultimate strength of the composite, σ_{blend}, is determined by the volume fraction of particles, ϕ, and information on the matrix behavior, σ_{matrix},

$$\sigma_{blend} = \sigma_{matrix}\left(1 - a \times \phi^{b}\right), \tag{3}$$

where a is a constant related to the stress concentration and the adhesion, b to the particle geometry. In the case of spherical particles without adhesion, a=1.21 and b=2/3. Eq. (3) is applicable to rigid material (e.g., glass beads). Previously, Chanvrier et al. (2006) reported the successful application of Nicolais and Nicodemo's model to starch-zein blends in a glassy state. However, due to the plasticizing effect that glycerol and water have over zein (Corradini et al., 2006; Lawton, 2002), Eq. (3) needs to include a correction factor due to the swelling of the protein phase, as follows:

$$\sigma_{blend} = \sigma_{matrix}\left[1 - 1.21 \times \left(\beta \times \phi\right)^{2/3}\right], \tag{4}$$

where β is the swelling factor obtained from the image analysis (Table 2).

Assuming that all processed blends are uniform and isotropic, as required by the stereological relationships (Russ, 2005), the volume fraction of zein could be approximated from the ZSR. As a result, the distribution of plasticizers between the two phases can be obtained by defining a swelling factor, as follows:

$$\beta = 1 + \frac{ZSR - \phi}{\phi}, \tag{5}$$

where ZSR is the surface ratio between the zein surface and the total surface of an image and ϕ is the volume fraction of zein particles in the blend. Table 2 shows the calculated vales of ZSR and β.

A reduction in β values upon increased zein concentration and shear rate was observed (Table 2). Since the ratio of plasticizer to starch in all blends was kept constant, increasing the zein concentration at constant shear rate ($\dot{\gamma}$ =72 s^{-1}) results in a decrease of the swelling factor as a consequence of the lower amount of plasticizer that was available for zein (higher dry weight). Moreover, when a higher shear rate is applied, the hydrophilic starch phase is more plasticized than the zein phase due to a possible migration of glycerol or water from the zein phase (less hydrophilic) to the thermoplastic starch phase upon processing and gelatinization.

The calculated values shown in Figure 7A from the modified composite model with no adhesion agree with the experimental data obtained for starch-zein blends. However, a deviation is observed for the 85:15 blend, which could be as a result of the low value found for β. Nevertheless, the results confirm our suggestions about poor adhesion between the starch matrix and zein particles.

4.2 The role of coalescence and breakup of zein in microstructure formation

The size and shape of the dispersed phase depend on several processing parameters, including rheology, interfacial properties, and the composition of the blend. The capillary number (*Ca*) quantifies the ratio between the viscous forces, which tend to deform and break the drop, and the counteracting interfacial force, which tries to reduce the deformation of the drop. The capillary number is defined as:

$$Ca = \frac{\dot{\gamma} \times \eta_C \times D}{2 \times \Gamma}, \tag{6}$$

where $\dot{\gamma}$ is the shear rate, η_c is the continuous phase viscosity, D is the diameter of the drop, and Γ is the interfacial tension. Applying a steady shearing flow that is not able to break the droplet will stretch a droplet into a nearly ellipsoidal steady-state shape. The steady-state degree of deformation, defined as the deformation parameter, *Def,* is approximately linear to the capillary number as (Taylor, 1932; 1934):

$$Def = \frac{a-b}{a+b} = Ca \frac{16 \times \frac{\eta_d}{\eta_c} + 16}{19 \times \frac{\eta_d}{\eta_c} + 16}, \tag{7}$$

where η_d is dispersed phase viscosity, and *a* and *b* are the lengths of the major and minor axes of the deformed droplet, respectively. Taylor (1934) found this relation to be valid for an isolated Newtonian droplet in a steady simple shearing flow of a surrounding Newtonian fluid. However, the non-Newtonian viscoelastic behavior of starch-zein blends manifested in shear thinning behavior is expected to influence the droplet deformation and breakup. Previous studies on viscoelastic droplet breakup showed that the stretching and deformation of droplets in the direction of the flow has been ascribed to a low elasticity system (Cherdhirankorn et al., 2004). The fact that we observed elongation allows us to assume that our system consists of Newtonian liquids.

The *Def* values for starch-zein blends were obtained from the CSLM images. The overall evaluation showed that for the blends analyzed, *Def* was less than 0.4. Hence, following Eq. (7), $Ca<0.5$. Taylor (1934) predicted that the critical point (Ca_c) at which the viscous force overcomes the interfacial force leading to droplet breakup occurs at $Ca\cong0.5$ and $Def\cong0.5$ when $\eta_d/\eta_c\approx1$. At $\eta_d/\eta_c>4$, Ca_c becomes infinite so that droplets are stable at all capillary numbers (Grace, 1982). For starch-zein blends, Ca_c was estimated using the graph obtained for Newtonian fluids. For starch-zein blends processed at $\dot{\gamma}=120\ s^{-1}$, we obtained an approximation of the viscosity ratio $\eta_d/\eta_c\geq2$ (Figure 3B). At $\eta_d/\eta_c\approx2$ under simple shear conditions, $Ca_{cr}\approx2.3$. Therefore, under the conditions studied no breakup occurred as $Ca<Ca_c$. That explains the microstructures described in this chapter.

Based on the discussion and observations presented above, a mechanism can be proposed. The overall microstructural picture that reconciles most of the information described above is summarized in Figure 8A. Under shearless conditions, starch-zein formed a co-continuous blend. This co-continuity is broken down under shear conditions to form zein aggregates (flocs). When shear forces increase, the dominant forces are of hydrodynamic character leading to small flocs aligned in the flow direction. On the other hand, larger clusters are formed for higher zein concentrations at constant shear rate. The addition of more zein to the blend leads to lower swelling factor (Table 2), which means that the resulting viscosity of the protein phase will probably be even higher, moving away from breakage and alignment of the continuous phase.

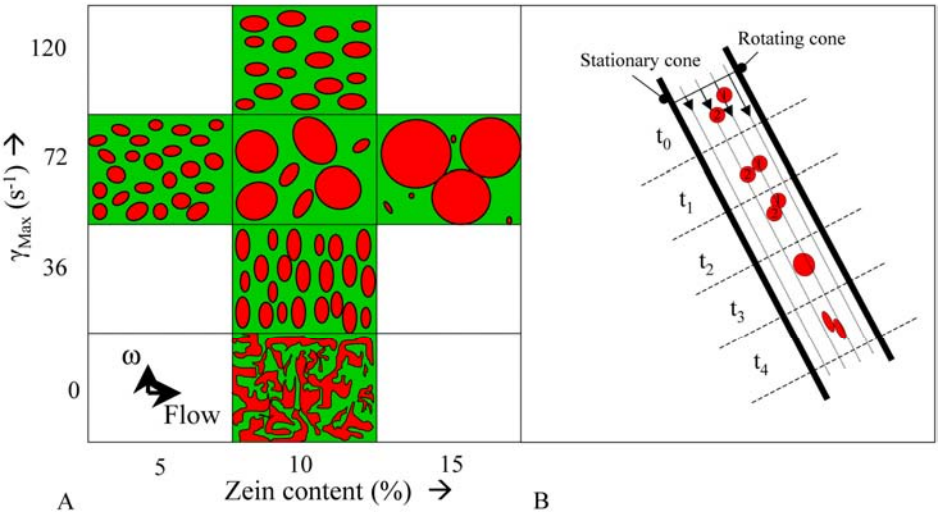

Figure 8. *Schematic illustration of morphology development of starch-zein under shear conditions. (A) Overview of the morphology of starch-zein blends at different shear rates and protein concentration during shear flow. (B) Mechanism of developing structure under simple shear.*

Figure 8B illustrates a possible mechanism. Consider two zein particles at positions (1) and (2) with the velocities v_1 and v_2 respectively at time t_0 following a simple shear field. Under these conditions, particle (1) moves faster than particle (2) and will join it at time t_1. As a consequence of attractive forces, the two particles will form a doublet, and start to rotate by the effect of the differences in velocities. They will form a floc at t_3. Later, this floc may capture more particles along its trajectory. This situation describes the coalescence situation observed upon addition of zein. On the other hand, if the shear conditions are high enough at t_2, the particles would not form a larger floc, but would be stretched in the flow direction. At t_4 the particles will eventually align along the flow direction ($\|$), as we observed for the 90:10 starch-zein blends processed at $\dot{\gamma}$ =120 s^{-1}.

5. Conclusions

The newly developed shearing device is a useful tool to explore the formation of new types of microstructures in starch-zein blends. The use of simple shear to process starch-zein blends led to the formation of larger zein flocs than reported in studies on similar blends obtained through extrusion and mixing. The main reason for this situation is the significantly lower dispersing (break-up) capacity in simple shear in comparison to mixing condition that comprise apart from simple shear flow also elongation and reorientation.

Processing a 90:10 starch-zein ratio at $\dot{\gamma}$=120 s^{-1} induced a certain degree of anisotropy. The poor compatibilization of the phases was responsible for the weakened behavior of starch-zein blends causing phase separation with simultaneous aggregation of zein.

Acknowledgments

The authors thank Dr. Henk Kieft for the confocal scanning laser microscopy measurements, H. Baptist for assistance with the tensile tests, and Jacqueline Donkers for the scanning electron microscope. This research was conducted within the framework of the Carbohydrate Research Centre at Wageningen.

References

1. Avérous, L. (2004). Biodegradable multiphase systems based on plasticized starch: a review. *Journal of Macromolecular Science Part C Polymer Reviews*, 44(3), 231-234.
2. Avérous, L., & Boquillon, N. (2004). Biocomposites based on plasticized starch: thermal and mechanical behaviours. *Carbohydrate Polymers*, 56(2), 111-122.
3. Batterman-Azcona, S.J., Lawton, J.W., & Hamaker, B.R. (1999). Microstructural changes in zein proteins during extrusion. *Scanning*, 21(3), 212-216.
4. Chanvrier, H., Colonna, P., Della Valle, G., & Lourdin, D. (2005). Structure and mechanical behaviour of corn flour and starch–zein based materials in the glassy state. *Carbohydrate Polymers*, 59(1), 109-119.
5. Chanvrier, H., Valle, G.D., & Lourdin, D. (2006). Mechanical behaviour of corn flour and starch–zein based materials in the glassy state: a matrix-particle interpretation. *Carbohydrate Polymers*, 65(3), 346-356.
6. Cherdhirankorn, T., Lerdwijitjarud, W., Sirivat, A., & Larson, R. (2004). Dynamics of vorticity stretching and breakup of isolated viscoelastic droplets in an immiscible viscoelastic matrix. *Rheologica Acta*, 43(3), 246-256.
7. Corradini, E., de Medeiros, E.S., Carvalho, A.J.F., Curvelo, A.A.S., & Mattoso, L.H.C. (2006). Mechanical and morphological characterization of starch/zein blends plasticized with glycerol. *Journal of Applied Polymer Science*, 101(6), 4133-4139.
8. Follain, N., Joly, C., Dole, P., & Bliard, C. (2005). Mechanical properties of starch-based materials. I. Short review and complementary experimental analysis. *Journal of Applied Polymer Science*, 97(5), 1783-1794.

9. Grace, H.P. (1982). Dispersion phenomena in high viscosity immiscible fluid systems and application of static mixers as dispersion devices in such systems. *Chemical Engineering Communications*, 14(3–6), 225-277.
10. Gross, R.A. & Kalra, B. (2002). Biodegradable polymers for the environment. *Science*, 297(5582), 803-807.
11. Habeych, E., Van der Goot, A.J., & Boom, R. (2007). Prediction of permeation fluxes of small volatile components through starch-based films. *Carbohydrate Polymers*, 68(3), 528-536.
12. Hoekstra, H., Vermant, J., Mewis, J., & Fuller, G. (2003). Flow-induced anisotropy and reversible aggregation in two-dimensional suspensions. *Langmuir*, 19(22), 9134-9141.
13. Khayat, R.E., Luciani, A., Utracki, L.A., Godbille, F., & Picot, J. (2000). Influence of shear and elongation on drop deformation in convergent-divergent flows. *International Journal of Multiphase Flow*, 26, 17-44.
14. Lawton, J.W. (1992). Viscoelasticity of zein-starch dough. *Cereal Chemistry*, 69(4), 351-355.
15. Lawton, J.W. (2002). Zein: a history of processing and use. *Cereal Chemistry*, 79(1), 1-18.
16. Lim, S.T. & Jane, J.L. (1993). Water-resistant starch-protein thermoplastics. Patent WO/1993/019125.
17. Lin, B., Sundararaj, U., Mighri, F., & Huneault, M.A. (2003). Erosion and breakup of polymer drops under simple shear in high viscosity ratio systems. *Polymer Engineering & Science*, 43(4), 891-904.
18. Liu, L.S., Fishman, M.L., & Hicks, K.B. (2007). Pectin in controlled drug delivery – a review. *Cellulose*, 14(1), 15-24.
19. Lyu, S.P., Bates, F.S., & Macosko, C.W. (2000). Coalescence in polymer blends during shearing. *AIChE Journal*, 46(2), 229-238.
20. Madeka, H. & Kokini, J.L. (1996). Effect of glass transition and cross-linking on rheological properties of zein: development of a preliminary state diagram. *Cereal Chemistry*, 73(4), 433-438.
21. Manski, J.M., Van der Goot, A.J., & Boom, R.M. (2007). Formation of fibrous materials from dense calcium caseinate dipersions. *Biomacromolecules*, 8(4), 1271-1279.
22. Manski, J.M., Van der Zalm, E.E.J., Van der Goot, A.J., & Boom, R.M. (2008). Influence of process parameters on formation of fibrous materials from dense calcium caseinate dispersions and fat. *Food Hydrocolloids*, 22(4), 587-600.

23. McClements, D.J. (Ed.). (2007). *Understanding and controlling the microstructure of complex foods*. Cambridge, England: Woodhead Publishing Ltd.
24. Nicolais, L. & Nicodemo, L. (1974). Effect of particles shape on tensile properties of glassy thermoplastic composites. *International Journal of Polymeric Materials*, 3(3), 229-243.
25. Park, J.W., Im, S.S., Kim, S.H., & Kim, Y.H. (2000). Biodegradable polymer blends of poly(l-lactic acid) and gelatinized starch. *Polymer Engineering and Science*, 40(12), 2539-2550.
26. Paulis, J.W. (1982). Recent developments in corn protein research. *Journal of Agricultural and Food Chemistry*, 30(1), 14-20.
27. Peighambardoust, S.H., Van der Goot, A.J., Hamer, R.J., & Boom, R.M. (2004). A new method to study simple shear processing of wheat gluten-starch mixtures. *Cereal Chemistry*, 81(6), 714-721.
28. Rudin, A. & Schreiber, H.P. (1983). Shear modification of polymers. *Polymer Engineering and Science*, 23(8), 422-430.
29. Russ, J.C. (2005). *Image Analysis of Food Microstructure*. Boca Raton, FL: CRC Press.
30. Shukla, R. & Cheryan, M. (2001). Zein: the industrial protein from corn. *Industrial Crops and Products*, 13(3), 171-192.
31. Sundararaj, U. & Macosko, C.W. (1995). Drop breakup and coalescence in polymer blends: the effects of concentration and compatibilization. *Macromolecules*, 28(8), 2647-2657.
32. Tan, I., Wee, C.C., Sopade, P.A., & Halley, P.J. (2004). Investigation of the starch gelatinisation phenomena in water-glycerol systems: application of modulated temperature differential scanning calorimetry. *Carbohydrate Polymers*, 58(2), 191-204.
33. Tao, Y., Lebovitz, A.H., & Torkelson, J.M. (2005). Compatibilizing effects of block copolymer mixed with immiscible polymer blends by solid-state shear pulverization: stabilizing the dispersed phase to static coarsening. *Polymer*, 46(13), 4753-4761.
34. Taylor, G.I. (1932). The viscosity of a fluid containing small drops of another fluid. *Proceedings of the Royal Society of London Series A*, 138, 41-48.
35. Taylor, G.I. (1934). The formation of emulsions in definable fields of flow. *Proceedings of the Royal Society of London Series A*, 146, 501-523.
36. Utracki, L.A. (1986). Flow and flow orientation of composites containing anisometric particles. *Polymer Composites*, 7(5), 274-282.

37. Utracki, L.A. (2002). Compatibilization of polymer blends. *Canadian Journal of Chemical Engineering*, 80(6), 1008-1016.
38. Van den Einde, R.M., Bolsius, A., Van Soest, J.J.G., Janssen, L.P.B.M., Van der Goot, A.J., & Boom, R.M. (2004). The effect of thermomechanical treatment on starch breakdown and the consequences for process design. *Carbohydrate Polymers*, 55(1), 57-63.
39. Van Den Einde, R.M., Van der Veen, M.E., Bosman, H., Van der Goot, A.J., & Boom, R.M. (2005). Modeling macromolecular degradation of corn starch in a twin screw extruder. *Journal of Food Engineering*, 66(2), 147-154.
40. Van Soest, J.J.G. & Vliegenthart, J.F.G. (1997). Crystallinity in starch plastics: consequences for material properties. *Trends in Biotechnology*, 15(6), 208-213.
41. Vermant, J., Van Puyvelde, P., Moldenaers, P., Mewis, J., & Fuller, G.G. (1998). Anisotropy and orientation of the microstructure in viscous emulsions during shear flow. *Langmuir*, 14(7), 1612-1617.
42. Wu, J. (2003). The interfacial properties and porous structures of polymer blends characterized by synchrotron small-angle x-ray scattering. *Polymer*, 44(26), 8033-8040.

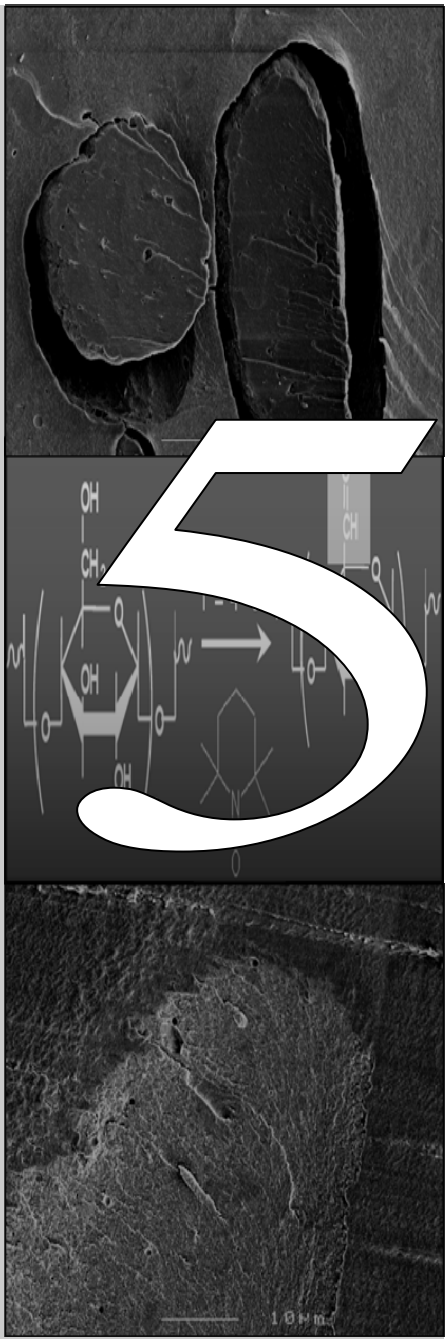

5

In situ compatibilization of starch-zein blends under shear flow

This chapter has been published as: Habeych, E., Van der Goot, A.J., & Boom, R. *In situ* compatibilization of starch-zein blends under shear flow. *Chemical Engineering Science*. 64(15), 3516-3524.

Abstract

Starch-zein blends show poor adhesion between the two phases. Aldehyde starch was investigated as compatibilizer for these blends. Wheat starch was oxidized under mild conditions using sodium hypochlorite in the presence of the 2,2,6,6-tetramethylpiperidine-1-oxyl radical (TEMPO) and NaBr to prepare aldehyde starch. The oxidized starch was characterized by Nuclear Magnetic Resonance and Rapid Visco-Analyser. Starch-zein blends plasticized with water and glycerol were prepared using simple shear flow in an in-house developed shearing device. Different zein ratios were tested to study the influence of aldehyde starch on the properties of the final material. The morphology of the blends was observed with confocal scanning laser microscopy and scanning electron microscopy. Tensile tests were used to evaluate the performance of the material. Both microscopy and tensile tests indicated that the blends had improved adhesion between the zein and starch phases, probably by reaction between the aldehyde groups in the starch molecules and zein. The aldehyde starch also influenced the properties of the starch matrix (higher viscosity, larger breakdown), which shows that physical or chemical crosslinks were formed inside the starch matrix.

1. Introduction

Polymers blends have emerged as an effective and economical way to create new materials (Ghodgaonkar & Sundararaj, 1996; Lin et al., 2005). Due to their low entropy of mixing, most polymer blends are immiscible and need to be compatibilized, which may be accomplished by addition of a compatibilizer or by reactive processing (Utracki, 2002). Compatibilization is required to: (i) enhance adhesion between the phases, (ii) stabilize the morphology against high stresses during forming, and (iii) reduce the interfacial tension; (Utracki, 2002). Good compatibilization has significant effects on the flow behavior and the final performance of the material.

Biodegradable materials such as starch-based blends have been widely studied as replacement for petroleum-based polymers (Avérous, 2004; Rouilly & Rigal, 2002; Wang et al., 2003). Blending of starch with agro-polymers such as proteins to produce biodegradable plastics is a promising topic for research and industrial development (Habeych et al., 2008; Huang et al., 1999). Recently, starch-zein blends have been reported as a method to reduce the sensitivity of starch for water (Corradini et al., 2007; Habeych et al., 2008; Shukla & Cheryan, 2001). Zein, the major protein of corn (approximately 45–50% of the total protein) contains a high content of hydrophobic amino acids (glutamic acid, leucine, proline, and alanine) (Paulis, 1982; Shukla & Cheryan, 2001), which makes this protein suitable to reduce the interaction with water (Habeych et al., 2007). The main drawback of the starch-zein blends is the lack of adhesion between the starch and the protein resulting in poor properties of the blend. To improve the adhesion between the two immiscible polymers, we propose the inclusion of a reactive functional group (aldehyde) on a starch phase to influence the interfacial properties of the blend (Lim & Jane, 1993). Aldehyde groups may react with neighbouring starch chains to form hemiacetals. The hemiacetals can react with amines to give imine and aminal covalent linkages. Li et al. (2005) identified this reaction as a method to improve wet strength of TEMPO oxidized cellulose with different proteins, including zein. Another possibility is a condensation reaction of an amine with a carboxyl to form an amide. Even though this reaction generally requires a high temperature (T>150 °C); amide formation at moderate temperatures (70–100 °C) has been reported (Morawetz and Otaki 1963). In this study, the oxidized starch is used to react with the protein during blending, creating a compatibilizer *in situ*.

Aldehyde starch (St-CHO) can be produced by oxidizing native starch with sodium hypochlorite in the presence of the 2,2,6,6-Tetramethylpiperidine-1-oxyl radical (TEMPO) and NaBr. TEMPO-mediated oxidation has been applied to the selective oxidation of

different polysaccharides (De Nooy et al., 1995a; 1995b; 1996). The functionality of the aldehyde groups has been widely explored in many industries, particularly the paper, textile, and building materials industries (Chang et al., 2008).

In a previous publication, we reported an investigation on the effect of simple shear on starch-zein blending (Habeych et al., 2008). For this, we developed a new in-house shearing device that induced different structures in starch-zein blends. Microscopic observations of the starch-zein blends revealed that the starch formed the continuous phase and zein a dispersed phase with a poor adhesion between the two. This poor adhesion was confirmed with mechanical tests. Therefore, the present chapter reports on the improvement of the adhesion properties of starch-zein blends by addition of a pre-made compatibilizer under simple shear conditions. To achieve this, starch-zein blends with different protein concentrations were combined with St-CHO under simple shear conditions at 95 °C. The interfacial adhesion of the starch-zein blends was evaluated with field emission scanning electron microscopy (FESEM) and confocal scanning laser microscopy (CSLM) imaging. Large deformation tests were carried out to evaluate the tensile properties of the compatibilized starch-zein blends.

2. Materials and methods

2.1 Materials

Native wheat starch was purchased from Latenstein BV (The Netherlands). The moisture content was 11.7±0.1% w/w. Corn zein (Z3625) was obtained from Sigma-Aldrich (Zwijndrecht, The Netherlands), with a moisture content of 5.8±0.1% w/w. Glycerol (<0.1% H_2O) was obtained from Acros Organics (Geel, Belgium) and ethanol (<5% H_2O) from Merck Chemicals (Germany). The moisture contents of the powders were determined using the Sartorius MA-30 moisture analyzer (Goettingen, Germany). The water content of the starch was taken into account in all experiments. 2,2,6,6-Tetramethylpiperidine-1-oxyl radical (TEMPO) (Fluka), sodium hypochlorite (Sigma-Aldrich), chloridric acid, sodium bromide, sodium hydroxide, and other chemicals and solvents were of analytical grade (Merck), and used without further purification. Acetic acid (Merck), fuchsin acid, and dimethylsulfoxide (DMSO) used for the sample preparation for NMR, FESEM, and CSLM were of analytical grade.

2.2 Oxidation preparation

A gelatinized starch solution of 4.4% w/v starch (80 g) was prepared while heated at 90 °C for 30 min. The solution was then cooled to 4 °C and subjected to the following oxidation: TEMPO (0.25 g) and sodium bromide (0.50 g) were dissolved in 30 ml water and added to the gelatinized starch solution. The pH of the solution was adjusted to 10 with 2 M NaOH. Then, 91 mL of 13% sodium hypochlorite solution was added drop by drop to the starch solution, while the pH was maintained at 10 by continuous addition of 2 M NaOH using a pH-stat (719 S - Titrino automatic titrator, Metrohm, The Netherlands). The volume of the added 2.0 M NaOH solution was monitored. The reaction time, determined as the time taken for the consumption of 2 M NaOH to maintain the pH at 10, was in the range between 80 to 90 min.

When the oxidation was finished, the pH was adjusted to 5 by adding 1.8 M HCl. The oxidized products were precipitated by adding 95% ethanol. The precipitated wet sample was washed twice with acetone followed by centrifugation. The resulting material was freeze dried in a Christ Epsilon 2-6D freeze dryer (Osterode am Harz, Germany). The freeze-dried samples were cryo-grinded in an analytical mill (type A10) from IKA (Staufen, Germany). The resulting fine powder was stored at –20 °C.

2.3 Sample preparation

Prior to shear processing, the starch-zein premix was prepared using the protocol described earlier (Habeych et al., 2008). The mixtures were freeze-dried, grinded, and stored as was indicated above for the oxidized starch. A homogenous mixture containing starch-zein and oxidized starch with dough-like consistency was then prepared by adding water and glycerol (plasticizers) 1 h before processing. When St-CHO was used, it was added at 5% (w/w) of the mixture. This implies that the ratio between native starch and zein was the same as in the uncompatibilized case but the total solids content was 5% higher. The effect of the solids content was tested by comparing the gelatinization process of the native starch with and without St-CHO with precisely the same amount of solid content.

2.4 Shear cell processing

The combined starch-zein mixture was transferred to the shear cell device (Wageningen University, The Netherlands), which is depicted in Figure 1A. Inside the shear cell (190 mL sample volume), the mixture is subjected to a simple shear flow field, established between the cone and the plate (i.e., the bottom cone) (i.e., angle α_{plate}=105°, α_{cone}=100°). The stationary cone and rotating plate were heated electrically and cooled with water. The cone

and plate contain separate heaters with temperature controller. The device was attached to a Brabender Do-Corder 330 (Brabender OHG, Duisburg, Germany) to enable shear rate control, and temperature and recording of the torque. After filling the shearing zone with the starch-zein mixture, the cone-plate cell was closed and a vertical pressure (250 kPa) was applied and kept constant during the experiments. The mixture was then subjected to the following shear treatment: 1 min at 2 rpm (4.3 s^{-1}), then an increase in 29 min from 2 rpm to the desired rpm value (30 or 50 rpm, equivalent to 72 and 120 s^{-1} respectively). This shear rate was continued for an additional 10 min. After processing, the material was cooled in the cell to room temperature at a rate of about 1.2 °C min^{-1}. The processed blends were then stored at –40 °C prior to further analysis. The measured torque curves were calibrated relative to the measured torque value at t=0. The shear rate ($\dot{\gamma}$ in s^{-1}), shear stress (τ in kPa), and specific mechanical energy input (SME in kJ kg^{-1}) into the material were calculated following the method described previously (Habeych et al., 2008). After shearing the starch-zein blends, a visual inspection of a homogenous surface with the presence of lines in the blends originated from the grooves in the cone and plate geometry was used as a signal of good shearing process without slippage.

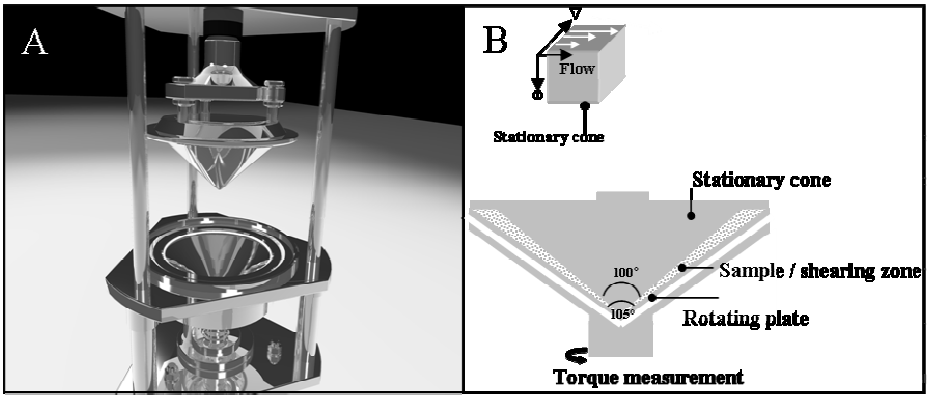

Figure 1. *An new, improved version of the shear cell device. (A) Animation and (B) schematic overview of the shear cell device. Cone angle=100°, angle between cone and plate (shearing zone), θ=2.5°.*

2.5 Compression molding

In order to separate the effect of heat from shear, starch-zein blends containing St-CHO were molded at 95 °C following the procedure reported earlier (Habeych et al., 2008).

2.6 Confocal scanning laser microscopy

The method used to analyze the microstructure of the blends by confocal scanning laser microscopy (CSLM) was described in the previous work (Habeych et al., 2008). Each presented image corresponds to a flat projection of the *Z* stack (512×512 μm^2). From these results, the morphology of materials was quantified by image analysis following the procedure reported earlier. From this analysis, the number of particles and the zein surface ratio (ZSR) defined as the ratio between the surface covered by zein and the total surface of an image were obtained.

2.7 Scanning electron microscopy

Microstructural aspects of the starch-zein blends were observed with a field emission scanning electron microscope (FESEM) at ambient temperature. Dry samples were prepared according to the method based on (Manski et al., 2007) to observe the blend without interference from a water phase.

Freeze fracturing was performed before the samples were glued onto a sample holder using conductive carbon cement (Leit-C, Neubauer Chemicalien, Germany) and subsequently sputter coated with 20 nm platinum (JFC 1200, JEOL, Japan). The fractured surfaces were analyzed with a FESEM (JEOL 6300 F, Tokyo, Japan) at room temperature using a working distance of 8 mm, with SE detection at 3.5–5 kV. All images were recorded digitally (Orion, 6 E.L.I. sprl., Belgium) at a scan rate of 100 s (full frame) at a size of 2528×2030, 8 bit. Noise reduction and resizing of the images were done using Adobe Photoshop CS.

2.8 Large-scale deformations

A Texture Analyzer T2 (Instron - 5564 Series Table Model Systems - Twin column design, USA) was used for large deformation tests. Before the measurement, the starch-zein blends were defrosted at room temperature. The samples were cut into a dog-bone shape with a custom-made mould, according to ASTM D638 type IV. The thickness ($e \approx 4$ mm), was measured precisely with a micrometer model 7305 (Mitutoyo, Japan) for each specimen. Uniaxial tensile tests were conducted with a constant crosshead speed of 3 mm min^{-1}, until sample fracture. All measurements were done at least in triplicate. From the obtained stress-strain curve, tensile strength (σ) and tensile elongation (ε) of the samples were calculated as follows:

$$\sigma = \frac{F}{A_0} \quad \text{(MPa)}, \tag{1}$$

where F (N) is the maximum tensile force and A_0 (mm^2) is the initial cross-section of the specimen at the start, and

$$\varepsilon = \frac{L_M - L_0}{L_0} \ 100 \ (\%), \tag{2}$$

where L_0 (mm) is the original length and L_M (mm) is the elongation length.

To test the anisotropy of the material, specimens were cut along the flow ($\parallel$) and vorticity ($\perp$) directions (see Figure 1B).

2.9 Rapid Visco-Analyser

The pasting properties of the starch samples were determined using a Rapid Visco-Analyser-4 (RVA) (Newport Scientific Pvt. Ltd., Warriewood, Australia). After grinding and sieving (500-µm wide mesh), 3.0 g of sample (dry base) and a weighed amount of distilled water were mixed and stirred in the aluminium RVA sample canister to make a 10.7% starch suspension (w/w). The time-temperature sequence was as follows: an initial stage at 50 °C for 2 min, followed by heating to 95 °C at a constant heating rate of 5–6 °C min^{-1}, maintaining temperature at 95 °C for 5 min and then cooling to 50 °C at the same rate. Pasting temperature (P_{temp}), peak viscosity, hot paste viscosity, breakdown (peak minus hot paste viscosity), and final or cold paste viscosity were obtained.

2.10 Nuclear Magnetic Resonance

The structure of St-CHO was confirmed by ^{1}H-nuclear magnetic resonance (NMR) spectroscopy. ^{1}H-NMR spectrum of St-CHO dissolved in 99.9% D_2O (Cambridge Isotope Laboratories, USA) was recorded with 2048 scans with a repetition delay of 11.4 s at 60 °C on a Bruker AMX-500 located at the Wageningen NMR Centre.

3. Results & discussion

3.1 ^{1}H-NMR spectra of the oxidized products

Figure 2 illustrates ^{1}H-NMR spectra of the oxidized products. A small signal due to C6 aldehyde protons were detected at 9.2 ppm for the oxidized products with 2.3% of the total C6 (see inset in Figure 2). For ^{1}H-NMR spectra of native starch, we refer to (Kato et al.,

2003). The TEMPO-mediated oxidation of primary hydroxyl to carboxyl groups can be expressed according to the stoichiometric formulae suggested by Kato (Kato et al., 2003). Two moles of NaClO and one mole of NaOH are consumed for the oxidation of one mole of primary hydroxyl group. Therefore, the amount of aldehyde species produced can be estimated by following the consumption of NaOH solution used to maintain the pH at 10. According to this scheme, the maximum theoretical percentage of oxidized species produced in the oxidised starch was calculated to be 7±1%, however, their quantities were lower (i.e., 2.3% of the total C6) as was indicated before. During the C6 selective oxidation process, side reactions, such as the degradation and the oxidation of reduced end groups formed by the degradation, are inevitable and have an effect on the consumption of NaOH (De Nooy et al., 1996; Kato et al., 2003). Therefore, the true amount of aldehyde groups is less than the stoichiometrically determined maximum amount. The next signal was observed in the range of 5.2 – 5.7 ppm, which is partially due to the formation hemiacetals in C6. Finally, a signal was observed at 4.2 ppm, which corresponds to the complete oxidized form of the C6 primary hydroxyl group of starch formation of α-1,4-linked polyglucuronic acid Na salt. Similar results were previously presented (Kato et al., 2003). In this manner, the material obtained after TEMPO-mediated oxidation showed the presence of the reactive functional group (aldehyde) on a starch.

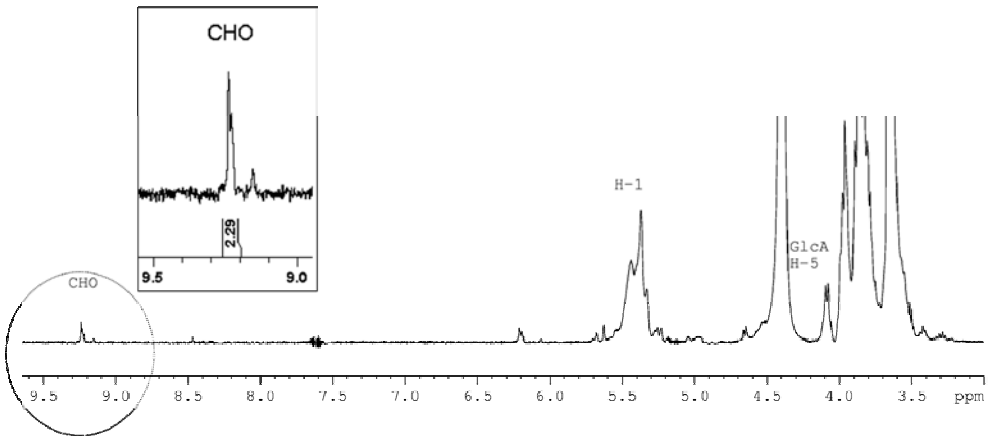

Figure 2. *^{1}H-NMR spectra of oxidized starch by the TEMPO-NaBr-NaClO system. The inset shows the enhanced ^{1}H-NMR signal for aldehyde starch; the value below represents the obtained percentage of this specie in the sample.*

3.2 Blends processing

Effect of St-CHO on native starch and on starch-zein blend

In contrast to the white color of the thermoplastic starch-water-glycerol mixture, the addition of St-CHO to this mixture under simple shear conditions led to a brown material (Figure 3). This colour suggests the occurrence of a type of browning reactions possibly caused by oxidation, non-enzymatic browning reactions, and Maillard reactions.

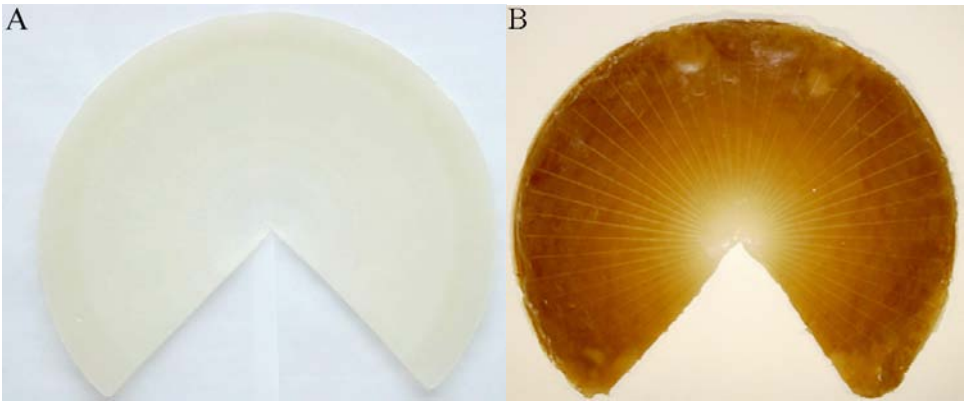

Figure 3. *(A) Thermoplastic starch sheared at $\dot{\gamma}$=72 s^{-1} for 40 min; (B) 90:10 starch-St-CHO blend sheared at $\dot{\gamma}$=72 s^{-1} for 40 min.*

Recordings of the torque during shearing of blends with different starch-zein ratios showed a single peak (Figure 4), which is the result of gelatinization of the starch. The addition of St-CHO gave higher torque values. This high shear stress obtained can be rationalized as an effect of chemical crosslinks of the starch induced under shear conditions. This effect was also reported by (Veelaert et al., 1997), who ascribed it to the formation of inter- and intramolecular hemiacetal and acetal linkages. In patent literature, aldehyde starch has been identified as an interesting additive to achieve fully gelatinized starch at relatively low temperature and plasticizer content (Thornton et al., 2005).

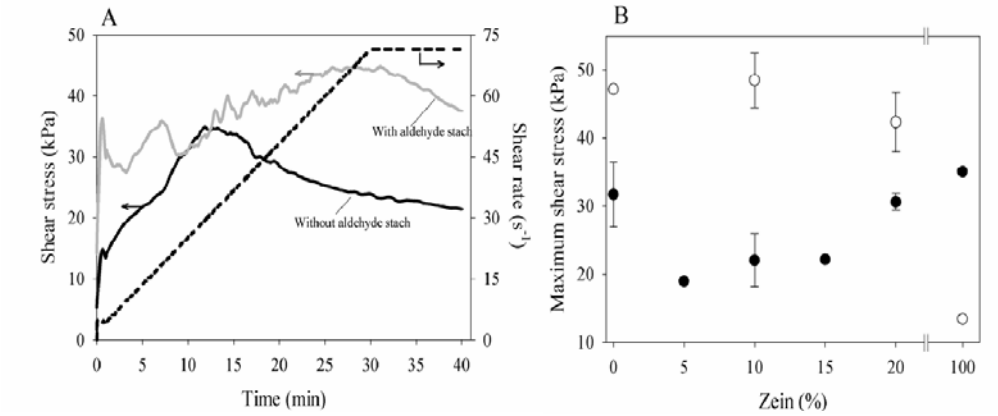

Figure 4. *(A) Shear stress profiles for thermoplastic starch (without zein) processed under the indicated shear treatment with a maximum shear rate of* $\dot{\gamma}$ *=72* s^{-1}*; (B) maximum shear stresses under simple shear flow as a function of the zein content. (●), uncompatibilized system; (○), compatibilized system.*

Table 1 presents the specific mechanical energy (SME) values obtained during blending. The addition of St-CHO to the starch-zein blends increases the SME values by a factor of two.

Table 1. *Treatment conditions and SME results for starch-zein blends processed in the shear cell at 95 °C for 40 min*

Starch:zein ratio (db)	Maximum shear rate (s^{-1})	SME (kJ kg^{-1})
100:0[a]	72	1397 (2430)[b]
95:05	72	801
90:10[a]	0	-
	72	728 (2349)[b]
	120	1310 (2971)[b]
85:15	72	974
80:20[a]	0	-
	72	964 (2170)[b]
	120	1558 (2230)[b]
0:100[a]	72	1449 (637)[b]

[a]Conditions tested also with the addition of St-CHO. [b]Blends containing St-CHO.

The addition of St-CHO to pure plasticized zein (0:100 blend), however, showed a notable reduction in SME. Figure 4B summarizes the peak values in the shear stress observed as a function of the zein concentration at $\dot{\gamma}$ =72 s^{-1}. The peak value increases with the presence of St-CHO. Previous work on starch degradation under simple shear condition showed a direct relation between maximal peak stresses during heating-shearing treatment with the reduction of molecular weight of starch (Van den Einde et al., 2004; 2005). Based on these studies, it is suggested that the degree of macromolecular degradation increases with the addition of St-CHO. However, the full extent of the increased breakdown is masked by the formation of additional chemical crosslinks.

Pasting behavior

Figure 5 shows the pasting viscosity profiles of starches analyzed using the Rapid Visco-Analyser (RVA). When native starch is heated above a certain temperature in the presence of excess water (>66% w/w), it gelatinizes (Ratnayake & Jackson, 2007). Nevertheless, the term gelatinization is not exactly appropriate to describe the changes that occur during heating of St-CHO because the formation of oxidized starch was done with fully gelatinized starch, and the random chemical modification inhibits retrogradation or recystallization.

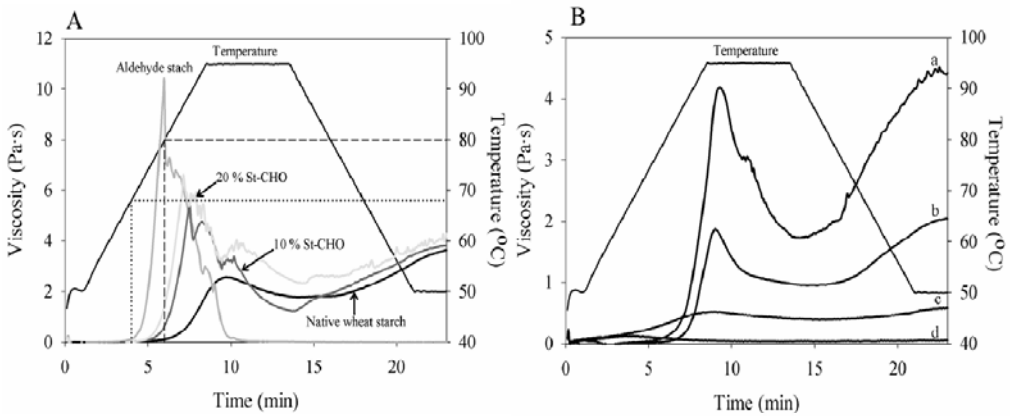

Figure 5. *(A) RVA pasting curves (A) native wheat starch, aldehyde starch (St-CHO), and blends with different St-CHO concentration; (B) Different starch-zein blends (a) 90:10 starch:zein with St-CHO, (b) 90:10 starch:zein, (c) Sheared 90:10 starch:zein, and (d) sheared 90:10 starch:zein with St-CHO. RVA: Rapid Viscous Analyzer. (a) and (b) are before, (c) and (d) are after shearing. Dash and dotted lines indicate the pasting temperatures for native wheat starch and aldehyde starch, respectively.*

Fig. 5A shows the effect of aldehyde starch (St-CHO) in starch-St-CHO mixtures (i.e., without zein). The highest pasting temperature (P_{temp}) was observed for unmodified native wheat starch (i.e., 80 °C - see dash line), which decreased with the addition of St-CHO, down to 68 °C for pure St-CHO (see dotted line). Similar results were reported for corn starch in presence of TEMPO-mediated partially oxidized corn starch (Suh et al. 2002). The peak viscosity was four times higher for St-CHO than for the native starch. A high peak viscosity is an indication of the water-binding capacity of the starch, which is related to the stronger hydrophilicity induced by the presence of carboxyl groups formed during the oxidation process (Chang et al. 2008; Suh et al. 2002). Suh et al. (2002) suggested that this high peak was probably the result of a network formation between soluble amylose and the oxidised starch. The addition of 10 and 20% (w/w) of St-CHO to the native wheat starch resulted in a broader gelatinization range and slightly higher final viscosity than the native starch alone.

Fig. 5B shows the effect of St-CHO on the pasting behavior of 90:10 starch-zein blends before and after processing. Before processing, the addition of St-CHO induced a faster swelling with a wider gelatinization range, and a peak viscosity that was twice as high as for the blend without St-CHO (compare curves a and b). This effect was also observed for mixtures without zein (Fig. 5A), suggesting that the pasting behaviour is dominated by the starch phase. The quick increase of the paste viscosity after processing at low temperatures indicated that starch granules were disrupted during shearing (see curve c with d). Comparing the pasting behaviour with the shear stress peaks in Fig. 4B, suggests that blends containing St-CHO (higher shear stress peak) suffer from significant molecular breakdown, resulting in a low peak viscosity.

3.3 Microstructure of the blends

FESEM was used to analyze the adhesion between starch and zein while CSLM was used to study the distribution, size, and orientation of the phases. Figure 6 shows characteristic images of the zein domains in the starch matrix, for uncompatibilized and compatibilized blends.

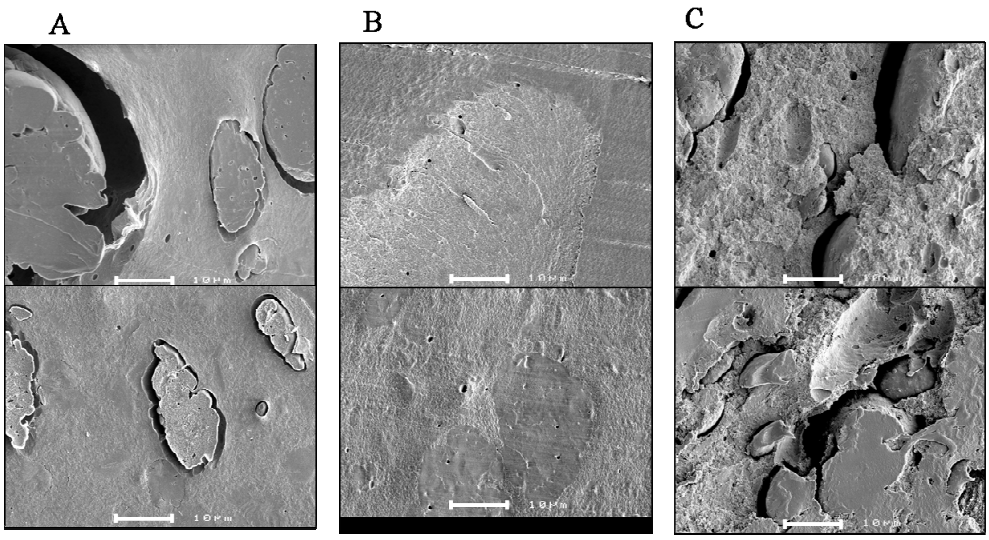

Figure 6. *Field emission electron micrograph showing the zein flocs in starch-zein blends processed at 95 °C. (A) uncompatibilized 90:10 starch-zein blend; (B) compatibilized 90:10 starch-zein blend; (C) compatibilized 80:20 starch-zein blend. Scale bar: 10 μm.*

In contrast to the voids observed between zein domains and the matrix in the uncompatibilized blend (Figure 6A), the compatiblized 90:10 starch-zein shows a continuous interface (Figure 6B). Thus, St-CHO may well act as a compatibilizer between the two phases, by introducing covalent bonds across the interface. In case of the compatibilized 80:20 starch-zein ratio the adhesion was not as good as with the 90:10 blends (Figure 6C). Because the absolute concentration of St-CHO was the same in all blends, it is possible that the amount of St-CHO added was not enough to obtained a fully compatabilized interface. Therefore, we conclude that the main aim of compatibilization, being the enhancement of adhesion between the phases, can be accomplished through the addition of St-CHO, but that it seems to be not very weight effective. This can be understood from the fact that a starch chain crosslinked to a zein molecule is a very large molecule, which will therefore not be weight effective. In other words, good compatabilization can only obtained though using a large amount of oxidized starch.

Figure 7 shows the morphological distribution of compatibilized starch-zein blends with 90:10 and 80:20 starch-zein ratios processed at three different shear rates. The red areas depict the protein phase and green areas represent the starch phase. Under shearless conditions (compression molding experiment), the analyzed starch-zein blends showed a

morphology similar to the uncompatibilized blend described earlier (Habeych et al., 2008). The values of the ZSR and the swelling factor obtained from image analysis for the compatibilized 90:10 starch-zein blend did not show statistical differences with the uncompatiblized blend (Table 2). This suggests that St-CHO does not have an effect on the development of the morphology of the blend under shearless conditions. Under shear conditions, small protein domains were formed without any specific orientation. Increasing the shear rate or the zein concentration, a reduction in the swelling factor (β) was observed (Table 2). This reduction is a result of the mass transfer of the plasticizers from zein phase (less hydrophilic) to the thermoplastic starch phase upon processing and gelatinization as was earlier reported (Habeych et al., 2008).

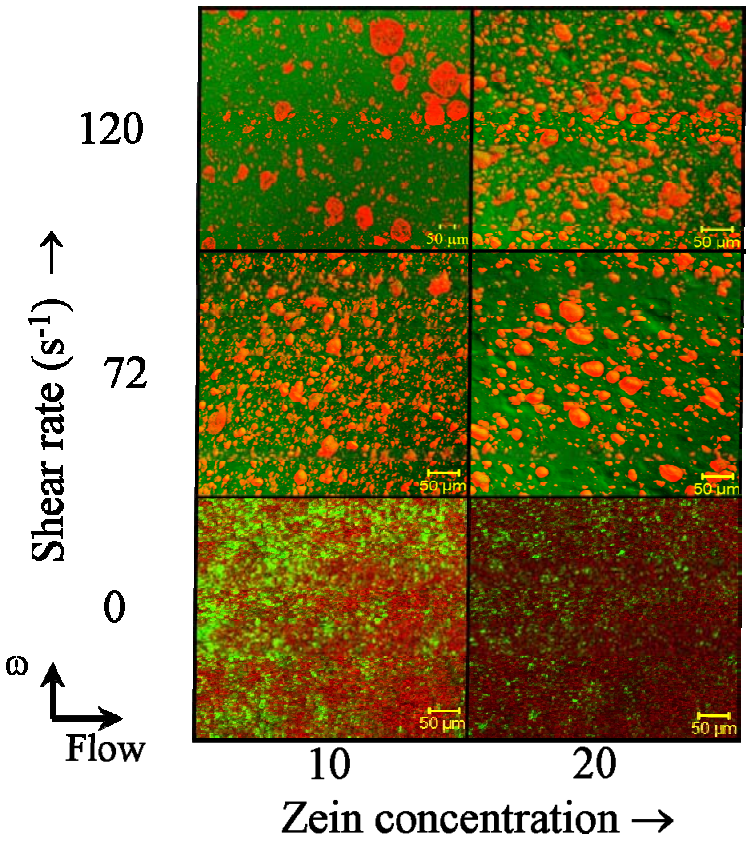

Figure 7. *Morphology of compatibilized starch-zein blends processed at 95 °C under different shear rates for 40 min (CSLM pictures). Flow direction: from left to right.*

Table 2. *Zein surface ratio (ZSR) and swelling factor (β) obtained for starch-zein blends by using CSLM image analysis*

Starch:zein ratio (db)	Maximum shear rate (s^{-1})	Zein surface ratio (ZSR)	Swelling factor (β)
95:05	72	16.9±2.3	3.4±0.5
90:10[a]	0	36.8±10.3 (43.9±4.1)[b]	3.7±1.0 (4.4±0.4)[b]
	72	14.6±7.3 (31.6±1.5)[b]	1.5±0.7 (3.2±0.2)[b]
	120	20.6±3.7 (14.9±2.4)[b]	2.1±0.4 (1.5±0.2)[b]
85:15	72	18.2±16.9	1.2±1.1
80:20[a]	0	(76.1±1.7)[b]	(3.9±1.1)[b]
	72	22.7±0.3 (22.7±2.6)[b]	1.2±0.0 (1.2±0.1)[b]
	120	30.2±6.4 (33.4±1.7)[b]	1.5±0.3 (1.7±0.1)[b]

[a]Conditions tested also with the addition of St-CHO. [b]Blends containing St-CHO.

Figure 8 shows the number of zein particles as a function of the starch:zein ratio. A drop in the number of zein particles was earlier observed as a signal of coalescence (Habeych et al., 2008).

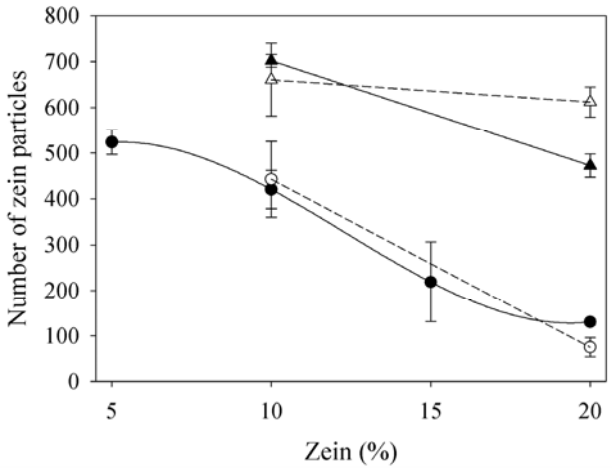

Figure 8. *Effect of St-CHO on the coalescent of zein particles. Circles: uncompatibilized blends; triangles: compatibilized blends. Filled symbols: blends processed at* $\dot{\gamma}$ *=72* s^{-1}*; open symbols: blends processed at* $\dot{\gamma}$ *=120* s^{-1}*.*

Unlike the uncompatibilized blends, the number of zein particles remains approximately constant for the 80:20 starch-zein blends. However, the 90:10 starch-zein blends showed a drop on the number of particles, albeit less steep than in the case of the uncompatibilized system. The addition of St-CHO thus partially suppressed the coalescence of the zein domains. In addition, aldehyde starch reduced the formation of large zein domains formed during shearing of starch-zein blends as was found earlier for the uncompatibilized 80:20 blend.

3.4 Mechanical properties

Effect of St-CHO on native starch

Figure 9 shows the stress-strain diagram for wheat starch with and without St-CHO blend. One can see a clear anisotropy, independent of the presence of St-CHO, where the tensile stress showed a marked difference along the flow (∥) and vorticity (⊥) directions, being higher along the flow direction. Along the flow, the starch molecules were subjected to larger stresses, leading to more molecular alignment, but, the addition of the St-CHO did not influence this effect significantly. The addition of St-CHO reduces the strength of the starch (due to increase molecular breakdown) and increases the elongation of sample. Long elongation at break is typically associated to a high degree of entanglement of the polymers, for example induced by the introduction of intermolecular crosslinks (Follain et al., 2005).

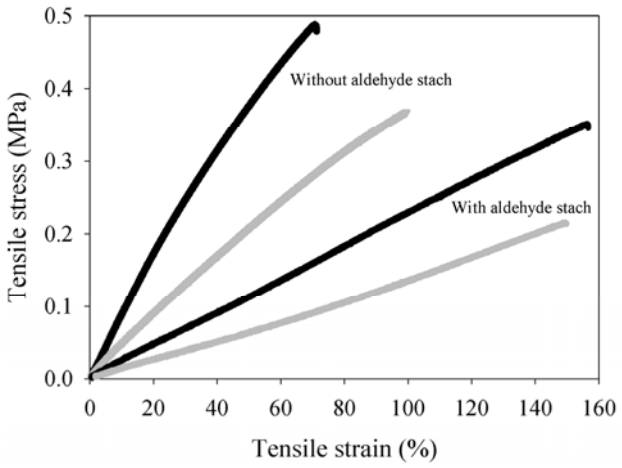

Figure 9. *Typical shear-stress-strain curve (obtained by tensile test) of thermoplastic starch in two different directions. The tensile properties were measured along the flow (∥) direction (in black) and vorticity (⊥) direction (in gray) in the shear cell device.*

Effect of St-CHO on starch-zein blends

Figure 10 depicts the normalized mechanical properties (tensile strength and tensile elongation) of uncompatibilized and compatibilized starch-zein blends as a function of the zein content.

The normalized values of the tensile strength of the uncompatibilized system dropped to about 60% of the initial value obtained for 100:0 starch-zein in the 80:20 starch-zein blend (Figure 10A). In contrast, compatibilized blends showed a remarkable constant value close to the tensile strength of the compatibilized starch matrix.

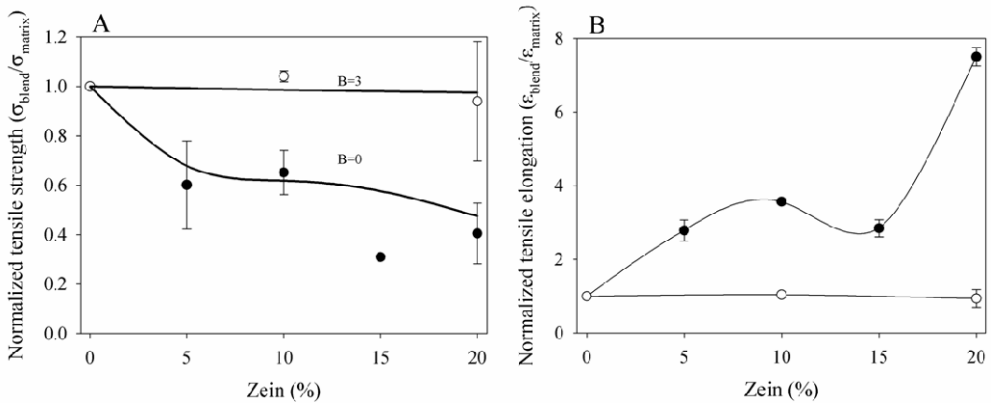

Figure 10. *Mechanical properties of starch-zein blends in two different directions as a function of the zein concentration. (A) Normalized tensile strength and (B) Normalized tensile elongation.* (●)*, uncompatibilized system;* (○)*, compatibilized system. The bars indicate the mean±average standard deviation.*

Depending on the adhesion between the zein particles and the starch matrix, a different degree of interfacial bonding can be defined: poor adhesion, good adhesion and some adhesion. Previous work showed that uncompatibilized starch-zein blends followed a modified model used for particle-matrix materials with weak adhesion between the phases (Habeych et al., 2008). Furthermore, a similar model developed to describe the strength of the blend with different degree of interfacial bonding as a function of the fillers concentration was proposed by Turcsányi (Turcsányi et al., 1988). The authors introduce a parameter proportional to the load carried by the dispersed component, *B*, and presented an empirical equation:

$$\frac{\sigma_{blend}}{\sigma_{matrix}} = \left(\frac{1-\phi}{1+2.5\phi} \right) e^{B\phi}, \quad (3)$$

in which the ultimate strength of the composite, σ_{blend}, relative to the strength of the matrix σ_{matrix}, is determined by the volume fraction of particles, ϕ. However, Eq. (3) needs to include a correction factor due to the swelling of the protein phase, as follows:

$$\frac{\sigma_{blend}}{\sigma_{matrix}} = \left(\frac{1-\beta\phi}{1+2.5\beta\phi} \right) e^{B\beta\phi}, \quad (4)$$

where β is a swelling factor that accounts for the increase of the volume fraction by swelling of the protein due to the presence of glycerol and water. This swelling factor was obtained from image analysis as was described earlier (Habeych et al. 2008). Table 2 shows the values for compatibilized and uncompatibilized blends obtained from image analysis. In spite of the lack of physical meaning of the fitting constant *B*, it has been connected with the interfacial properties of the system. For systems with poor adhesion, B=0 is found (Liang & Li, 1998; Turcsanyi et al., 1988), while in systems where the strength increases with higher ϕ (a sign of good adhesion), $B \geq 3$ (Liang & Li, 1998). As can be seen in Figure 10A, the compatibilized starch-zein blends follow the modified Turcsányi model with good adhesion, while the uncompatibilized blends behaves according to the non-adhesive model. Interfacial adhesion is therefore improved by addition of St-CHO.

Please note that the normalization on the strength of the pure starch corrects for changes in the properties of the starch matrix, which was noted before. The analysis here is therefore exclusively coupled to the presence of the zein phase.

The normalized tensile elongation for the uncompatibilized blends increases with zein concentration while the compatibilized blends remain approximately constant (Figure 10B). High elongation of the starch-zein blends has been associated to poor adhesion (Habeych et al., 2008) and therefore this confirms the conclusion that the uncompatibilized blend has poor adhesion, while the compatibilized blends shows good adhesion.

4. Conclusions

Blends of starch and zein were found to exhibit poor adhesion between the starch matrix and the zein domains. A compatibilizer was prepared by oxidizing starch, which introduced aldehyde groups. Addition of this component to a starch-zein blend resulted in good adhesion and mechanical properties indicative of that good adhesion.

The mechanism probably is that some of the aldehyde groups in the starch react with zein, forming a compatibilizer *in situ*. The large molecular weight of the resulting compatibilizer implies that the system was not weight effective: addition of 5% (w/w) to a 90:10 starch:zein blend was sufficient, but not for an 80:20 blend.

The mechanical properties of the starch matrix itself were modified by addition of the oxidised starch, showing much higher viscosities, and larger breakdown, which indicates formation of physical or chemical crosslinks inside the starch phase as well.

Acknowledgments

The authors thank Jacqueline Donkers for assistance with the scanning electron microscope, Frans Kappen for the RVA, Peter de Waar for the ^{1}H-NMR, and Dr. Carmen Boeriu for the stimulating conversations over TEMPO. This research was conducted within the framework of the Carbohydrate Research Centre at Wageningen.

References

1. Avérous, L. (2004). Biodegradable multiphase systems based on plasticized starch: A review. *Journal of Macromolecular Science - Polymer Reviews*, 44(3), 231-274.
2. Chang, P.S., Park, K.O., Shin, H.K., Suh, D.S., & Kim, K.O. (2008). Physicochemical properties of partially oxidized corn starch from bromide-free tempo-mediated reaction. *Journal of Food Science*, 73(3), C173-C178.
3. Corradini, E., de Carvalho, A.J.F., Curvelo, A.A.daS., Agnelli, J.A.M., & Mattoso, L.H.C. (2007). Preparation and characterization of thermoplastic starch/zein blends. *Materials Research*, 10(3), 227-231.
4. De Nooy, A.E.J., Besemer, A.C., & Van Bekkum, H. (1995a). Highly selective nitroxyl radical-mediated oxidation of primary alcohol groups in water-soluble glucans. *Carbohydrate Research*, 269(1), 89-98.
5. De Nooy, A.E.J., Besemer, A.C., & Van Bekkum, H. (1995b). Selective oxidation of primary alcohols mediated by nitroxyl radical in aqueous solution. Kinetics and mechanism. *Tetrahedron*, 51(29), 8023-8032.
6. De Nooy, A.E.J., Besemer, A.C., Van Bekkum, H., Van Dijk, J.A.P.P., & Smit, J.A.M. (1996). Tempo-mediated oxidation of pullulan and influence of ionic strength and linear charge density on the dimensions of the obtained polyelectrolyte chains. *Macromolecules*, 29(20), 6541-6547.

7. De Nooy, A.E.J., Besemer, A.C., & Van Bekkum, H. (1996). On the use of stable organic nitroxyl radicals for the oxidation of primary and secondary alcohols. *Synthesis*, 10, 1153-1174.
8. Follain, N., Joly, C., Dole, P., & Bliard, C. (2005). Mechanical properties of starch-based materials. I. Short review and complementary experimental analysis. *Journal of Applied Polymer Science*, 97(5), 1783-1794.
9. Ghodgaonkar, P.G. & Sundararaj, U. (1996). Prediction of dispersed phase drop diameter in polymer blends: The effect of elasticity. *Polymer Engineering and Science*, 36(12), 1656-1665.
10. Habeych, E., Van der Goot, A.J., & Boom, R. (2007). Prediction of permeation fluxes of small volatile components through starch-based films. *Carbohydrate Polymers*, 68(3), 528-536.
11. Habeych, E., Dekkers, B., Van der Goot, A.J., & Boom, R. (2008). Starch-zein blends formed by shear flow. *Chemical Engineering Science*, 63(21), 5229-5238.
12. Huang, H.C., Chang, T.C., & Jane, J. (1999). Mechanical and physical properties of protein-starch based plastics produced by extrusion and injection molding. *JAOCS, Journal of the American Oil Chemists' Society*, 76(9), 1101-1108.
13. Kato, Y., Matsuo, R., & Isogai, A. (2003). Oxidation process of water-soluble starch in tempo-mediated system. *Carbohydrate Polymers*, 51(1), 69-75.
14. Li, X. & Pelton R. (2005). Enhancing wet cellulose adhesion with proteins. *Industrial and Engineering Chemistry Research*, 44 (19), 7398–7404.
15. Liang, J.Z. & Li, R.K.Y. (1998). Prediction of tensile yield strength of rigid inorganic particulate filled thermoplastic composites. Journal of Materials *Processing Technology*, 83(1-3), 127-130.
16. Lim, S.T. & Jane, J.L., 1993. Water-resistant starch-protein thermoplastics. WO9319125.
17. Lin, B., Mighri, F., Huneault, M.A., & Sundararaj, U. (2005). Effect of premade compatibilizer and reactive polymers on polystyrene drop deformation and breakup in simple shear. *Macromolecules*, 38(13), 5609-5616.
18. Manski, J.M., Van der Goot, A.J., & Boom, R.M. (2007). Formation of fibrous materials from dense calcium caseinate dipersions. *Biomacromolecules*, 8(4), 1271-1279.
19. Morawetz, H. & Otaki, P.S. (1963). Kinetics and equilibria of amide formation in aqueous media. *Journal of American Chemistry Society*, 85, 463–468.
20. Paulis, J.W. (1982). Recent developments in corn protein research. *Journal of Agricultural and Food Chemistry*, 30(1), 14-20.

21. Ratnayake, W.S. & Jackson, D.S. (2007). A new insight into the gelatinization process of native starches. *Carbohydrate Polymers*, 67(4), 511-529.
22. Rouilly, A. & Rigal, L. (2002). Agro-materials: A bibliographic review. *Journal of Macromolecular Science - Polymer Reviews*, 42(4), 441-479.
23. Shukla, R. & Cheryan, M. (2001). Zein: The industrial protein from corn. *Industrial Crops and Products*, 13(3), 171-192.
24. Suh, D.S., Chang, P.S., & Kim, K.O. (2002). Physicochemical properties of corn starch selectively oxidized with 2,2,6,6-tetramethyl-1-piperidinyl oxoammonium ion. *Cereal Chemistry*, 79(4), 576-581.
25. Thornton, J.W., Slaghek, T.M., Timmermans, J.W., Jetten, J.M., & Thiewes, H.J., (2005). Process for gelatinising starch using a biodegradable polymer material bearing aldehyde groups. WO2005/090462 A1.
26. Turcsányi, B., Pukanszky, B., & Tudos, F. (1988). Composition dependence of tensile yield stress in filled polymers. *Journal of Materials Science Letters*, 7(2), 160-162.
27. Utracki, L.A. (2002). Compatibilization of polymer blends. *Canadian Journal of Chemical Engineering*, 80(6), 1008-1016.

28. Van den Einde, R.M., Akkermans, C., Van der Goot, A.J., & Boom, R.M. (2004). Molecular breakdown of corn starch by thermal and mechanical effects. *Carbohydrate Polymers*, 56(4), 415-422.
29. Van den Einde, R.M., Van der Veen, M.E., Bosman, H., Van der Goot, A.J., & Boom, R.M. (2005). Modeling macromolecular degradation of corn starch in a twin screw extruder. *Journal of Food Engineering*, 66(2), 147-154.
30. Veelaert, S., De Wit, D., Gotlieb, K.F., & Verhe, R. (1997). Chemical and physical transitions of periodate oxidized potato starch in water. *Carbohydrate Polymers*, 33(2-3), 153-162.
31. Wang, X.L., Yang, K.K., & Wang, Y.Z. (2003). Properties of starch blends with biodegradable polymers. *Journal of Macromolecular Science - Polymer Reviews*, 43(3), 385-409.

6

Compatibilization of starch-zein blends under shear flow

This chapter has been published as: Habeych, E., Van der Goot, A.J., Adachi, S., & Boom, R. (**2009**). Compatibilization of starch-zein blends under shear flow. *Proceedings 5th International Symposium on Food Rheology and Structure (ISFRS).*

Abstract

Blends of starch and zein were shown to have poor adhesion between the starch matrix and the zein domains. Aldehyde starch and rice bran extract could compatibilize these blends. Starch-zein blends plasticized with water and glycerol were prepared using an in-house developed shearing device. The adhesion between the phases was studied with scanning electron microscopy and by measuring the deformation properties of the blends. Both compatibilizers improved the adhesion between the zein and starch phases. Aldehyde starch formed additional crosslinks in the starch matrix which changed the matrix properties. However, after storage under controlled conditions, this blend showed a reduced effect on the mechanical properties, possibly caused by retrogradation of starch. The use of rice bran extract had high impact on the final product properties after storage; good compatibilization was achieved, which was not reduced after storage. The compatibilization by rice bran extract may be due to the presence of polysaccharide-protein complexes, which have emulsifying properties.

1. Introduction

Biodegradable materials such as starch-based blends have been widely studied as replacement for petroleum-based polymers (Avérous, 2004). Thermoplastic starch (TPS) can be prepared from granular starch mixed with plasticizers (glycerol, water and other polyols) using heat and shear. Both mechanical and thermal energy are generally needed to obtain the bioplastic polymer. However, starch-based plastics have some drawbacks, being swelling or even dissolution caused by water absorption, bad processability, ageing, and poor mechanical properties (Follain, 2005). To overcome these limitations while maintaining its biodegradability, blending of plasticized starch with another biodegradable polymer is a way to obtain composite materials with physical properties that are different from those of the pure components (Gáspár et al., 2005).

Recently, starch-zein blends have been reported to reduce the sensitivity of starch to water (Habeych et al., 2008). Zein, the major protein of corn (approximately 45-50% of the total protein) contains a high content of hydrophobic amino acids (Shukla & Cheryan, 2001), which makes this protein suitable to reduce the water diffusion trough starchy materials (Habeych et al., 2007). Nevertheless, the main drawback of the starch-zein blends is represented by the lack of adhesion between the polysaccharide and the protein giving consequently poor final properties (Habeych et al., 2008). In a recent publication, we reported on the use of aldehyde starch (St-CHO) as a manner to improve the adhesion between starch and zein (Habeych et al., 2009). Mechanical tests of fresh starch-zein samples blended with St-CHO showed enhancement on the performance of the material as a result of the better interaction between the starch and zein phase. However, St-CHO is not food-grade, which limits its applicability. Another possibility is the use of rice bran, a by-product obtained during the rice polishing process (Hata et al., 2008). Its possess functional properties such as radical scavenging, antioxidative and emulsifying activities, and negative mutagenecity, which make rice bran extract a interesting candidate to obtained a food-grade compatibilizer for starch-zein blend. Therefore, the aim of the present chapter is to compare the influence of St-CHO and rice bran extract as compatibilizers for starch-zein blends under shear conditions.

2. Materials and Methods

2.1 Materials

Native wheat starch was purchased from Latenstein BV (The Netherlands). Its moisture content was 11.7±0.1% w/w. Corn zein (Z3625) was obtained from Sigma-Aldrich

(Zwijndrecht, The Netherlands), with moisture content of 5.8±0.1% w/w. Rice bran extract was obtained by extraction with subcritical water according to (Khuwijitjaru et al., 2004) and provided by Tsuno Food Industrial Co. (Wakayama, Japan). Aldehyde starch (St-CHO) was prepared as described earlier (Habeych et al., 2009). Glycerol (<0.1% H_2O) was obtained from Acros Organics (Geel, Belgium) and ethanol (<0.05% H_2O) from Merck Chemicals (Germany). The moisture contents of the powders were determined using a moisture analyzer (Sartorius MA-30, Goettingen, Germany). The water content of the starch was taken into account in all experiments. Dimethylsulfoxide (DMSO) used for the sample preparation for FESEM was of analytical grade.

2.2 Sample preparation

Prior to shear processing, the 90:10 starch-zein premix was prepared using the protocol described earlier (Habeych et al., 2008). A homogenous mixture containing 90:10 starch-zein with and without compatibilizer with dough-like consistency was prepared by adding water and glycerol (plasticizers). In the case of compatibilized blends, rice bran extract and St-CHO were added at 2.5% and 5% (w/w) of the mixture, respectively.

2.3 Shear cell processing

The combined starch-zein mixture was transferred into the shear cell device (Wageningen University, The Netherlands). Details of the device can be found in a previous report (Habeych et al., 2008). The mixture was subjected to a simple shear field; its typical behavior is presented in Figure 1.

2.4 Microscopy

Microstructural aspects of the starch-zein blends were observed with a field emission scanning electron microscope (FESEM) at ambient temperature. Dry samples were prepared according to the method based on (Manski et al., 2007) to observe the blend without interference by water.

2.5 Large-scale deformations

Directly after processing, the blends were cut into a dog-bone shape according to ASTM method D638 type IV and stored for two weeks at 50% RH and 25°C. A model T2-5564 Series Instron Testing machine coupled to a humidity chamber (Weiss Enet, NL) was used for tensile testing operating at a constant crosshead speed of 3 mm min^{-1}. To test the anisotropy of the material, the specimens were cut parallel and perpendicular to the flow.

All measurements were done at least in triplicate. Tensile strength and tensile elongation of the samples were calculated as reported previously (Habeych et al., 2008).

2.6 Rapid Visco-Analyser

The pasting properties of the starch samples were determined using a Rapid Visco-Analyser-4 (RVA) (Newport Scientific Pvt. Ltd., Warriewood, Australia). After grinding and sieving (500-µm wide mesh), 3.0 g of sample (dry base) and a weighed amount of distilled water were mixed and stirred in the aluminium RVA sample canister to make a 10.7% starch suspension (w/w). The time-temperature sequence was as follows: an initial stage at 50 °C for 2 min, followed by heating to 95 °C at a constant heating rate of 5–6 °C min^{-1}, maintaining temperature at 95 °C for 5 min and then cooling to 50 °C.

3. Results and Discussion

3.1 Blends processing

Figure 1 shows the viscous response of the starch-zein blends under simple shear flow with and without compatibilizer. In all three treatments, a single peak in the shear stress curves was observed as a result of starch gelatinization. Addition of a compatibilizer retarded this peak. In the case of rice bran extract, the larger delay in the peak may be related to its high water-binding capacity (Wiboonsirikul et al., 2007).

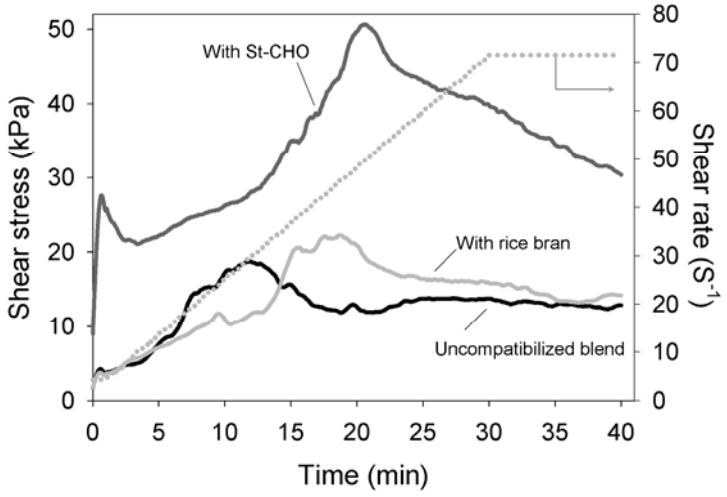

Figure 1. *Shear stress profiles for compatibilized and uncompatibilized starch-zein blends.*

The addition of St-CHO increased the viscous response of the shearing process and had a stronger effect than rice bran extract. This high shear stress obtained can be rationalized as an effect of chemical crosslinks of the starch induced under shear conditions. Previous work on starch degradation under simple shear condition showed a direct relation between maximum peak stresses during heating-shearing treatment with the reduction of molecular weight of starch (Van den Einde et al., 2004). Based on these studies, we suggest that the degree of macromolecular degradation increases with the addition of St-CHO.

Figure 2 shows the effect of the compatibilizers on the pasting behavior of 90:10 starch-zein blends after shearing, as measured with the Rapid Visco-Analyser (RVA). A quick increase of the paste consistency at low temperatures indicates that starch granules were disrupted during shearing. This is evident with the uncompatibilized (a) and in the rice bran extract compatibilized (b) samples; however the St-CHO compatibilized system shows hardly any pasting. The shear stress peak observed during preparation for the St-CHO system (Figure 1) probably implies that significant molecular breakdown occurred, which explains the a low viscosity in Figure 2.

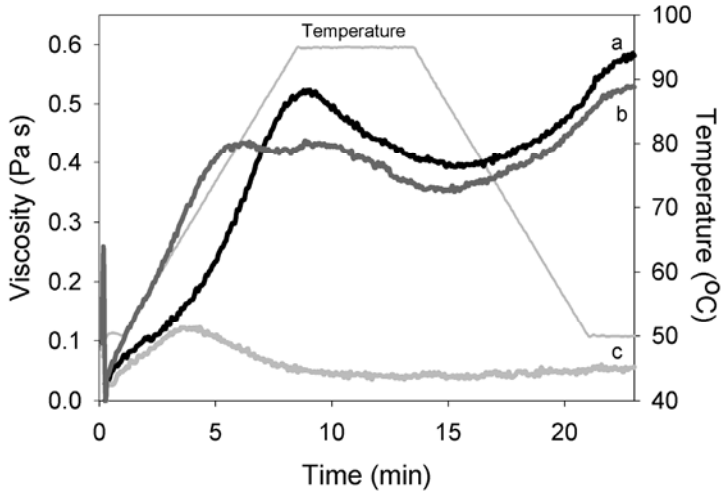

Figure 2. *RVA pasting curves of sheared 90:10 starch-zein blends with different treatments (a) uncompatibilized, (b) compatibilized with rice bran extract, and (c) compatibilized with St-CHO. RVA: Rapid Viscous Analyzer.*

3.2 Microstructure of the blends

Figure 3 shows the interface between the starch matrix and zein domains, for uncompatibilized and compatibilized blends. In contrast to the voids at the interface of the uncompatibilized blend (Figure 3A), the blend compatibilized with St-CHO (Figure 3B) and rice bran extract (Figure 3C) show adhesion. Polysaccharides and protein are generally immiscible (De Kruif & Tuinier, 2001; Tolstoguzov, 2003), and due to the different nature of starch and zein, poor adhesion is expected. Enhancement of the adhesion between the phases can be achieved by the addition of either St-CHO or rice bran extract. The tested compatibilizers act as 'adhesive' between the two polymers, but the two tested components act most likely via a different binding mechanism. Aldehyde starch is reactive and may generate covalent bonds by reacting with some of the proteins at the interface, thus generating a compatibilizer *in situ*. Rice bran extract contains polysaccharide-protein complexes (possibly Maillard products) which then have to migrate towards the interface, where they can act as a surfactant. One can observe in the blend compatibilized with rice bran extract (Figure 3C) that the matrix layer around the zein shows some thin, ribbon-like regions. This may suggest that the starch matrix in this region under deformation first yields by plastic deformation and develops crazes (stress whitening) because of the concentration of stress around the zein domain under an external force. This plastic deformation absorbs deformation energy which shows in an improvement of the tensile toughness of the blend (Liang & Li, 2000).

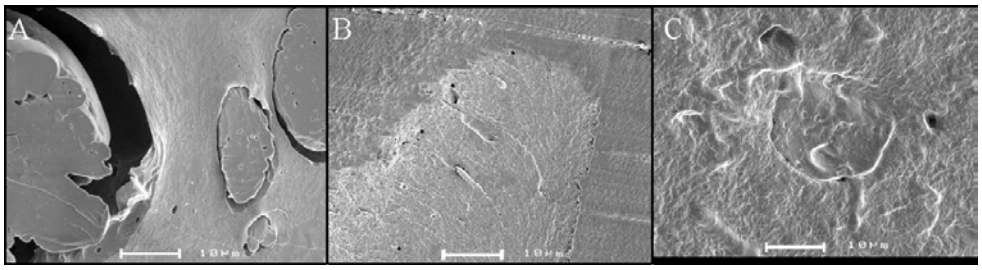

Figure 3. *Field emission electron micrograph showing the zein particles in starch-zein blends processed at 95 °C. (A) uncompatibilized blend; (B) compatibilized blend with TEMPO; (C) compatibilized blend with rice bran extract. Scale bar: 10 μm.*

3.3 Mechanical properties

Figure 4 shows the stress-strain diagram for thermoplastic starch and starch-zein blends with and without compatibilizer. Anisotropy can be observed independent of the presence of compatibilizer or even the presence of zein: the tensile stress shows a difference along

the flow and vorticity directions, being higher along the flow direction. This effect can be understood by the fact that along the flow, the starch molecules were subjected to larger stresses, which leads to a certain degree molecular alignment. The addition of compatibilizer does not change this. The addition of rice bran extract to the sample improves the adhesion of the blend, which localizes the formation of crazes and thus prevents them for forming throughout the material, which causes a rapid change in the slope of the stress-strain curve as is observed for the uncompatibilized starch-zein blend (d) and blend compatibilized with St-CHO (c). Similar behavior was reported for compatibilized synthetic polymers, (e.g., polyethylene and polypropylene blends compatibilized with ethylene-propylene random copolymer (EPR) (Teh et al., 1994)).

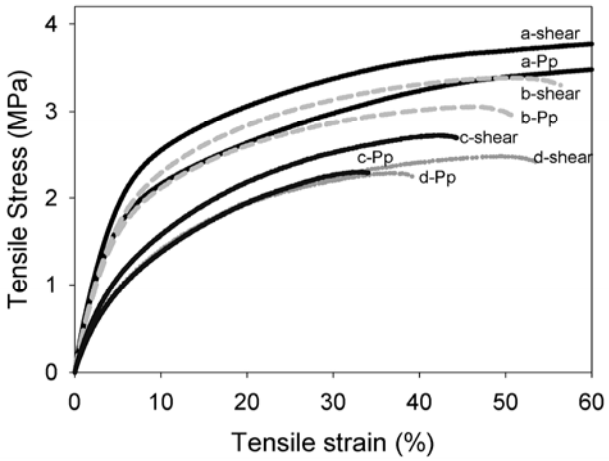

Figure 4. *Stress-strain curve (a) thermoplastic starch, (b) starch-zein with rice bran, (c) starch-zein with St-CHO, (d) uncompatibilized starch-zein. The tensile properties were measured along the flow (shear) and perpendicular to the flow (Pp) in the shear cell device.*

In such blends, the fracture behavior was suggested to change from brittle crazing to a combination of shear yielding and multicrazing. The EPR acted as an 'interfacial' or 'emulsifying' agent, improving the adhesion between the phases. We postulate analogously that the conjugates of polysaccharides with proteinous substances in rice bran (Hata et al., 2008) may similarly act as an interfacial or emulsifying agent.

The enhancement of the mechanical properties of fresh starch-zein samples blended with St-CHO reported previously (Habeych et al., 2009) decreased when the materials had been stored for two weeks under controlled humidity conditions. This effect may be related to

variations in water content or starch (re)crystallization/retrogradation upon storage (Van Soest et al., 1996).

4. Conclusions

Starch-zein blends prepared under shear flow were shown to have poor adhesion between the two phases. The system could be compatibilized by adding aldehyde starch or rice bran extract. After storage under controlled conditions, the blend compatibilized with aldehyde starch showed a reduced effect on the mechanical properties, which may be due to retrogradation. Compatibilization with rice bran extract had high impact on the material properties before and after storage. We hypothesize that the polysaccharide-protein conjugates in the rice bran extract may act as an interfacial or emulsifying agent for the starch-zein blends, thus improving the adhesion between the starch matrix and the zein domains. Rice bran extract as a compatibilizer for starch-zein blends therefore has potential for the preparation of food grade, compatibilized polysaccharide - protein blends.

Aknowledgements

The authors thank Jacqueline Donkers for assistance with the scanning electron microscope and Frans Kappen for the RVA. Rice bran extract was prepared in the Cooperation for Innovative Technology and Advanced Research in Evolutional Area (CITY AREA) program of the Ministry of Education, Culture, Sports, Science and Technology, Japan. This research was conducted within the framework of the Carbohydrate Research Centre at Wageningen.

References

1. Avérous, L. (2004). Biodegradable multiphase systems based on plasticized starch: A review. *Journal of Macromolecular Science - Polymer Reviews*, 44(3), 231-274.
2. De Kruif, C.G. & Tuinier, R. (2001). Polysaccharide protein interactions. *Food Hydrocolloids*, 15(4-6), 555-563.
3. Follain, N., Joly, C., Dole, P., & Bliard, C. (2005). Mechanical properties of starch-based materials. I. Short review and complementary experimental analysis. *Journal of Applied Polymer Science*, 97(5), 1783-1794.
4. Gáspár, M., Benko, Z., Dogossy, G., Réczey, K., & Czigány, T. (2005). Reducing water absorption in compostable starch-based plastics. *Polymer Degradation and Stability*, 90(3), 563-569.

5. Habeych, E., Van der Goot, A.J., & Boom, R. (2007). Prediction of permeation fluxes of small volatile components through starch-based films. *Carbohydrate Polymers*, 68(3), 528-536.
6. Habeych, E., Dekkers, B., Van der Goot, A.J., & Boom, R. (2008). Starch-zein blends formed by shear flow. *Chemical Engineering Science*, 63(21), 5229-5238.
7. Habeych, E., Van der Goot, A.J., & Boom, R. (2009). *In situ* compatibilization of starch-zein blends under shear flow. *Chemical Engineering Science*, 64(15), 3516-3524.
8. Hata, S., Wiboonsirikul, J., Maeda, A., Kimura, Y., & Adachi, S. (2008). Extraction of defatted rice bran by subcritical water treatment. *Biochemical Engineering Journal*, 40(1), 44-53.
9. Khuwijitjaru, P., Fujii, T., Adachi, S., Kimura, Y., & Matsuno, M. (2004). Kinetics on the hydrolysis of fatty acid esters in subcritical water. *Chemical Engineering Journal*, 99(1), 1-4.
10. Liang, J.Z. & Li, R.K.Y. (2000). Effect of filler content and surface treatment on the tensile properties of glass-bead-filled polypropylene composites. *Polymer International*, 49(2), 170-174.

11. Manski, J.M., Van der Goot, A.J., & Boom, R.M. (2007). Formation of fibrous materials from dense calcium caseinate dipersions. *Biomacromolecules*, 8(4), 1271-1279.
12. Shukla, R. & Cheryan, M. (2001). Zein: The industrial protein from corn. *Industrial Crops and Products*, 13(3), 171-192.
13. Teh, J.W., Rudin, A., & Keung, J.C. (1994). Review of polyethylene-polypropylene blends and their compatibilization. *Advances in Polymer Technology*, 13(1), 1-23.
14. Tolstoguzov, V. (2003). Some thermodynamic considerations in food formulation. *Food Hydrocolloids*, 17(1), 1-23.
15. Van den Einde, R.M., Akkermans, C., Van der Goot, A.J., & Boom, R. M. (2004). Molecular breakdown of corn starch by thermal and mechanical effects. *Carbohydrate Polymers*, 56(4), 415-422.
16. Van Soest, J.J.G., Hulleman, S.H.D., De Wit, D., & Vliegenthart, J.F.G. (1996). Changes in the mechanical properties of thermoplastic potato starch in relation with changes in B-type crystallinity. *Carbohydrate Polymers*, 29(3), 225-232.
17. Wiboonsirikul, J., Hata, S., Tsuno, T., Kimura, Y., & Adachi, S. (2007). Production of functional substances from black rice bran by its treatment in subcritical water. *LWT - Food Science and Technology*, 40(10), 1732-1740.

General discussion

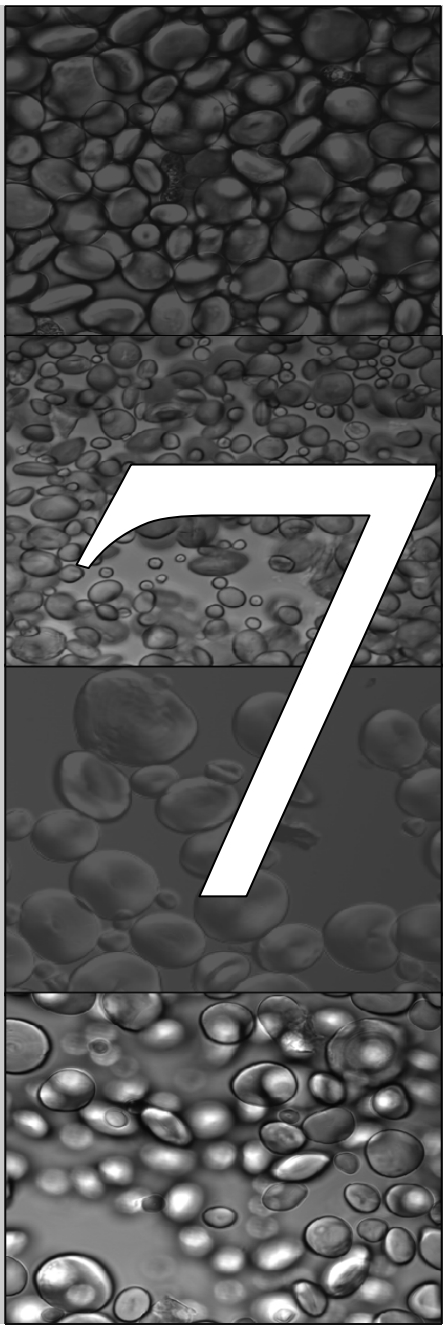

1. Introduction

The aim of this thesis was to develop insight on how the properties of starch-based materials emerge from the combination of processing and ingredients, and to develop and explore new processing routes based on these insights. This chapter evaluates the strategies that have been used to do this. Initial perspective in all chapters was the existing theoretical and practical understanding of synthetic polymers. It was analyzed how this could be applied to starch-based systems, being much more complex than most synthetic polymeric systems, and what new insights could be obtained.

2. Development of starch-based materials

Thermoplastic starch (TPS) based materials are considered to be promising alternatives for the replacement of petroleum-derived polymers, because of their low cost and availability (Avérous, 2004; Van Soest et al., 1996; Van Soest & Knooren, 1997; Wang et al., 2003). However, their properties often do not yet match with the envisaged applications. For rational development of better materials, it is essential to know the relation between these properties and the formulation and conditions during preparation and processing (Goddard III et al., 2001).

Therefore, in **Chapter 3** an adapted form of the well-known Flory–Huggins theory was used to quantitatively predict the reduction in crystallinity of starch under the action of heat in presence of different plasticizers. Further, in **Chapter 2**, it was demonstrated that the permeation of volatile components in fully gelatinized starch could be predicted semi-quantitatively using a combination of the Flory-Huggins, free volume, and Maxwell-Stefan theories.

Generally, TPS-materials are water sensitive and rubbery in the presence of moisture. From the perspective of synthetic polymer technology, two general routes exist to change polymer properties. One is to chemically modify the polymer; however, such modifications are normally accompanied by high development and production costs (Avérous, 2004). Another approach is to use blends of polymers, usually leading to inhomogeneous blends (i.e., a blend that contains more than a single phase). By varying the components in the blend and applying the right process conditions, the morphology and hence the properties can be controlled; this was discussed in **Chapter 4**.

However, due to the poor adhesion between the phases, one often needs to enhance the interphase adhesion, which is termed compatibilization. Compatbilization can be done by

the addition of an amphiphilic component that has affinity for both phases, or by creating such a component *in situ* by local chemical modification. These routes were explored in **Chapters 5** and **6**. **Chapter 5** describes the use of a compatibilizer that was prepared *in situ*. Starch was oxidized, which introduced reactive aldehyde groups in the polymer. Addition of this component to a starch-zein blend resulted in good interphase adhesion and thus better mechanical properties. The probable mechanism is that some of the aldehyde groups in the starch react with zein, forming a compatibilizer *in situ*. In **Chapter 6**, rice bran extract was explored as a non-reactive, food-grade compatibilizer for starch-zein blends. This extract was found to be a suitable compatibilizer, while the resulting blends showed more stable properties in time, compared to the reactively compatibilized blends discussed in **Chapter 5**.

In **Chapters 4** to **6**, a new class of process equipment was introduced and applied, that applies well-defined shear flow during processing, combined with large shear stresses on the material. These devices allow better control over the structure of the material, and permit the exploration of processing conditions that were previously unattainable. We found in **Chapter 4** that these process conditions indeed show promise for the practical structuring of starch-zein blends.

3. Design of TPS-based materials

Designing TPS-based materials with the correct combination of properties is still a challenge at this moment. In this section we summarize the concepts, considered and developed for this aim in this thesis.

The properties of a blend are dependent on the equilibrium properties, and the kinetics of its constituents and of the total system. Rational design of TPS based blends will therefore include two stages:

1. The evaluation of the thermodynamics and kinetic properties. The gelatinization and plasticization behavior can be predicted well using relatively simply thermodynamic concepts theories originally developed for much simpler polymeric systems. In addition, some of the material properties, such as permeability can be (semi-quantitatively) predicted.
2. The use of a compatibilizer. Blending starch with a protein was found to show the same challenges as blending of synthetic polymers. While a chemical modification was found to be effective, a non-reactive, food-grade compatibilizer was found to give similar compatibilization combined with more stable mechanical properties.

One has several parameters available in the design of better TPS-based materials to influence a variety of properties of the final material. Table 1 suggests a number of relations between these parameters and the properties. One should bear in mind that these suggestions are neither exhaustive nor quantitative, but the table will give a general impression on how to proceed towards a more rational design of TPS based materials.

Table 1. *Influences of process and formulation parameters on the final properties of the resulting TPS based material*

Control parameter / Target Functionality	Composition (relative to continuous phase)			Process	
	Addition of Plasticizer	Addition of compatibilizer	Addition of dispersed phase	Heating	Shear flow
Ductility	++	+	+ (dependent on adhesion)	+ (gelatinization)	+
Strength	-	-	+ (dependent on adhesion)	+ (creation of continuous matrix)	+ (continuous matrix and well defined dispersed phase)
Permeability	+ (higher permeability)	0 (no direct influence)	- (lower permeability)	- (Anisotropic dispersed phase gives slower permeation)	0 No direct effect
Stability of mechanical properties	+ (lower T_g, T_c)	+ non-reactive / - reactive	0 (no direct influence)	+/- (retrogradation needs attention)	+

Even though this thesis showed that design of better TPS based materials is feasible, several areas need further attention. Some of them are discussed below.

As was shown in this thesis, biopolymer product and process development can obtain inspiration from polymer technology. While we have here explored the use of blends from two polymers, it is now common practice in the field of synthetic polymers to develop materials comprising more than two polymers (Utracki, 2002a). Although the use of more

than two biopolymers is unexplored to our knowledge, we expect that further improvement can result from such an approach.

The results in this thesis also show that there is potential in improving the interfacial properties of biopolymeric blends. However, the dynamics of the transfer of added compatibilizers to the interface, the resulting dynamic interfacial tensions during processing and its influence on the evolution of the morphology, are still largely unknown. The situation is even more complex when using a reactive additive, which will only develop its amphiphilic properties during the blending process. Thus, a better understanding of the interfacial dynamics is highly important for the prediction of the effects of the compatibilizer on the blend (Koning et al., 1998). To achieve this, and to achieve further quantification on the relevant processes and morphologies, better characterization methods are important. Three-dimensional quantification of the morphology of a blend is a challenge; quantification of the location of various components is even more difficult. Development of in-line measurement methods during processing will elucidate many of the dynamic effects. One can think here of in-line rheological measurements, shear-induced phase behavior, and rheo-optics suitable for concentrated systems are subjects for consideration (Utracki, 2002b). It should be mentioned that once more, the field of synthetic polymer technology may be an inspiration.

4. Towards other applications

Even though we focused on the development of starch-based biopolymeric materials in this thesis, some of the insights obtained are also relevant to different (but related) subjects that have societal relevance. To illustrate this, we will discuss just one example, which is the hydrolysis of starch using the theory developed in **Chapter 3**.

Starch can be enzymatically hydrolyzed to obtain several products of industrial relevance, such as starch hydrolysates, glucose, maltose and fructose syrups, maltodextrins, and cyclodextrins (Akoh et al., 2008). This process typically consists of three steps: gelatinization, liquefaction, and saccharification. In the first step, starch is gelatinized using a total starch content of about 35% by incubation at temperatures of about 110 °C. In the second step, starch is hydrolyzed into soluble oligosaccharides (mainly 8-12 glucose units) of lower molecular weight with a thermo-stable α-amylase at temperatures of up to 110 °C (Akoh et al., 2008; Van der Veen et al., 2006). In the saccharification step, the oligosaccharides may be further hydrolyzed, catalyzed by glucoamylase, at temperatures of around 60 °C to form glucose syrup. Alternative processes combine step one and two. After

complete hydrolysis, the final product is further purified and concentrated to about 80% w/w dry matter. (Van der Veen et al., 2006).

Several authors have identified starch hydrolysis as a process that would benefit from intensification (Baks et al., 2008; Van der Veen et al., 2006). For example, increasing the total solid contents to 60% – 70% w/w could lead to significant savings in equipment volume, water consumption, and energy usage. However, Van der Veen et al. (2006) indentified two critical issues that limit the intensification. First of all, low water content will hinder the gelatinization or melting of starch. Secondly, the increase of the dry matter content might lead to more undesired byproducts.

Chapter 3 provides the necessary concepts for analyzing the first issue on starch melting. The phase diagram for the system starch-water-glucose can be used to analyze the effect of water and glucose content on the melting of starch.

Process intensification would require increasing the dry matter content. One can either increase the total initial starch concentration (Figure 1A) or one can recycle part of the hydrolyzed product (glucose) produced to replace water (Figure 1B).

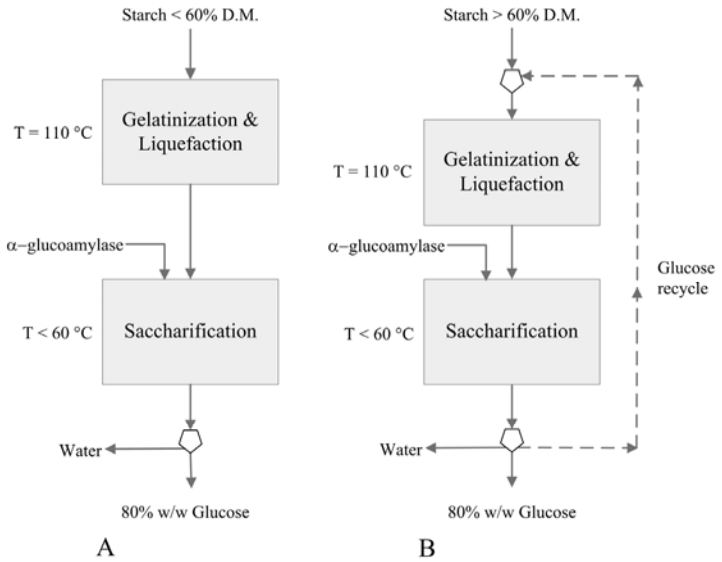

Figure 1. *The hydrolysis of starch. (A) current intensified process; (B) intensification with glucose recycle.*

We assume a maximum process temperature of 110 °C, normally applied for enzymatic hydrolysis (Van der Veen et al., 2006). Figure 2 shows that a maximum dry matter content of 60% can be achieved under those conditions in a starch-water mixture (arrow 1). A higher concentration will lead to incomplete melting of the starch.

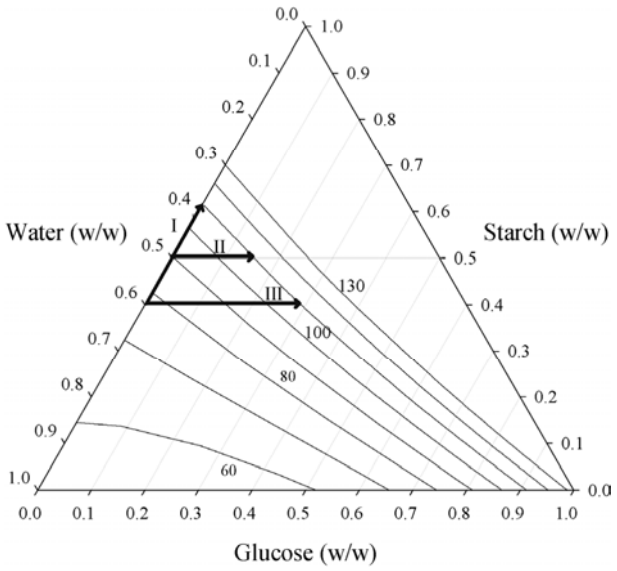

Figure 2. *Ternary phase diagram for the gelatinization/melting of the water-starch-glucose system. The solid lines refer to the corresponding predicted equilibrium gelatinization/melting isotherm. Numbers in the graph represent the corresponding isotherm in ascending order starting from T = 60 ℃ to T = 130 ℃.*

In option II, water has been partly replaced by glucose resulting in a dry matter concentration of 65% w/w (consisting of 50% starch and 15% glucose). Option III describes a further reduction of water from 40% down to 31 %, resulting in a dry matter content of 69% (40% starch and 29% glucose). Considering the chemical gain, this leads to a dry matter content after reaction of about 73%. Thus, the ternary diagram shows that a glucose addition may lead to a reduced dilution with water, which implies that less water has to be removed by evaporation in a later stage, leading to lower energy consumption. Compared to option I, option III allows a reduction of 92% of the water to be evaporated (see Table 2). This makes option III very attractive, but it involves a recycle stream, which could imply larger overall volumes to be processed. However, mass balance calculations show that the throughput through the reactor is not increased compared to the original

situation. Obviously the recycle of glucose is fully compensated by the fact that less water goes through the system. Table 2 shows the results of the mass balance calculations for the four study processes.

Table 2. *Comparative table for water reduction in intensification of the production of glucose syrup*

Process	Water reduction (%) w/w	Throughput through reactor[a]
Traditional (35% D.M)	-	2.1
Alternative I (60% D.M)	81	1.2
Alternative II (65% D.M)	87	1.4
Alternative III (69% D.M)	92	1.8

[a]scaling factor in relative to the volumetric throughput of the product.

In summary, the thermodynamic insight obtained in **Chapter 3** of this thesis may point to more effective routes of processing starch into valuable products, potentially opening possibilities for lower energy consumption and smaller processing equipment. Analogously, the other chapters might inspire better insights in other applications.

5. Final conclusions

- Using some of the established theories developed for synthetic polymers, several aspects of biomaterials based on thermoplastic starch could be quantified.
- The development of TPS based blends was found to rely on good compatibilization of the phases, which was found to be possible in a number of ways.
- New processing equipment, allowing processing under well-defined (shear flow) conditions was found to be very useful for the preparation of blends with the right morphology.
- The concepts discussed may be useful as well for different applications having societal relevance. This was illustrated with the intensification of industrial enzymatic starch hydrolysis as an example.

Many of the aspects discussed in this thesis will need further elaboration and understanding, especially better understanding of the dynamics of dispersed phase breakup and the dynamics of the interfacial properties, and better methods for characterization of the process and the materials will be important.

References

1. Akoh, C.C., Chang, S.W., Lee, G.C., & Shaw, J.F. (2008). Biocatalysis for the production of industrial products and functional foods from rice and other agricultural produce. *Journal of Agricultural and Food Chemistry*, 56(22), 10445-10451.
2. Avérous, L. (2004). Biodegradable multiphase systems based on plasticized starch: A review. *Journal of Macromolecular Science - Polymer Reviews*, 44(3), 231-274.
3. Baks, T., Kappen, F.H.J., Janssen, A.E.M., & Boom, R.M. (2008). Towards an optimal process for gelatinisation and hydrolysis of highly concentrated starch-water mixtures with alpha-amylase from b. Licheniformis. *Journal of Cereal Science*, 47(2), 214-225.
4. Goddard III, W.A., Cagin, T., Blanco, M., Vaidehi, N., Dasgupta, S., Floriano, W., Belmares, M., Kua, J., Zamanakos, G., Kashihara, S., Iotov, M., & Gao, G. (2001). Strategies for multiscale modeling and simulations of organic materials: Polymers and biopolymers. *Computational and Theoretical Polymer Science*, 11(5), 329-343.
5. Koning, C., Van Duin, M., Pagnoulle, C., & Jerome, R. (1998). Strategies for compatibilization of polymer blends. *Progress in Polymer Science (Oxford)*, 23(4), 707-757.
6. Utracki, L.A. (2002a). Compatibilization of polymer blends. *Canadian Journal of Chemical Engineering*, 80(6), 1008-1016.
7. Utracki, L.A. (2002b). *Polymer blends handbook*. Dordrecht, The Netherlands: Kluwer Academic Publishers.
8. Van der Veen, M.E., Veelaert, S., Van der Goot, A.J., & Boom, R.M. (2006). Starch hydrolysis under low water conditions: A conceptual process design. *Journal of Food Engineering*, 75(2), 178-186.
9. Van Soest, J.J.G., De Wit, D., & Vliegenthart, J.F.G. (1996). Mechanical properties of thermoplastic waxy maize starch. *Journal of Applied Polymer Science*, 61(11), 1927-1937.
10. Van Soest, J.J.G. & Knooren, N. (1997). Influence of glycerol and water content on the structure and properties of extruded starch plastic sheets during aging. *Journal of Applied Polymer Science*, 64(7), 1411-1422.
11. Wang, X.L., Yang, K.K., & Wang, Y.Z. (2003). Properties of starch blends with biodegradable polymers. *Journal of Macromolecular Science - Polymer Reviews*, 43(3), 385-409.

Summary

Starch-based materials show potential as fully degradable plastics. However, the current applicability of these materials is limited due to their poor moisture tolerance and mechanical properties. Starch is therefore frequently blended with other polymers to make the material more suitable for special or severe circumstances. By varying the components of the blend and the process conditions, the morphology and hence the properties can be controlled. A clear understanding over the structure formation process will allow the development of new, biodegradable blends based on starch-based materials with better properties. The overall goal of this thesis was thus to develop insight in how the material (blend) properties depend on the processing, and based on this insight, explore new processing routes.

Structure-function relationships: exploring a polymer science approach

In Chapter 2, we discuss the relation between the performance of a plasticized starch-based film, in terms of permeation of volatile components, and its composition. Estimations of the Maxwell-Stefan diffusion rates of trace volatile components through plasticized starch films were developed based on free-volume theory and the Flory-Huggins-Maxwell-Stefan (FHMS) equation. The model correctly predicted the order of magnitude of the permeation fluxes of diacetyl and carvone through starch films. The results of this chapter show that blending of starch with hydrophobic polymers could be an effective way to improve the barrier properties of the film.

In Chapter 3, the influence of alternative plasticizers (i.e., glucose and glycerol) on the gelatinization and melting of concentrated starch mixtures was studied, using differential scanning calorimetry (DSC) and wide angle X-ray scattering (WAXS). The results were interpreted using an extended form of the well-known Flory-Huggins equation. The chapter exemplified the possibilities of using theories that were traditionally applied to synthetic polymers, to biomaterials, in spite of their much greater complexity. This approach led to quantitative and qualitative understanding of the influence of small plasticizers of industrial relevance on the gelatinization and melting of starch. Comparing the Flory-Huggins model results with experimental results, showed that the approach is useful for interpreting and predicting the gelatinization and melting behavior of ternary starch-based systems. It also showed that since the experiments were complex, systems were often not in true equilibrium and other disturbing effects were easily encountered. Therefore, one should be cautious to use experimental results for characterizing the thermodynamics of gelatinization in multicomponent systems.

Processing: the use of simple shear

In Chapter 4, the use of simple shear as an instrument for structure formation of plasticized starch-protein blends was introduced. A novel shearing device was developed to explore the formation of new types of microstructures in concentrated starch-zein blends. This device was used to process different ratios of starch and zein (0–20% zein, dry basis) to study the influence of the matrix composition and processing conditions on the properties of the final material. Confocal scanning laser microscopy and field emission scanning electron microscopy showed that under shearless conditions, the starch-zein blend forms a co-continuous blend. Shear transformed this structure into a dispersion, with zein being the dispersed phase. The large deformation properties were examined by tensile tests in the flow and the vorticity directions; they could be described using a model for blends having poor adhesion between the continuous and dispersed phases.

In Chapter 5, we studied the effect of compatibilization, i.e., improvement of the adhesion between the continuous and dispersed phases in starch-zein blends through the incorporation of a component having affinity for both phases. Aldehyde starch was synthesized by introducing a reactive functional group (aldehyde). This group then reacted in the blend with zein (and/or other components), forming a macromolecular compatibilizer *in situ*. The effect of this compatabilizer on the interfacial properties of the blend was studied using different zein ratios. The blends showed improved adhesion between the zein and starch phases compared to the blends described in **chapter 4**. The aldehyde starch however also influenced the properties of the starch matrix (higher viscosity, stronger molecular breakdown, browning), which indicates that indeed physical or chemical crosslinks were formed inside the starch matrix, but on the other hand posed a limitation for practical applicability.

Chapter 6 presented the use of rise bran extract as a food-grade compatibilizer for starch-zein blends. This material was extracted from rice brans using super-critical water, probably contains Maillard components and shows activity as radical scavenger, antioxidant and surfactant. The influence of rice bran extract as compatibilizer was compared with that of aldehyde starch by preparing blends under shear conditions. Field emission scanning electron microscopy showed that both compatibilizers improved the adhesion between the zein and starch phases. The mechanical properties of the blends compatibilized with aldehyde starch showed poorer mechanical properties after storage under controlled conditions, possibly caused by retrogradation of starch. The use of rice bran extract as compatibilizer however led to good compatibilization with good stability

during storage. The good compatibilization by rice bran extract was suggested to be caused by polysaccharide-protein complexes, which are also responsible for its emulsifying properties.

Application

In Chapter 7, the conclusions of the preceding chapters were collectively interpreted. First, the use of a heuristic approach for the rational design of thermoplastic starch-based materials was described. Then the use of the ternary diagram for the system starch-water-glucose developed in **Chapter 3** was used to evaluate alternatives routes for the intensification of the enzymatic hydrolysis of starch.

Finally, future trends in the development of starch-based materials were presented following the insights obtained in this thesis. These include the use of established theories developed for synthetic polymers, further exploration of the concept of compatibilization of starch-based blends, and the development of new processing equipment dedicated to material structuring.

Resumen

Materiales a base de almidón muestran un gran potencial como plásticos biodegradables. Sin embargo, hasta el momento la aplicabilidad de estos materiales ha estado limitada debido a su baja tolerancia a la humedad y sus deficientes propiedades mecánicas. En consecuencia, el almidón es con frecuencia combinado con otros polímeros que contribuyen a mejorar sus propiedades, haciéndolo resistente a condiciones mas severas. Adicionalmente, al variar los componentes de la mezcla y las condiciones del proceso la morfología de la mezcla y por lo tanto las propiedades de la misma pueden ser controladas. De esta manera el entendimiento adecuado del o los mecanismos involucrados en la formación de la estructura de la mezcla permiten el desarrollo de nuevas mezclas a base de almidón completamente biodegradables con propiedades mejoradas. En consecuencia, el objetivo general de esta tesis fue desarrollar el conocimiento que conduzca al entendimiento de como las propiedades del material (mezcla de polímeros) se relacionan con el proceso aplicado e igualmente explorar sobre la base de dicho conocimiento nuevas vías de procesamiento.

Relación entre estructura y desempeño: exploración de un enfoque basado en la ciencia de los polímeros

En el capítulo 2, analizamos la relación entre la composición de películas a base de almidón con su permeabilidad para con compuestos aromáticos volátiles. La estimación de las difusividades de Maxwell-Stefan de compuestos aromáticos volátiles a través de películas de almidón fue desarrollado mediante el uso combinado de la teoría del volumen libre y las ecuaciones de Flory-Huggins y Maxwell-Stefan (FHMS). El modelo obtenido predijo correctamente el orden de magnitud de los flux de diacetil y carvone a través de películas de almidón. Los resultados de este capítulo demuestran que el mezclado de almidón con polímeros hidrofóbicos podría ser una forma eficaz de mejorar las propiedades de barrera de película a base de almidón.

En el capítulo 3, la influencia de plastificantes alternativos como glucosa y glicerol sobre la gelatinización y la fusión de mezclas concentradas de almidón se estudió mediante calorimetría de barrido diferencial (en inglés: DSC) y cristalografía de rayos X a ángulos grandes (en inglés: WAXS). Los resultados obtenidos fueron interpretados utilizando una extensión de la ecuación de Flory-Huggins. En el capítulo se ejemplifican las posibilidades de utilización de las teorías tradicionalmente usadas en polímeros sintéticos en biomateriales; a pesar de la mayor complejidad de estos últimos. Este enfoque condujo a un entendimiento cuantitativo y cualitativo del efecto de plastificantes de uso amplio en la industria sobre la gelatinización y fusión del almidón. Al comparar las predicciones del

modelo basado en la ecuación de Flory-Huggins con los resultados experimentales se obtuvo que el enfoque teórico utilizado resulto útil para interpretar y predecir el comportamiento de gelatinización y fusión de sistemas ternarios a base de almidón. También se puso de manifiesto la dificultad para la interpretación de los resultados dada la complejidad de los experimentos, el no equilibrio de los sistemas y la posible acción de otros efectos perturbadores fácilmente encontrados. Por lo tanto, se recomienda ser cauteloso al utilizar los resultados experimentales para caracterizar la termodinámica de gelatinización en sistemas múlticomponentes.

Procesamiento: el uso de esfuerzos de cizalla simple

En el capítulo 4, el uso de esfuerzos de cizalla simple es introducido como un instrumento para el estructuramiento de mezclas de almidón con proteína. Un novedoso dispositivo para la aplicación de esfuerzos de cizalla simple fue desarrollado para estudiar la formación de nuevos tipos de microestructuras en mezclas concentradas de almidón y zeina. Este dispositivo se utilizó para estudiar el efecto de la composición de la matriz y las condiciones de proceso sobre las propiedades del material resultante. De esta manera, mezclas de almidón y zeina con diferentes concentraciones (0-20% zeina, base seca) fueron evaluadas bajo diferentes condiciones de proceso. La evaluación del material obtenido se llevó acabo mediante el uso de microscopía confocal láser de barrido y microscopía electrónica de barrido. Los resultados obtenidos mostraron que cuando ningún esfuerzo es aplicado a la mezcla de almidón y zeina, esta forma una mezcla co-continua que se transforma en una dispersión de zeina en almidón al aplicársele esfuerzos de cizalla simple. Las propiedades mecánicas de las mezclas fueron examinadas en muestras tomadas en dirección paralela y perpendicular al flujo aplicado, mostrando una buena correlación con un modelo desarrollado para predecir las propiedades mecánicas de mezclas con baja adherencia entre las fases.

En el capítulo 5, se estudió el efecto de compatibilización de mezcla, es decir, el mejoramiento de la adhesión entre las fases en mezclas de almidón y zeina mediante la incorporación de un agente con afinidad con ambas fases. Para dicho fin, se sintetizó almidón aldehídico mediante la introducción de un grupo funcional reactivo (aldehído). Este grupo reaccionó posteriormente en la mezcla con zeina (y/o otros componentes), formando un compatibilizante macromolecular *in situ*. El efecto de este compatibilizante sobre las propiedades interfaciales de la mezcla fue evaluado variando la concentración de zeina en la mezcla. Las mezclas obtenidas mostraron un mejoramiento de la adhesión entre el almidón y la zeina comparado con las mezclas descritas en el **capitulo 4**.

Adicionalmente, el almidón aldehídico influyó en las propiedades del almidón (mayor viscosidad, mayor rompimiento molecular, oscurecimiento del material, las cuales indican la formación de reticulado por vía química o física en el almidón, limitando la aplicabilidad de esta ruta.

En el capítulo 6 se presentó el uso de extracto de salvado de arroz como compatibilizante de grado alimentario para mezclas de almidón y zeina. Este compatibilizante fue obtenido mediante extracción en agua supercrítica, probablemente conteniendo compuestos producto de la reacción de Maillard con actividad reductora, antioxidante y tensoactiva. El efecto de extracto de salvado de arroz como compatibilizante fue comparado con el presentado por el almidón aldehídico en mezclas preparadas bajo condiciones de cizalla simple. Análisis mediante microscopía electrónica de barrido mostró que ambos compatibilizantes mejoraron la adhesión entre la zeina y el almidón. Sin embargo, la evaluación de las propiedades mecánicas de las mezclas bajo condiciones controladas de humedad mostró que las mezclas compatibilizadas con almidón aldehídico perdieron su mejoría posiblemente a causa de la retrogradación del almidón. Por otro lado, la adición del extracto de salvado de arroz a la mezcla condujo a una buena compatibilización de estas con una buena estabilidad durante el almacenamiento. El efecto positivo compatibilizador del extracto de salvado de arroz se cree atribuido a la presencia de complejos proteína-polisacárido, responsables de sus propiedades emulsionantes.

Aplicación

En el capítulo 7, las conclusiones de los capítulos precedentes fueron interpretadas en conjunto. En primer lugar, se describe la utilización de un enfoque heurístico para el diseño racional, de materiales a base de almidón termoplástico. En segundo lugar, se evaluaron rutas alternativas para la intensificación de la hidrólisis enzimática del almidón mediante la utilización del diagrama ternario agua-almidón-glucosa desarrollados en el **capítulo 3**.

Finalmente, con base en los resultados obtenidos fueron presentadas en esta tesis tendencias futuras para el desarrollo de materias a base de almidón. Estas incluyen la aplicación de teorías desarrolladas para polímeros sintéticos en biopolímeros, la exploración del concepto de compatibilización de las mezclas a base de almidón, y el desarrollo de nuevos equipos de procesamiento de material dedicado a la estructuración de materiales.

Samenvatting

Materialen op basis van zetmeel zijn volledig biologisch afbreekbaar. De huidige toepassingen van deze materialen worden echter beperkt door de slechte vochttolerantie en mechanische eigenschappen. Daarom wordt het zetmeel vaak gemengd met andere (bio)polymeren om een composiet materiaal te verkrijgen dat geschikt is voor bijzondere of extreme omstandigheden. Door de componenten in het mengsel of de procescondities aan te passen kunnen de morfologie en daarmee de eigenschappen van de composiet gecontroleerd worden. Een goed begrip van het structuurvormingsproces zal de ontwikkeling van nieuwe, biologisch afbreekbare composieten met verbeterde eigenschappen stimuleren. Het doel van dit proefschrift was daarom het genereren van inzichten hoe materiaaleigenschappen afhangen van de procesomstandigheden en het exploreren van nieuwe procesmethoden gebaseerd op deze nieuw verkregen inzichten.

Structuur-functie-relaties: een polymeerwetenschappelijke benadering verkend

In **hoofdstuk 2** bespreken we de relatie tussen de permeatie van vluchtige componenten door een zetmeelgebaseerde film en de samenstelling van de film. Schattingen voor de Maxwell-Stefan diffusiesnelheden van vluchtige componenten door zetmeelfilms zijn gebaseerd op de vrije-volume theorie en de Flurry-Huggins-Maxwell-Stefan (FHMS) vergelijking. Het model voorspelt de juiste orde van grootte voor de permeatieflux van diacetyl en Carvon door de zetmeelfilm. De in dit hoofdstuk beschreven resultaten laten zien dat verbeteringen van de barrière-eigenschappen van zetmeelfilms mogelijk zijn door het inmengen van hydrofobe polymeren in de zetmeelfilm.

Hoofdstuk 3 beschrijft de invloed van alternatieve weekmakers, glucose en glycerol, op de het geleer- en het smeltgedrag van zetmeel in geconcentreerde systemen door middel van “differenential scanning calorimetry (DSC) en röntgendiffractie (wide angle X-ray scattering, WAXS). De resultaten zijn geanalyseerd met behulp van een Florry-Huggins vergelijking die is uitgebreid naar een ternair systeem. Het gebruik van de Florry-Huggins-vergelijking is een voorbeeld van het toepassen van polymeerchemische theorieën op de complexere biopolymeren. Dit leidt tot een kwalitatief en kwantitatief begrip hoe industrieel relevante weekmakers het geleren en smelten van zetmeelsystemen beïnvloeden. De experimentele uitkomsten kwamen goed overeen met de voorspelling van het Florry-Huggins systeem, hetgeen de bruikbaarheid van de benadering aangeeft. Verder bleek uit de vergelijking van experimentele uitkomsten en modelvoorspellingen dat de systemen vaak niet in thermodynamisch evenwicht zijn, wat kan leiden tot verstorende effecten. Daarom moeten de uitkomsten aangaande de thermodynamica van het geleergedrag van multicomponent systemen met de nodige voorzichtigheid worden gebruikt.

Het gebruik van lineaire afschuiving bij het verwerken van zetmeelhoudende materialen.

In hoofdstuk 4 wordt afschuiving geïntroduceerd als een methode om structuren aan te brengen in zetmeel-zeïnemengsels. Een nieuw afschuifapparaat is ontwikkeld om de vorming van nieuwe microstructuren in geconcentreerde zetmeel-zeïnemengsels te exploreren. Het apparaat werd gebruikt om de invloed van procescondities op de materiaaleigenschappen voor verschillende samenstellingen te exploreren. Verschillende microscopische technieken (met name confocal scanning laser microscopy CSLM en field emission scanning electron microscopy FESM) lieten zien dat zetmeel met zeïne een bicontinu composiet vormt wanneer dit mengsel verwarmd wordt zonder vervorming. Door afschuiving ontstond een composiet, met zeïne als disperse fase. Trektesten toonden aan dat er een geringe interactie is tussen het zetmeel en het zeïne.

In **hoofdstuk 5** hebben we bekeken hoe de interactie tussen de continue en de disperse fase verbeterd kan worden door het toevoegen van componenten die interactie kunnen aangaan met beide fasen. Deze componenten worden vaak compatibilizers genoemd. In dit onderzoek is geoxideerd zetmeel onderzocht. Geoxideerd zetmeel bevat een reactieve groep (een aldehyde). Tijdens het mengen van zetmeel en zeïne reageerde deze reactieve groep met het eiwit, waardoor een macromoleculaire compatibilizer werd gevormd. Het effect van dit additief op de grenslaageigenschappen van de composiet werd bestudeerd voor verschillende zeïne concentraties. Het bleek dat de interactie tussen de zetmeel en zeïnefase sterk was verbeterd. Echter, het geoxideerde zetmeel beïnvloedde ook de eigenschappen van de zetmeelmatrix. Deze werd meer viskeus, bruin van kleur, wat duidt op chemische veranderingen in de zetmeelfase. Geconcludeerd werd dat het toevoegen van geoxideerd zetmeel de interactie tussen het zetmeel en het zeïne verbetert, maar dat het ook de zetmeelmatrix sterk beïnvloedt. Dat laatste kan de toepasbaarheid van geoxideerd zetmeel beperken.

Hoofdstuk 6 presenteert het gebruik van rijstzemelen extract als een compatibilizer. Het voordeel van dit extract is dat het mag worden toegepast in levensmiddelen. Het wordt verkregen door extractie van rijstzemelen met superkritisch water. Het extract bevat waarschijnlijk Maillard componenten en heeft als eigenschap dat het radicalen kan wegvangen. Het effect van dit extract is vergeleken met de werking van geoxideerd zetmeel. Ook het rijstzemelen extract verbetert de interactie tussen de zetmeel en zeïnefase. De mechanische eigenschappen verslechteren na opslag onder gecontroleerde condities, wat waarschijnlijk veroorzaakt wordt door zetmeelretrogradatie. Het gedrag van het extract

werd toegeschreven aan aanwezigheid van koolhydraat-eiwit complexen, die emulgerende eigenschappen bezitten.

Toepassing

In hoofdstuk 7 zijn de conclusies van de voorgaande hoofdstukken gezamenlijk geïnterpreteerd. Het hoofdstuk begint met het beschrijven van een heuristische benadering voor een wetenschappelijk ontwerp van thermoplastische, zetmeelgebaseerde materialen. Daarna is beschreven hoe het in **hoofdstuk 3** ontwikkelde ternaire diagram voor het zetmeel-water-glucose systeem toegepast kan worden om een alternatieve methode te vinden voor het intensiveren van het zetmeel hydrolyseproces.

Tenslotte zijn toekomstige ontwikkelingen voor zetmeelgebaseerde materialen gepresenteerd die kunnen volgen uit de nieuwe inzichten, beschreven in dit proefschrift. Deze omvatten het toenemend gebruik van theorieën die zijn ontwikkeld voor synthetische polymeren, het verder exploreren van het concept van compatibilisatie in zetmeelhoudende materialen en het ontwikkelen van nieuwe procesapparatuur specifiek ontworpen voor structureringsdoeleinden.

Acknowledgements

Even though this thesis bears the name of just one person, achieving this work would not have been possible without the help and support of a number of people; in consequence I would like to take this opportunity to acknowledge them. Due to my lousy memory, I apologize in advance to those that I might have forgotten in these lines.

First of all, I would like to thank my parents for their unconditional support and encouragement since the beginning of this challenge. Papi & Mami, thanks a lot for all the love that you have given me, the lessons that you have taught me, and the education that you have provided me. Everything I am, I owe you. I would like to thank my brother David (*Nacho*) who has been a motive of inspiration to pursue this dream. Without intending, you have always triggered my curiosity to go further with my studies. Thanks a lot *Flaco*.

I would like to express my deepest acknowledgments to my co-supervisor, Dr. Atze Jan van der Goot. I thank you Atze Jan for believing in me, for your continuous guidance, your unconditional support and scientific insight, and for your friendship. Furthermore, I want to thank you for the scientific freedom that you gave me during these years, which allowed me to explore multiple fields within the scientific domain. In spite of this freedom, you always found a way to put me back on track when my thoughts were getting a bit dispersed. Your sharpness and efficient work were highly valuable for the accomplishment of this thesis.

I am deeply indebted to my promotor, Prof. Remko Boom. Dear Remko, your clever ideas gave me the light to accomplish this research. Your kindness and politeness are highly appreciated. Under your supervision during these four years, I have learned a lot from you both professional and non-professional aspects.

I would like to express my thanks to all my colleagues at Food & Bioprocess Engineering department. I really enjoy all the scientific and playful activities that we did together. Many thanks for sharing with me coffee breaks, We-days, “labuitjes”, “borrels”, “kerstdiners”, “AIO reizen”, soccer games, and of course the unique “gezellige” atmosphere. Special thanks to my roommates: Hady Peighambardoust, Julita van Oosten-Manski, Jan Swarts, Janneke van Seters, and Nanik Purwanti. It has been wonderful to have shared and worked with all of you. Heel veel dankt!!

I would like to thank my students Bram Dekkers & Xiojing Guo. Thank you very much for your valuable contribution to this thesis; it was really a pleasure to work with you two.

Many thanks to Frans Kappen, Martien van den Oever, Herman de Beukelaer, Guus Frissen, and Wouter Teunissen for your kindness and help during my work at the Agrotechnology & Food Sciences Group. Moreover, I would like to thank Jacqueline Donkers and Henk Kieft for the nice talks and the invaluable help with the microscopes. Additionally, I would like to express my most sincere admiration and acknowledgments to the people of the "werkplaats" in the Biotechnion (Hans de Rooij, Hans Meijer, and Reinoud Hummelen) for the excellent job done during the design and assembling of the shear cell. Bedankt!

I would like to specially acknowledge my friends in The Netherlands: Claudio Finol & Veronica Rivas for you unconditional friendship; Carlos Florez & Margarita Kielman for being my overseas family; Yoav Dienes, Diego Romero, Esteban Jaramillo, and Victor Beslier for all the unbelievable times that we lived together; and many thanks to Andrey Lizyayev and Francisco Rossier.

Last and not least, I would like to express my most sincere acknowledgments to my dearest and lovely wife Rosana. You left everything behind to come to The Netherlands to be with me and become my pillar. Thanks a lot *Pecas* for your support, your understanding, your confidence in me, your sincere love, and for making me a happy person sharing every moment of our lives.

October, 2009

Publication List

Edwin Habeych, Atze Jan van der Goot, Remko Boom. **2009**. *In situ* compatibilization of starch–zein blends under shear flow. *Chemical Engineering Science*, 64 (15): 3516-3524.

Edwin Habeych, Xiaojing Guo, Jeroen van Soest, Atze Jan van der Goot, Remko Boom. **2009**. On the applicability of Flory–Huggins theory to ternary starch–water–solute systems. *Carbohydrate Polymers*, 77(4): 703-712.

Edwin Habeych, Bram Dekkers, Atze Jan van der Goot, Remko Boom. **2008**. Starch–zein blends formed by shear flow. *Chemical Engineering Science*, 63 (21): 5229-5238.

Edwin Habeych, Atze Jan van der Goot, Remko Boom. **2007**. Prediction of permeation fluxes of small volatile components through starch-based films. *Carbohydrate Polymers*, 68 (3): 528-536.

Lina María Ruiz, Gemma Armengol, Edwin Habeych, Sergio Orduz A. **2006**. Theoretical analysis of codon adaptation index of the *Boophilus microplus* bm86 gene directed to the optimization of a DNA vaccine. *Journal of Theoretical Biology*, 239 (4): 445-449.

Conference proceeding

Edwin Habeych, Atze Jan van der Goot, Shuji Adachi, Remko Boom. **2009**. Compatibilization of starch-zein blends under shear flow. *Proceedings 5th International Symposium on Food Rheology and Structure (ISFRS)*. Zurich: 446-449.

Edwin Habeych, Atze Jan van der Goot, Remko Boom. **2009**. Estudio de estructuramiento y compatibilización de mezclas de Almidón con Zeina bajo condiciones de cizalla simple. *Proceedings IV Simposio sobre Biofábricas*. Medellín - Colombia.

Overview of Completed Training Activities

Discipline specific activities

Courses
Rheological Measurements (Leuven University, 2005)
Computational Fluid Dynamics I (Delft University, 2006)
Numerical Methods in Chemical Engineering, (OSPT, 2006)
Summer Course Glycosciences (VLAG, 2006)
Polysaccharides as Food Colloids and Biomaterials (VLAG, 2007)
Extrusion Training (AFSG – Wageningen, 2007)

Conferences and meetings
Bionanotechnology Congress (VLAG, 2005)
XV International Starch Convention (Moscow - Russia, 2007)
Meetings: Carbohydrate Research Center (Wageningen, 2006, 2007)
Netherlands Process Technology Symposium (OSPT, 2005, 2006, 2008)
10th International Congress of Engineering and Food (Viña del Mar – Chile, 2008)
Meeting: NMR and MRI Applications in Food Systems (VLAG, 2008)
5th International Symposium on Food Rheology and Structure (Switzerland, 2009)

General courses
VLAG PhD week (VLAG, 2005)
Academic writing II (Wageningen University, 2006)
Scientific writing (Wageningen University, 2007)
Organizing and supervising thesis projects (Wageningen University, 2007)
Philosophy and Ethics of Food Science & Technology (VLAG, 2007)
Career assessment (VLAG, 2007)

Optional courses and activities
PhD study tour Food & Bioprocess Engineering group (Denmark & Sweden, 2006)
PhD study tour Food & Bioprocess Engineering group (Japan, 2008)
Brainstorm-week Food and Bioprocess Engineering group (2005)

Curriculum Vitae

Edwin A. Habeych Narváez was born in Santa Marta (Colombia) on the 14th of December in 1977. In 1994 he completed his high-school studies and graduated from the Colegio San Luis Beltrán (Santa Marta) with distinction and best grade average. He attended the Universidad Nacional de Colombia (sede Medellín), graduating in 2001 with a degree in Chemical Engineering with emphasis in biotechnology. He conducted his bachelor thesis at the Corporacion para Investigaciones Biologicas (CIB, Medellín) where he continued after his graduation working as a bioprocess engineer. Before his graduation, he was awarded a scholarship from the Agencia Española de Cooperación Internacional para el Desarrollo (Ministry of Foreign Affairs of Spain) conducted at the University of Valladolid (Valladolid, Spain). In September 2002, he joined the post-master program on Bioprocess Design at Delft University of Technology (Delft, The Netherlands) receiving his diploma as Professional Doctorate in Engineering (PDEng) in September 2004. In March 2005, he started his PhD research at the Food and Bioprocess Engineering department at Wageningen University, The Netherlands. The results of this research are described in this thesis. On the 1st of April of 2009, Edwin started working as Research & Development specialist at the Nestlé Research Center in Lausanne (Switzerland) in the department of Food Science and Technology.

Cover: animation of the shear cell with microscopic pictures of wheat starch and a scheme of a proposed mechanism of developing structure under simple shear. Shear cell animation: Hans de Rooij. Cover design: Rosana Ceballos.

The research described in this PhD thesis was co-financed by Carbohydrate Research Center - Wageningen.